ISSN 2523-6881

Volume 9, Issue 21 – e20250921 January – December 2025

Journal Renewable Energy

ECORFAN®

Journal Renewable Energy, Volume 9, Issue 21: e20250921 January – December 2025, is a Continuous publication - Journal edited by ECORFAN-Peru. 1047 La Raza Avenue -Santa Ana, Cusco-Peru. WEB: www.ecorfan.org/taiwan, revista@ecorfan.org. Chief Editor: Serrano-Pacheco, Martha. PhD. ISSN-On line: 2523-6881. Responsible for the latest update of this number ECORFAN Computer Unit. Escamilla-Bouchán, Imelda. PhD, Luna-Soto, Vladimir. PhD. 1047 La Raza Avenue -Santa Ana, Cusco-Peru, last updated December 30, 2025.

Journal Renewable Energy

Definition of Research Journal

Scientific Objectives

Support the international scientific community in its written production Science, Technology and Innovation in the Field of Engineering and Technology, in Subdisciplines Solar energy and its applications, renewable energies and climate change, environmental impact, hydroelectric plants, renewable energies, energy geothermal power in the world.

ECORFAN-Mexico SC is a Scientific and Technological Company in contribution to the Human Resource training focused on the continuity in the critical analysis of International Research and is attached to SECIHTI-RENIECYT number 1702902, its commitment is to disseminate research and contributions of the International Scientific Community, academic institutions, agencies and entities of the public and private sectors and contribute to the linking of researchers who carry out scientific activities, technological developments and training of specialized human resources with governments, companies and social organizations.

Encourage the interlocution of the International Scientific Community with other Study Centers in Mexico and abroad and promote a wide incorporation of academics, specialists and researchers to the publication in Science Structures of Autonomous Universities - State Public Universities - Federal IES - Polytechnic Universities - Technological Universities - Federal Technological Institutes - Normal Schools - Decentralized Technological Institutes - Intercultural Universities - S & T Councils - SECIHTI Research Centers.

Scope, Coverage and Audience

Journal Renewable Energy is a Research Journal edited by ECORFAN-Mexico S.C in its Holding with repository in Republic of Peru, is a scientific publication arbitrated and indexed with semester periods. It supports a wide range of contents that are evaluated by academic peers by the Double-Blind method, around subjects related to the theory and practice of Solar energy and its applications, renewable energies and climate change, environmental impact, hydroelectric plants, renewable energies, energy geothermal power in the world with diverse approaches and perspectives , That contribute to the diffusion of the development of Science Technology and Innovation that allow the arguments related to the decision making and influence in the formulation of international policies in the Field of Engineering and Technology. The editorial horizon of ECORFAN-Mexico® extends beyond the academy and integrates other segments of research and analysis outside the scope, as long as they meet the requirements of rigorous argumentative and scientific, as well as addressing issues of general and current interest of the International Scientific Society.

Editorial Board

Arbitration Committee

Castillo - Quiñones, Javier Emmanuel. PhD
Universidad Autónoma de Baja California • • 0000-0002-2478-3375 • 228521

Chávez-Lugo, Pedro. PhD
Universidad Michoacana de San Nicolás de Hidalgo • JMR-0073-2023 • 0000-0002-1681-3503 • 44921

Flores - Ramírez, Oscar. PhD
Universidad Politécnica de Amozoc • 0000-0002-9780-937X • 92914

Gómez - Mercado, Abdiel
Instituto Tecnológico de Pachuca • P-7684-2018 • 0000-0002-3409-6851 • 58742

Hernández - Gómez, Víctor Hugo. PhD
Universidad Nacional Autónoma de México • S-6575-2018 • 0000-0001-9315-5869 • 122247

Herrera - Romero, José Vidal. PhD
Universidad Veracruzana • 0000-0001-9462-0160 • 163163

Mejias - Brizuela, Nildia Yamileth. PhD
Universidad Politécnica de Sinaloa • • 0000-0003-2973-473X • 253092

Pérez - Robles, Juan Francisco. PhD
Instituto Politécnico Nacional • B-8421-2016 • 0000-0001-9738-6795 • 3240

Aguilar - Virgen, Quetzalli. PhD
Universidad Autónoma de Baja California • K-2317-2017 • 0000-0002-4514-760X

Ramírez - Coutiño, Víctor Ángel. PhD
Universidad Tecnológica de Querétaro • 0000-0003-2510-2030 • 212480

Assignment of Rights

The sending of an Article to Journal Renewable Energy emanates the commitment of the author not to submit it simultaneously to the consideration of other series publications for it must complement the Originality Format for its Article.

The authors sign the Authorization Format for their Article to be disseminated by means that ECORFAN-Mexico, S.C. In its Holding Republic of Peru considers pertinent for disclosure and diffusion of its Article its Rights of Work.

Declaration of Authorship

Indicate the Name of Author and Coauthors at most in the participation of the Article and indicate in extensive the Institutional Affiliation indicating the Department.

Identify the Name of Author and Coauthors at most with the CVU Scholarship Number-PNPC or SNI-SECIHTI- Indicating the Researcher Level and their Google Scholar Profile to verify their Citation Level and H index.

Identify the Name of Author and Coauthors at most in the Science and Technology Profiles widely accepted by the International Scientific Community ORC ID - Researcher ID Thomson - arXiv Author ID - PubMed Author ID - Open ID respectively.

Indicate the contact for correspondence to the Author (Mail and Telephone) and indicate the Researcher who contributes as the first Author of the Article.

Plagiarism Detection

All Articles will be tested by plagiarism software PLAGSCAN if a plagiarism level is detected Positive will not be sent to arbitration and will be rescinded of the reception of the Article notifying the Authors responsible, claiming that academic plagiarism is criminalized in the Penal Code.

Arbitration Process

All Articles will be evaluated by academic peers by the Double Blind method, the Arbitration Approval is a requirement for the Editorial Board to make a final decision that will be final in all cases. MARVID® is a derivative brand of ECORFAN® specialized in providing the expert evaluators all of them with Doctorate degree and distinction of International Researchers in the respective Councils of Science and Technology the counterpart of SECIHTI for the chapters of America-Europe-Asia- Africa and Oceania. The identification of the authorship should only appear on a first removable page, in order to ensure that the Arbitration process is anonymous and covers the following stages: Identification of the Research Journal with its author occupation rate - Identification of Authors and Coauthors - Detection of plagiarism PLAGSCAN - Review of Formats of Authorization and Originality-Allocation to the Editorial Board-Allocation of the pair of Expert Arbitrators-Notification of Arbitration -Declaration of observations to the Author-Verification of Article Modified for Editing-Publication.

Instructions for Scientific, Technological and Innovation Publication

Knowledge Area

The works must be unpublished and refer to topics of Solar energy and its applications, renewable energies and climate change, environmental impact, hydroelectric plants, renewable energies, energy geothermal power in the world and other topics related to Engineering and Technology.

Presentation of the content

In the first article we present, *Analysis of the installation of photovoltaic panels interconnected to the electrical grid to illuminate the parking lot of the Higher Technological Institute of Huatusco* by Molina-García, Moisés, Fuentes-Ramos, Francisco Javier, Melchor-Hernández, Cesar Leonardo and Díaz-Cogco, Jonathan, with adscription in the Instituto Tecnológico Superior de Huatusco, as the next article presents, *Comparative analysis of evacuated flat plate solar collectors under clean and fouled conditions* by Lugo-Granados, Hebert Gerardo, Canizalez-Dávalos, Lázaro and Picón-Núñez, Martín, with adscription in the Universidad Autónoma de Zacatecas and Universidad de Guanajuato, as the next article presents, *Sizing parabolic trough solar thermal collector networks for Industrial Application – Case study* by Lizárraga-Morazán, Juan-Ramón & Picón-Núñez, Martín, with adscription in the Universidad de Guanajuato, as the next article presents, *Effects of photovoltaic systems on power quality and power factor in industry, simulation and experimental validation in Mexico* by Tellez-Hernandez, Felipe, Pineda-Piñón, Jorge, Sánchez-Vega, Guadalupe O. and Mota-Del Carpio, Jimena, with adscription in the Instituto Politécnico Nacional and Uco Mondragón, as the next article presents, *SOLNIDO: A novel solar-powered incubator model for advancing sustainable poultry farming* by Marroquín-De Jesús, Ángel, Castillo-Martínez, Luz Carmen, Soto-Álvarez, Sandra and Olivares-Ramírez, Juan Manuel, with adscription in the Universidad Tecnológica de San Juan del Río, as the next article presents, *Analysis of the ultraviolet radiation profile based on measurements from the UTVM-UNAM solarimetric station and its effects on health* by Demillón-Pascual, Rufino, López-Mendoza, Israel, Trejo-Leal, Huber Baltazar and Callejas-Mejía, Miriam, with adscription in the Universidad Tecnológica del Valle del Mezquital, as the last article presents, *Sweet sustainability: Comparative study of solar and electric cooking in the production of crystallized orange peel Candy* by Castillo-Martínez, Luz-Carmen, Marroquín-De Jesús, Ángel, Alonso-Arroyo, Juana and Olivares-Ramírez, Juan Manuel, with adscription in the Universidad Tecnológica de San Juan del Río.

Content

Journal Renewable Energy 9[21]1-5: e10921105
Article

Analysis of the installation of photovoltaic panels interconnected to the electrical grid to illuminate the parking lot of the Higher Technological Institute of Huatusco

Análisis de instalación de paneles fotovoltaicos interconectados a la red eléctrica para iluminar el estacionamiento del Instituto Tecnológico Superior de Huatusco

Molina-García, Moisés*[a], Fuentes-Ramos, Francisco Javier[b], Melchor-Hernández, Cesar Leonardo[d] and Díaz-Cogco, Jonathan[d]

[a] Tecnológico Nacional de México - Instituto Tecnológico Superior de Huatusco • KCZ-3165-2024 • 0000-0002-4213-9591 • 311075
[b] Tecnológico Nacional de México - Instituto Tecnológico Superior de Huatusco • KYR-9317-2024 • 0000-0002-7490-784X • 732279
[c] Tecnológico Nacional de México - Instituto Tecnológico Superior de Huatusco • AAU-3491-2021 • 0000-0003-2154-6654 • 161766
[c] Tecnológico Nacional de México - Instituto Tecnológico Superior de Huatusco • OUJ-8970-2025 0000-0002-5201-5517 • 1267487

SECIHTI classification:

Area: Engineering
Field: Engineering
Discipline: Energy Engineering
Subdiscipline: Solar energy

https://doi.org/10.35429/JRE.2025.9.21.1.1.5
Article History:
Received: January 20, 2025
Accepted: December 04, 2025

* ✉ [ingmoymolina@gmail.com]

Abstract

Solar energy is the main source of life on the planet; directs the biophysical, geophysical and chemical cycles that maintain life on earth. The sun supplies us with food through photosynthesis, it is used to generate electrical energy. The solar radiation that falls on the earth can be actively used, through the implementation of photovoltaic modules or cells, from which electrical energy can be obtained to illuminate different areas. The present investigation shows the different electrical variables of these modules interconnected to the electrical network and how the connection is derived to illuminate the parking lot of the Higher Technological Institute of Huatusco (ITSH).

Objetivos: análisis de instalación, iluminación led, energía renovable, ahorro de energía		
Objetivos	Metodología	Contribución
Análisis de instalación, iluminación led, energía renovable, ahorro de energía.	Uso de energía renovable Análisis de consumo mediante software	Iluminación led a través de energía solar Reducción de consumo de recibo de energía eléctrica.

Solar, Energía, Electricidad

Resumen

La energía solar es la fuente principal de vida en el planeta; dirige los ciclos biofísicos, geofísicos y químicos que mantienen la vida en la tierra. El sol nos suministra alimentos mediante la fotosíntesis, se utiliza para la generación de energía eléctrica La radiación solar que incidente en la tierra puede aprovecharse activamente, a través de la implementación de módulos o celdas fotovoltaicas, de los cuales se puede obtener energía eléctrica para iluminar diferentes áreas. La presente investigación muestra las diferentes variables eléctricas de estos módulos interconectados a la red eléctrica y de cómo se deriva la conexión para iluminar el estacionamiento del Instituto Tecnológico Superior de Huatusco (ITSH).

Objectives: installation analysis, LED lighting, renewable energy, energy savings		
Goals	Metodología	Contribución
Installation analysis, LED lighting, renewable energy, energy savings.	Use of renewable energy Consumption analysis using software.	LED lighting through solar energy Reduction of electricity bill consumption.

Solar, Energy, Electricity

Area: Development of strategic leading-edge technologies and open innovation for social transformation

Citation: Molina-García, Moisés, Fuentes-Ramos, Francisco Javier, Melchor-Hernández, Cesar Leonardo and Díaz-Cogco, Jonathan. [2025]. Analysis of the installation of photovoltaic panels interconnected to the electrical grid to illuminate the parking lot of the Higher Technological Institute of Huatusco. Journal Renewable Energy. 9[21] 1-5: e10921105.

Introduction

Photovoltaic solar energy is defined as the process of obtaining electrical energy using photovoltaic panels. Photovoltaic modules or collectors are made up of semiconductor diode devices, which, upon receiving solar radiation, undergo a chemical process that excites the electrons in the modules, causing electrons to jump; this is known as the photoelectric effect. This phenomenon generates a potential difference across the ends of the conductors. The result is a direct current (DC) voltage that can be harnessed and transformed into an alternating current (AC) voltage, which can then be fed into the electrical grid or an interconnected system. (Sánchez, 2011).

The fascinating world of lighting is art, technique, and science all at once. Today, electric lighting plays a fundamental role in all human activities, and all disciplines and professions depend on it to a large extent, even those that are predominantly daytime. It is difficult to imagine today's world without modern lighting systems. (Rivero, 2018)

The electricity used by the Huatusco Higher Technological Institute (ITSH) comes from the Federal Electricity Commission (CFE). The parking lot generates 36 kWh/month.

Development

Currently, the Huatusco Higher Technological Institute (ITSH) consumes approximately 1,320 Wh/day for parking area lighting, which increases the cost on its electricity bill. With the installation of solar panels, a portion of the consumed MWh can be generated on-site, with the remainder being fed back into the Federal Electricity Commission (CFE) grid, thus reducing the cost of the electricity bill.

LED lighting

In LED lighting, the drivers are responsible for maintaining a completely constant current to prevent changes in junction temperature, efficiency, color rendering, and lifespan. New doped materials and improved phosphor coatings are generating efficiencies exceeding 200 lm/W. (Rivero, 2018)

Installations connected to the electrical grid

These are installations where the energy generated by the photovoltaic array is delivered directly to the distribution grid. This type of installation does not have batteries or regulators, only the photovoltaic elements and the inverter. The inverter must have a system for measuring the energy consumed and delivered, capable of interrupting or resuming the supply depending on the field status of the module and adapting the alternating voltage produced by the inverter to the grid's power phase.

Photovoltaic module

The main function of a photovoltaic module is to capture and convert solar radiation into electrical voltage. Modules can be connected in series or parallel. When connected in series, the total voltage is the sum of the individual voltages of each module. The output voltage will be equal to the voltage of a single module. When connected in parallel, the total voltage is the same as that of a single module. Therefore, the number of modules connected in series determines the voltage, and the number of modules in parallel determines the current that can be supplied to a load.

Investor

It is responsible for converting the continuous voltage produced by the photovoltaic generator to the electrical characteristics required by the loads to be powered.

Methodology to be used

5.79 are the peak solar hours of the City of Huatusco, specifically in the parking area of ITS Huatusco.

$$(5.79\ )(5.32\ A) = 31.20\ Ah7día \quad [1]$$

This data is for use with a 45° tilt angle.

Each panel consumes 100W

$$(100\ W)(12\ h) = 1{,}200\ Wh/día \quad [2]$$

$$(1{,}200\ Wh/día)(1.1) = 1{,}200\ Wh/día \quad [3]$$

$$(1{,}200\ Wh/día)(1.1) = 1{,}320\ W \quad [4]$$

$$\frac{(1{,}320\ W)}{(18.78)} = 95.79\ Ah/día \quad [5]$$

ISSN: 2523-6881
RENIECYT-SECIHTI: 1702902

Molina-García, Moisés, Fuentes-Ramos, Francisco Javier, Melchor-Hernández, Cesar Leonardo and Díaz-Cogco, Jonathan. [2025]. Analysis of the installation of photovoltaic panels interconnected to the electrical grid to illuminate the parking lot of the Higher Technological Institute of Huatusco. Journal Renewable Energy. 9[21] 1-5: e10921105.
https://doi.org/10.35429/JRE.2025.9.21.1.1.5

The number of panels in parallel

$$\frac{\left(95.79\frac{Ah}{día}\right)}{\left(31.20\frac{Ah}{día}\right)} = 3\ paneles \quad [6]$$

100 W with twelve hours of use

$$(100\ W)(12\ h) = 1{,}200\ Wh/día \quad [7]$$

We added 10% security

$$\left(12{,}000\,\frac{Wh}{día}\right)(1.1) = 13{,}200\ Wh/día \quad [8]$$

$$\frac{\left(13{,}200\frac{Wh}{día}\right)}{22.64} = 583.03\ Ah/día \quad [9]$$

Number of panels in parallel

$$\frac{583.03\frac{Ah}{día}}{31.20\frac{Ah}{día}} = 18.68 = 19\ paneles \quad [10]$$

Box 1

Table 1
Calculation of the number of parking posts at ITSH

Parking length	80 meters
Parking width	44 meters
Total area	3,520 m²
Projected light output	20 lx
Luminous flux	9000 lm
Power input	100 W
Number of lamps per pole	2 de 50 W
Lamp height	3.65 m
Length, space 2H	7.3 m
Width, space 3H	10.95 m
Space 4H	14.6 m
Sidewalk length	5.83 m
Street width	2.40 m
Actual space	It is decided with design
Number of poles	14.03
Coefficient curve	
Forward	1
Forward	2

Source: Own Elaboration

The Instituto Tecnológico Superior de Huatusco is located at Avenida 25 poniente No. 100 Colonia Reserva Territorial, Huatusco, Ver. (Google/maps, 2025)

The dimensions of the parking lot are shown in.
Figure 1.

Box 2

Figura 1
West Zone Dimension
Source: Own Elaboration

The utilization factor yielded

Box 3

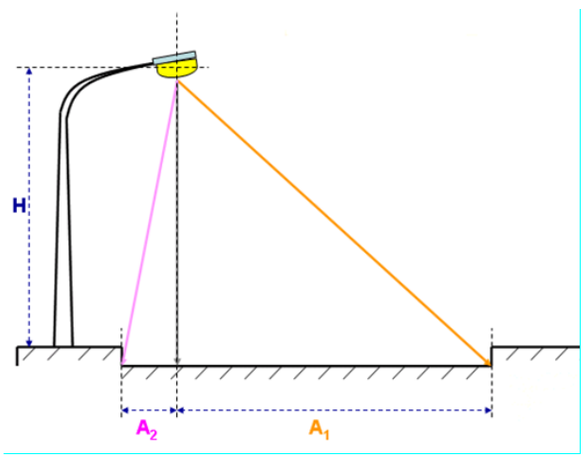

Figura 2
Utilization factor
Source: Own Elaboration

The coefficient curve is shown in Figure 4, which gives us a value of.

ISSN: 2523-6881
RENIECYT-SECIHTI: 1702902

Molina-García, Moisés, Fuentes-Ramos, Francisco Javier, Melchor-Hernández, Cesar Leonardo and Díaz-Cogco, Jonathan. [2025]. Analysis of the installation of photovoltaic panels interconnected to the electrical grid to illuminate the parking lot of the Higher Technological Institute of Huatusco. Journal Renewable Energy. 9[21] 1-5: e10921105.
https://doi.org/10.35429/JRE.2025.9.21.1.1.5

Box 4

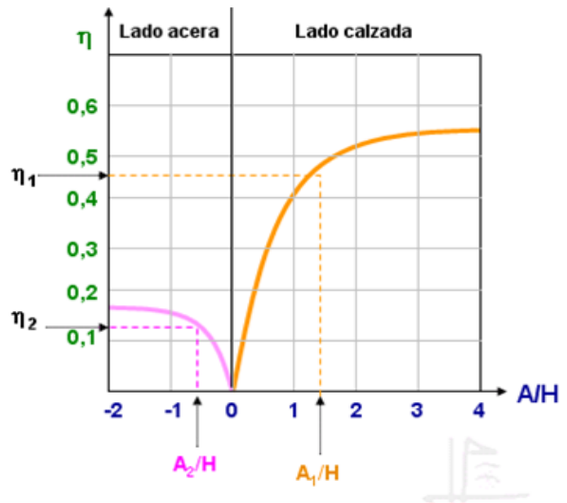

Figura 3
Utilization factor
Source: Own Elaboration

According to the Official Mexican Standard NOM-025-STPS-2008, Lighting conditions in workplaces. In the general outdoor work area: patios and parking lots, the minimum lighting level is 20 lux.

Costs

The proposed system is for an installed capacity of approximately 2 kW.

The price may vary depending on costs, but a proposal has already been prepared.

Box 5

Table 2
System quotation

Quantity	Description	Unit Price	Amount
19	100W solar module	$ 2,070.28	$ 39,335.27
1	Micro inverter with 2 kW power 220 VCA.	$7,270.50	$7,270.50
1	Bus cable end cap for ds3d 10 AWG/12 AWG	$175.86	$175.86
1	Apsystems ecu-r	$4,197.85	$4,197.85
1	Y3 bus cable for DS3D 10 AWG 2.4 m	$805.53	$805.53
8	Anodized aluminum structure cross rail	$1,276.37	$10, 210.98
1	AC combiner box, a micro-inverter arrangement	$2,266. 27	$2,266. 27
1	Engineering services, installation labor	$9,150.00	$9,150.00
		Subtotal	$73,412.
		IVA	$11,745.96
		Total	**$85,158.23**

Source: Own Elaboration

Conclusions

This analysis provides the necessary basis for installing the system. Generally, the monthly savings will be approximately 36 kWh, which, over 30 days, gives us a value of 1080 kWh. At $2.35 per kWh, this results in savings of approximately $2,538 per month, totaling $30,456 over 12 months. Analyzing the data obtained analytically, it is observed that the amount of kWh generated by the panels is specifically sufficient to properly supply the area; the in-depth analysis of the costs will be carried out in the next investigation.

Conflict of interest

The authors of this article decelerate that they have no conflicts of interest. They have no competing financial interests or known personal relationship that could have influenced the work presented in this article.

Author contribution

Ramos-Fuentes, Francisco Javier: conducted the analysis and feasibility study of the system interconnected to the electrical grid of the institute's parking lot

Molina-García, Moises: performed the calculation and sizing of the photovoltaic system, reviewed the data, and analyzed and studied the documented research for publication.

Melchor-Hernández, César Leonardo and Diaz-Cogco Jonathan: performed the general review and correction of the article.

Availability of data and materials

Mexican standards were used to calculated solar powered and evaluate photovoltaic module.

Financing

Financial found were provided by professors and staff involved into the scholar project.

Acknowledgments

To the Electromechanical Engineering division of the Higher Technological Institute of Huatusco (ITSH), for the facilities provided.

ISSN: 2523-6881
RENIECYT-SECIHTI: 1702902

Molina-García, Moisés, Fuentes-Ramos, Francisco Javier, Melchor-Hernández, Cesar Leonardo and Díaz-Cogco, Jonathan. [2025]. Analysis of the installation of photovoltaic panels interconnected to the electrical grid to illuminate the parking lot of the Higher Technological Institute of Huatusco. Journal Renewable Energy. 9[21] 1-5: e10921105.
https://doi.org/10.35429/JRE.2025.9.21.1.1.5

Abbreviations

LED Light Emitting Diode

DC Direct current

AC Alternate current

CFE Federal Electricity Commission

ITSH Huatusco Higher Technological Institute

References

Antecedents

Rivero, A. R. (2018). Iluminación y eficiencia energética . *Revista del fideicomiso para el ahorro de energía eléctrica* , 36 - 37.

Basic

Sánchez, D. A. (2011). *Libro Interactivo sobre energía solar y sus aplicaciones*. Pereira : Universidad Tecnológica de Pereira .

Supports

Google/maps. (04 de 07 de 2025). HYPERLINK "https://maps.app.goo.gl/3EKjhfW5ComX2uZv6" (Google/maps, 2025) Obtenido de https://maps.app.goo.gl/3EKjhfW5ComX2uZv6

Differences

Sánchez, D. A. (2011). *Libro Interactivo sobre energía solar y sus aplicaciones*. Pereira : Universidad Tecnológica de Pereira

ISSN: 2523-6881
RENIECYT-SECIHTI: 1702902

Molina-García, Moisés, Fuentes-Ramos, Francisco Javier, Melchor-Hernández, Cesar Leonardo and Díaz-Cogco, Jonathan. [2025]. Analysis of the installation of photovoltaic panels interconnected to the electrical grid to illuminate the parking lot of the Higher Technological Institute of Huatusco. Journal Renewable Energy. 9[21] 1-5: e10921105.
https://doi.org/10.35429/JRE.2025.9.21.1.1.5

Journal Renewable Energy 9[21]1-12: e20921112
Article

Análisis comparativo de colectores solares de placa plana evacuados bajo condiciones limpias y de ensuciamiento

Comparative analysis of evacuated flat plate solar collectors under clean and fouled conditions

Lugo-Granados, Hebert Gerardo*[a], Canizalez-Dávalos, Lázaro[b] and Picón-Núñez, Martín[c]

[a] Autonomous University of Zacatecas • F-2050-2019 • 0000-0002-0027-3418 • 487049
[b] Autonomous University of Zacatecas • ABW-3215-2022 • 0000-0002-3126-8574 • 164509
[c] University of Guanajuato • AHA-5481-2022 • 0000-0002-0793-192X • 12408

SECIHTI classification:

Area: Engineering
Field: Engineering
Discipline: Mechanical Engineering
Subdiscipline: Thermal Engineering

https://doi.org/10.35429/JRE.2025.9.21.2.1.12
Article History:
Received: June 20, 2025
Accepted: December 05, 2025

* ✉ [lugh871024@gmail.com]

Abstract

This study evaluates the thermal performance of two configurations of evacuated flat-plate solar collectors: serpentine-type and parallel-type, under both clean conditions and fouling caused by calcium carbonate ($CaCO_3$) scaling. The aim is to determine which of the two technologies offers higher efficiency and requires fewer units to achieve an outlet temperature of 90 °C. Results indicate that parallel collectors reach a higher thermal efficiency (0.80 compared to 0.76 for the serpentine configuration) and require fewer units to attain the target temperature. In the presence of scaling, 20 parallel collectors are needed, compared to 23 in the serpentine arrangement — representing a 15% increase in the number of collectors required. These findings suggest that the parallel configuration not only enhances thermal performance but also offers a more cost-effective and efficient solution.

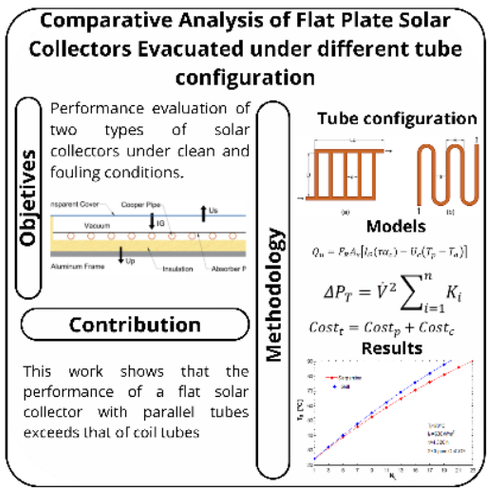

Evacuated Solar Collector, Parallel Tubes, Serpentine Tubes

Resumen

Este estudio evalúa el desempeño térmico de dos configuraciones de colectores solares planos evacuados: tipo serpentín y tipo paralelo, tanto en condiciones limpias como bajo ensuciamiento por incrustaciones de carbonato de calcio ($CaCO_3$). El objetivo es determinar cuál de las dos tecnologías ofrece mayor eficiencia y menor requerimiento de equipos para alcanzar una temperatura de salida de 90 °C. Los resultados muestran que los colectores en paralelo alcanzan una eficiencia térmica superior (0.80 frente a 0.76 del serpentín) y requieren menos unidades para lograr dicha temperatura. En presencia de incrustaciones, se necesitan 20 colectores en paralelo, comparados con 23 en configuración serpentín, lo que implica un aumento del 15 % en el número de colectores requeridos. Estos hallazgos sugieren que la configuración en paralelo no solo mejora el rendimiento térmico, sino que también representa una opción más rentable y eficiente.

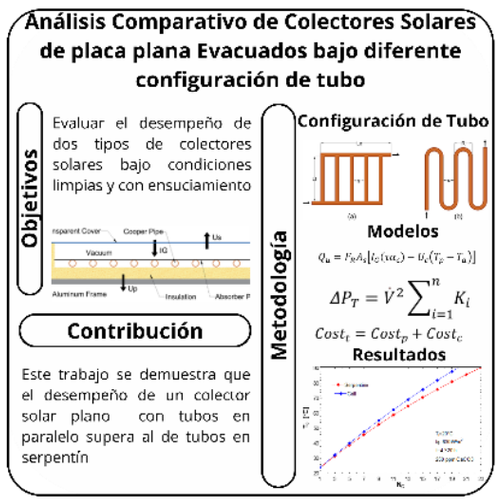

Colector Solar evacuado, tubos en Paralelo, Tubos en Serpentín

Area: Dissemination and universal access to science

Citation: Lugo-Granados, Hebert Gerardo, Canizalez-Dávalos, Lázaro and Picón-Núñez, Martín. [2025]. Análisis comparativo de colectores solares de placa plana evacuados bajo condiciones limpias y de ensuciamiento. Journal Renewable Energy. 9[21] 1-12: e10921112.

1. Introduction

The growing need to adopt renewable energy sources has driven the development of more efficient solar thermal technologies. Solar thermal energy offers a sustainable and effective means of generating heat for residential, commercial, and industrial applications. Among the most commonly used technologies are flat plate collectors (FPC) and evacuated tube collectors (ETC), both of which convert solar radiation into thermal energy with notable efficiency (Kalogirou, 2004).

In a comparative study, Ayompe et al. (2011) demonstrated that evacuated tube collectors outperform flat plate collectors in terms of efficiency. By combining both technologies, the evacuated flat plate collector (EFPC) emerges, harnessing the advantages of each type. However, despite their high efficiency, EFPCs are not yet widely available on the market. It is therefore necessary to explore new designs that enhance durability and performance, while reducing operational and investment costs (Kalair et al., 2022).

Beyond design considerations, the performance of these systems depends on factors such as materials, thermal fluid, operating conditions, and, crucially, the hydraulic flow configuration (Pandey et al., 2017). Whether configured as a coil or in parallel, the flow arrangement directly influences thermo-hydraulic performance.

Gao et al. (2020) developed a solar thermal system using optimised evacuated flat plate collectors designed to operate at medium temperatures. They achieved a peak thermal efficiency of 59.6% and an outlet temperature of 123 °C under solar irradiance of 835.2 W/m². Similarly, Hassan et al. (2023) evaluated an evacuated flat plate collector with spiral tubes, using a water-glycol mixture as the thermal fluid. Their system reached a maximum efficiency of 78% and temperatures of up to 98 °C. In another study, Deng and Zhao (2013) analysed a flat solar collector incorporating microchannels and heat-pipe tubes (MHPA-FPC), highlighting its rapid thermal response and effective temperature distribution. The system achieved an instantaneous peak efficiency of 80%. Numerous studies have examined the performance of solar collectors under various configurations and climatic conditions.

However, most have focused on ideal scenarios, without accounting for the impact of mineral scaling. It is therefore essential to assess the thermal, hydraulic, and economic behaviour of these systems under scaling conditions, to establish technical criteria for more robust and efficient designs.

Scaling is one of the principal challenges in the long-term operation of solar collectors, particularly in regions with high water hardness. The accumulation of mineral salts reduces thermal efficiency, increases pressure drop, and raises pumping costs (Bott, 1995). In recent years, Lugo Granados et al. (2023) demonstrated that reducing the free flow area by 40% significantly decreases scale formation without compromising thermal performance. Subsequently, Lugo Granados et al. (2024) evaluated the redesign of collector networks under scaling conditions, concluding that existing systems can be reconfigured using flow velocity as a key parameter to mitigate fouling.

To address these effects, several solutions have been proposed, including the use of water-glycol mixtures and nanofluids, which may enhance thermal efficiency by 5% to 35% compared to conventional fluids. However, their application presents limitations. Nanoparticle sedimentation can reduce heat transfer by up to 11%, increase viscosity, and lead to greater hydraulic losses (García-Rincón & Flores-Prieto, 2024). Although Bocanegra et al. (2025) highlight the improved optical and thermal properties of nanofluids, colloidal stability remains a challenge for long-term use. For instance, Deshmukh et al. (2025) reported an efficiency of up to 80.47% using titanium nitride (TiN) nanofluids and twisted tape inserts, but with a 64% increase in pressure drop and higher pumping requirements.

Box 1

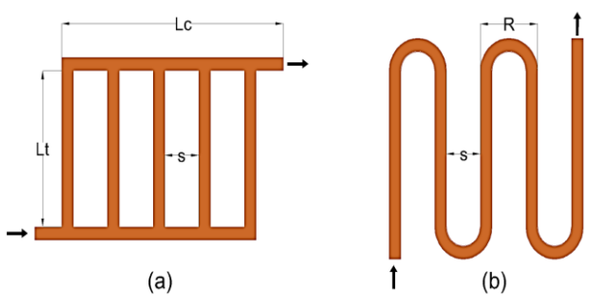

Figure 1
Internal tube layout within the solar collector: a) parallel configuration, b) spiral configuration
Source: Own Elaboration

ISSN: 2523-6881
RENIECYT-SECIHTI: 1702902

Lugo-Granados, Hebert Gerardo, Canizalez-Dávalos, Lázaro and Picón-Núñez, Martín. [2025]. Análisis comparativo de colectores solares de placa plana evacuados bajo condiciones limpias y de ensuciamiento. Journal Renewable Energy. 9[21] 1-12: e10921112.
https://doi.org/10.35429/JRE.2025.9.21.2.1.12

The use of nanofluids or water-glycol mixtures presents significant limitations, notably their high cost, which restricts their application in large-scale solar systems or in regions with limited resources. For these technical and economic reasons, this study focuses on the use of water as the thermal fluid, with particular emphasis on analysing scaling-related fouling which can lead to the development of cleaning strategies based on the prediction of scale formation over time. The objective of this work is to compare the performance of flat-plate solar collectors with evacuated tubes under two hydraulic configurations: serpentine and parallel (Figures 1 and 2). Both clean and fouled conditions are evaluated, considering key variables such as thermal efficiency, useful energy output, pressure drop, and operational costs. The results will help identify the most suitable configuration for environments with high water hardness and provide recommendations for implementing more efficient and sustainable solar thermal systems.

Box 2

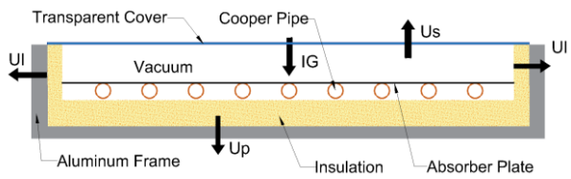

Figure 2
Evacuated flat-plate solar collector.
Source: Own Elaboration

2. Methodology

The methodology of this study aims to compare the thermal, hydraulic, and economic performance of two configurations of evacuated flat-plate solar collectors: one with tubes arranged in parallel, and the other featuring a serpentine-shaped tube. The analysis is conducted under clean conditions as well as considering the impact of scaling-related fouling.

2.1 Thermohydraulic Model:

Mathematical models were adapted to simulate the thermal and hydraulic behaviour of both configurations. These models incorporate parameters such as pressure drop, thermal efficiency, heat transfer coefficients, and head loss, following the approach proposed by Duffie & Beckman (2013).

The properties of the thermal fluid (water) and local climatic conditions were considered to represent realistic scenarios. The amount of useful heat Qu (W) absorbed by a solar collector depends on the incident solar radiation IG (W/m²), the cover transmittance (τ), the plate absorptance (α), and thermal losses, represented by the overall heat loss coefficient Uc (W/m²·°C) and the temperature difference between the absorber plate Tp (°C) and the ambient Ta (°C). This useful energy is adjusted by the heat removal factor (FR), which indicates how efficiently the heat is transferred to the fluid, and by the collector area, As (m²). This relationship is expressed in Equation (1):

$$Q_u = F_R A_s \left[I_G(\tau\alpha_c) - U_c\left(T_p - T_a\right) \right] \quad (1)$$

Figure 3 illustrates the thermal model representing the relationship between the absorber plate temperature T_{pm} (°C) and the ambient temperature T_a (°C). The overall heat loss coefficient U_C (W/m²°C) combines three components: the top loss coefficient U_s (W/m²°C), the back loss coefficient U_P (W/m²°C), and the side loss coefficient U_l (W/m²°C), as shown in Eq (2).

$$U_c = U_s + U_p + U_l \quad (2)$$

Heat loss from the top of the collector arises from convection and radiation between the absorber plate and the cover. The top loss coefficient (Us)is calculated as the inverse of the sum of two internal thermal resistances: R1 (°C/W) and R2 (W/m·°C), as shown in Equation (3).

The thermal resistance R1 (Equation 4) represents heat transfer between the absorber plate and the ambient, accounting for both convection (hc_{c-a}) and radiation (hr_{c-a}).

ISSN: 2523-6881
RENIECYT-SECIHTI: 1702902

Lugo-Granados, Hebert Gerardo, Canizalez-Dávalos, Lázaro and Picón-Núñez, Martín. [2025]. Análisis comparativo de colectores solares de placa plana evacuados bajo condiciones limpias y de ensuciamiento. Journal Renewable Energy. 9[21] 1-12: e10921112.
https://doi.org/10.35429/JRE.2025.9.21.2.1.12

Box 3

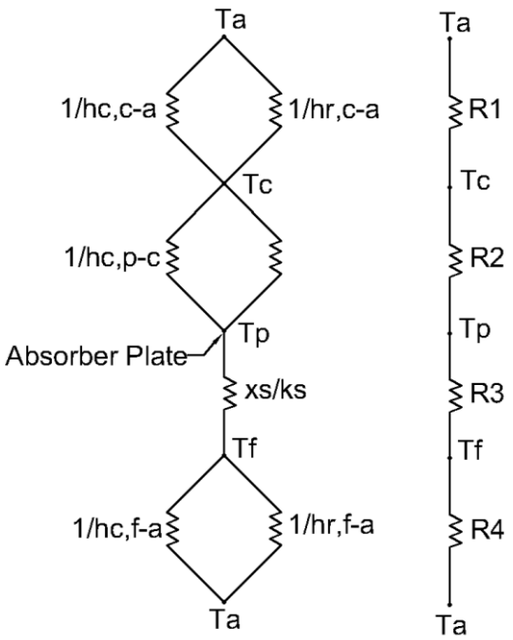

Figure 3
Heat transfer resistances within the solar collector.
Source: Own elaboration

In contrast, resistance R2 (Equation 5) corresponds to the space between the plate and the cover, where heat is transferred solely by radiation (hr_{p-c}), a characteristic feature of evacuated collectors.

$$U_s = \frac{1}{R_1+R_2} \quad (3)$$

$$R_1 = \frac{1}{hr_{c-a} + hc_{c-a}} \quad (4)$$

$$R_2 = \frac{1}{hr_{p-c}} \quad (5)$$

The back loss coefficient (U_p) depends on thermal resistances due to conduction through the insulation (R_3(°C/W)) and from combined convection and radiation (R_4 (°C/W)) between the backplate and the surroundings, Eq(6). As (R_4) is negligible compared to (R_3), its effect is typically ignored (Eq (8)). Here, ks (W/m °C) is the thermal conductivity and xs (m) is the thickness of the back insulation material.

$$U_p = \frac{1}{R_3+R_4} \quad (6)$$

$$R_3 = \frac{k_s}{x_s} \quad (7)$$

$$R_4 = \frac{1}{hr_{f-a} + hc_{f-a}} \quad (8)$$

The side heat loss coefficient (U_l) is derived considering one-dimensional thermal flux across the system perimeter and referenced to the total collector area (A_c), as shown in Eq(9). Where A_c is the collector surface area, x_l is the side insulation thickness, p and h are the perimeter and the height of the collector.

$$U_l = \left(\frac{k_s}{x_l}\right) \cdot \left(\frac{p\ h}{A_c}\right) \quad (9)$$

The heat removal factor (F_R) described in Eq(10), is a function of the mass flow rate $\dot{m}_f$ (kg/s), and the efficiency factor of the collector. The term F´ in Eq(11) is a function of the tube spacing S (m), the inner diameter di (m) and outer diameter do (m) of the tubes, and the resistance to heat transfer from the absorber plate to the working fluid. It also includes the resistance arising from convection between the inner tube wall and the working fluid Rh (m^2°C/W). The resistance due to the tube wall Rt (m^2°C/W) and the fouling layer resistance Rs (m^2°C/W). Cb (m^2°C/W) is the resistance caused by the tube/plate bond and is described in Eq(12).

$$F_{R,\theta} = \frac{\dot{m}_f Cp_f}{A_s U_c}\left[1 - e^{\frac{-A_s U_c F'}{\dot{m}_f Cp_f}}\right] \quad (10)$$

$$F' = \frac{1/U_c}{S\left[\frac{1}{U_c[d_0 + F_A(S-d_0)]} + \frac{1}{C_b} + \frac{R_h}{\pi d_s} + \frac{R_t}{\pi d_s} + \frac{R_s}{\pi d_s}\right]} \quad (11)$$

$$C_{b,\theta} = k_b W/\gamma \quad (12)$$

Where k_b (W/m °C) is the thermal conductivity of the junction, W (m) is the width, and γ (m) is the thickness of the junction between the plate and the tube. Eq(13) is described by the hydraulic diameter ds (m), and x_f (m) is the thickness of the scaling layer.

$$d_s = d_i - 2x_f \quad (13)$$

Additionally, F´ depends on the thermal efficiency of the metal fin (F_A) as given by Eq(14).

$$F_A = \frac{Tanh[M_\theta(S-d_0)/2]}{M_\theta(S-d_0)/2} \quad (14)$$

$$M_\theta = \sqrt{(U_{c,\theta}/(k_{p,\theta})\delta)} \quad (15)$$

ISSN: 2523-6881
RENIECYT-SECIHTI: 1702902

Lugo-Granados, Hebert Gerardo, Canizalez-Dávalos, Lázaro and Picón-Núñez, Martín. [2025]. Análisis comparativo de colectores solares de placa plana evacuados bajo condiciones limpias y de ensuciamiento. Journal Renewable Energy. 9[21] 1-12: e10921112.
https://doi.org/10.35429/JRE.2025.9.21.2.1.12

The terms k_p (W/m°C) and δ (m) represent the thermal conductivity and plate thickness, respectively and the parameter M (m^{-1}), is defined in Eq(15). The overall efficiency (η_f) can be evaluated from Eq(16):

$$\eta_f = \frac{\dot{Q}_u}{I_G A_s} \tag{16}$$

From Equation (17), we can determine the pressure drop within the collector network, which is proportional to the sum of hydraulic resistances K_i (kPa s^2/m^6) and the square of volumetric flow rate $\dot{V}$ (m^3/s).+

$$\Delta P_T = \dot{V}^2 \sum_{i=1}^{n} K_i \tag{17}$$

Equations (18) and (19) represent the main sources of hydraulic resistance. The frictional term, K1 (kPa·s^2/m^6), accounts for pressure losses along the pipe length, while K2 (kPa·s^2/m^6) reflects additional losses caused by fittings such as elbows and valves. Fouling introduces thermal resistance, which in turn affects the overall hydraulic behaviour of the system.

$$K_1 = \frac{8 L_t}{\pi^2 {d_s}^5} f \tag{18}$$

$$K_2 = \frac{8\rho}{\pi^2 {d_s}^5} k_f \tag{19}$$

Here, f denotes the friction factor associated with flow along the pipe, and k_f represents the resistance coefficient for individual fittings. L_t (m) and ds (m) refer to the tube's length and hydraulic diameter, respectively. A reduction in diameter results in greater flow resistance, which in turn causes a higher pressure drop.

2.2 Scaling Simulation

The model proposed by Lugo-Granados and Picón-Núñez (2018) was employed to predict the accumulation of mineral deposits ($CaCO_3$) on the inner walls of the tubes. These deposits affect both the thermal conductivity and the effective flow cross-section. The model is based on prior experimental data obtained from systems operating with hard water, and it enables an assessment of how scaling influences the thermal and hydraulic performance of solar collectors, as shown in Equation (20).

$$\dot{m}_d = \frac{\beta}{2}\left(\frac{\beta}{\alpha k_r} + (C_1 + C_2) - \sqrt{\frac{[\beta + (C_1 + C_2)\,\alpha k_r]^2 + 4\,\alpha^2 {k_r}^2 (K_{sp} - [C_1][C_2])}{\alpha^2 {k_r}^2}}\right) \tag{20}$$

The model calculates the mass flow rate of calcium carbonate deposition, $\dot{m}_d$ (kg/m²·s), within the tubes, based on the key factors that influence scaling. These include the pH of the fluid, the concentrations of calcium ions (Ca^{2+}, denoted as C_1 in kg/m³) and carbonate ions (CO_3^{2-}, denoted as C_2 in kg/m³), as well as the solubility product (K_{sp}) (kg²/m⁶) for $CaCO_3$ in water. Design variables are also considered. Temperature plays a central role, as it affects the rate of the chemical reaction responsible for crystal formation, which is governed by the reaction rate constant k_r (m²/kg·s). Fluid velocity is another important factor, influencing the rate of deposition through the mass transfer coefficient β (m/s).

The deposition resistance factor α, introduced in Equation (21), is a dimensionless quantity that reflects the influence of viscous and inertial stresses on the adherence of crystals to the surface. This factor was determined from published experimental data. As scaling progresses, it alters the internal surface of the tubes, roughness increases and the effective diameter decreases, leading to a higher pressure drop across the system.

$$\alpha = \frac{191}{f \cdot Re^{1.67}} \tag{21}$$

The thermal resistance due to fouling, Rs (m²·°C/W), depends on the mass flux of calcium carbonate deposited on the tube surfaces, $\dot{m}_d$, and the rate at which it is removed, $\dot{m}_r$ (kg/m²·s). It also incorporates the density of the deposit, ρ_f (kg/m³), and its thermal conductivity, λ_f (W/m·°C), as expressed in Equation (22).

$$\frac{dR_s}{dt} = \frac{\dot{m}_d - \dot{m}_r}{\rho_f \lambda_f} \tag{22}$$

The thickness generated by scaling can be determined to by Eq(23).

$$x_f = R_s \lambda_f \tag{23}$$

An economic analysis was carried out considering the following aspects:

ISSN: 2523-6881
RENIECYT-SECIHTI: 1702902

Lugo-Granados, Hebert Gerardo, Canizalez-Dávalos, Lázaro and Picón-Núñez, Martín. [2025]. Análisis comparativo de colectores solares de placa plana evacuados bajo condiciones limpias y de ensuciamiento. Journal Renewable Energy. 9[21] 1-12: e10921112.
https://doi.org/10.35429/JRE.2025.9.21.2.1.12

- Initial costs for both models, including equipment procurement.
- Energy consumption associated with the pumping systems, which is directly affected by the increase in pressure drop.

This approach allows for a comparison not only of thermal and hydraulic performance, but also of the economic and operational feasibility of each collector type. It provides clear criteria for selecting the most suitable option based on the intended application and the quality of the available water.

The total operating cost, $Cost_{total}$ (USD), is obtained by adding the pumping costs, $Cost_p$ (USD), to the annualised cost of the collectors, $Cost_c$ (USD), as indicated in Equation (24). This cost breakdown offers a clearer view of the economic factors involved in running solar thermal systems.

$$Cost_{total} = Cost_p + Cost_c \quad (24)$$

Equation (25) defines the operating cost of the pump, $Cost_p$, which is directly proportional to the unit cost of electricity $Cost_u$, the pumping power $\dot{w}$, and the operating time t, the duration required to reach the target temperature. In this study, the unit cost of electricity is taken as \$0.30 USD/kWh.

$$Cost_p = cost_u \dot{w}\, t \quad (25)$$

The pumping power $\dot{w}$is calculated using Equation (26), based on the pressure drop across the system. It is defined as the product of the volumetric flow rate $\dot{V}$ (m³/s) and the pressure drop ΔP (kPa), divided by the pump efficiency η_b:

$$\dot{w} = \frac{\dot{V}\,\Delta P}{\eta_b} \quad (26)$$

The annualised cost of the collectors, $Cost_c$, is given by Equation (27). It is calculated as the product of the unit cost per collector C_u (USD), the annualization factor Fa, and the total number of collectors Nc. The commercial cost per collector is estimated at \$811.76 USD. To determine the annualization factor Fa, Equation (28) is used. It considers a collector lifespan ω of 20 years and an annual interest rate $\imath$ of 10%:

$$Cost_c = C_u \cdot Fa \cdot N_c \quad (27)$$

$$F_a = \left[\frac{\imath(1+\imath)^{\omega}}{(1+\imath)^{\omega}-1}\right] \quad (28)$$

The simulations assessed the thermohydraulic performance as a function of the number of solar collectors, considering two configurations: flat-plate collectors with parallel tubes and flat-plate collectors with a spiral tube. The system operated under the following conditions:

- Irradiance: 630 W/m²
- Inlet temperature: 20 °C
- Flow rate: 4 L/min
- Water hardness: 250 ppm as $CaCO_3$

A thermal network was designed to reach an outlet temperature of 90 °C. System behaviour was analysed under both clean conditions and after scaling due to mineral deposits, following 4,320 hours of continuous operation.

3.1 Comparison between Collector Configurations

At this stage, the number of collectors required to reach the target temperature was determined. From that point onward, the two configurations (parallel tubes and spiral tube) were compared in terms of thermal efficiency, useful energy transfer, pressure drop, and operating costs.

Box 4

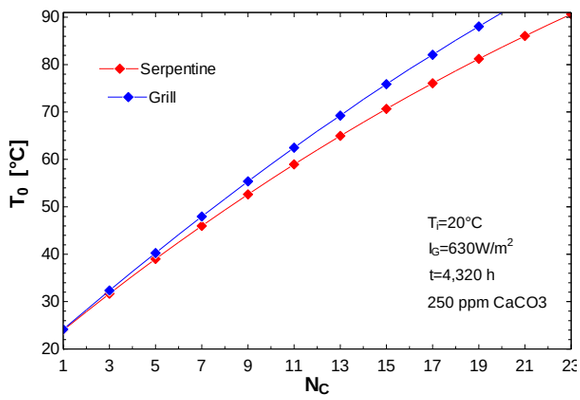

Figure 4

Outlet temperature as a function of the number of collectors for parallel and spiral configurations

Source: Own Elaboration

ISSN: 2523-6881
RENIECYT-SECIHTI: 1702902

Lugo-Granados, Hebert Gerardo, Canizalez-Dávalos, Lázaro and Picón-Núñez, Martín. [2025]. Análisis comparativo de colectores solares de placa plana evacuados bajo condiciones limpias y de ensuciamiento. Journal Renewable Energy. 9[21] 1-12: e10921112.
https://doi.org/10.35429/JRE.2025.9.21.2.1.12

Figure 4 illustrates the number of collectors required to reach an outlet temperature of 90 °C under extended operating conditions and in the presence of $CaCO_3$ scaling.

The results show that the parallel-tube configuration requires 20 collectors, whereas the spiral-tube design needs 23 to achieve the same target. This reflects a 13% improvement in efficiency for the parallel arrangement, as fewer collectors are needed. The difference implies lower capital costs, and reduced demands on the pumping system.

Box 5

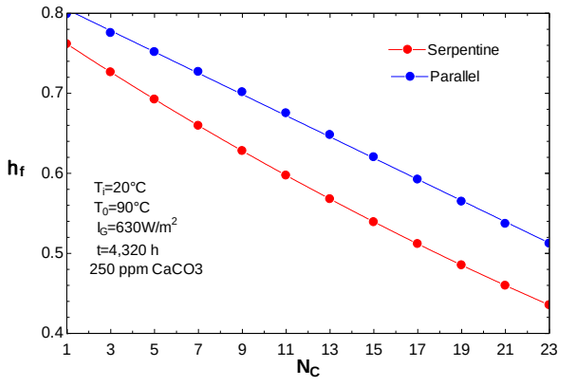

Figure 5

Thermal efficiency as a function of the number of installed solar collectors

Source: Own Elaboration

Figure 5 shows how thermal efficiency varies with the number of solar collectors for the two configurations: parallel tubes and spiral tubes.

With a single collector, the parallel-tube setup reaches an efficiency of 0.80, while the spiral-tube design achieves 0.76. However, as the number of collectors increases to 20, both efficiencies decline due to greater thermal losses and the cumulative effect of fouling.

At that point, efficiency drops to 0.55 for the parallel arrangement and to 0.48 for the spiral configuration—corresponding to reductions of 31.25% and 36.84%, respectively. Moreover, at the upper end of the range, the parallel configuration maintains an efficiency approximately 14.6% higher than that of the spiral design. This suggests that the parallel layout not only performs better initially but also retains superior efficiency as the system scales.

Box 6

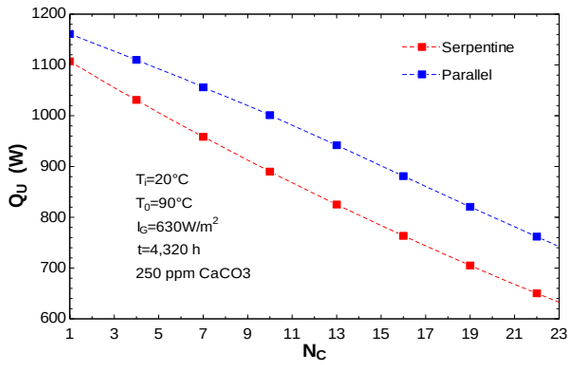

Figure 6

Comparison of thermal load according to the number of solar collectors

Source: Own Elaboration

Figure 6 illustrates the relationship between thermal load and the number of solar collectors for two configurations. Although thermal load decreases linearly with the number of collectors in both cases, the parallel-tube configuration consistently delivers better thermal performance.

As shown in the graph, the parallel collectors (blue line) outperform the spiral ones (red line), with the gap widening as the system grows. For instance, with two collectors, the parallel setup delivers approximately 70 W more than the spiral, representing a 7.14% improvement. With eight collectors, the difference increases to 100 W, equivalent to a 10.6% gain in thermal load.

This trend suggests that the parallel design is not only more efficient under extended operating conditions and calcium carbonate fouling, but its advantage becomes increasingly pronounced as the collector network expands.

Box 7

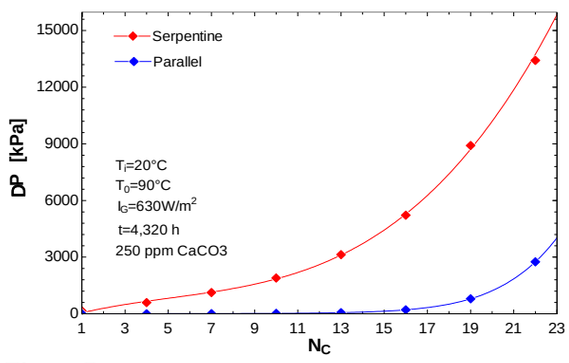

Figure 7

Variation in pressure drop with respect to the number of collectors in both configurations

Source: Own elaboration

ISSN: 2523-6881
RENIECYT-SECIHTI: 1702902

Lugo-Granados, Hebert Gerardo, Canizalez-Dávalos, Lázaro and Picón-Núñez, Martín. [2025]. Análisis comparativo de colectores solares de placa plana evacuados bajo condiciones limpias y de ensuciamiento. Journal Renewable Energy. 9[21] 1-12: e10921112.
https://doi.org/10.35429/JRE.2025.9.21.2.1.12

Figure 7 shows how pressure drop varies with the number of connected solar collectors. As more collectors are added, the pressure drop increases due to the longer fluid path and greater frictional losses.

A clear distinction emerges between the two configurations. Collectors with spiral tubes (red line) exhibit significantly higher pressure losses compared to those with parallel tubes (blue line). For instance, with 20 collectors, the pressure drop in the spiral arrangement reaches approximately 11,000 kPa, whereas the parallel setup registers only 1,000 kPa, a reduction of 90.9% when opting for the parallel configuration.

Figure 8 presents the system cost as a function of the number of collectors. Like the pressure drop, total cost rises with the number of units, as both parameters are closely linked.

For example, with 20 collectors, the estimated cost for the spiral configuration is $500, while the parallel arrangement amounts to just $100. This translates into a cost saving of 83.3% when choosing the parallel-tube design.

Box 8

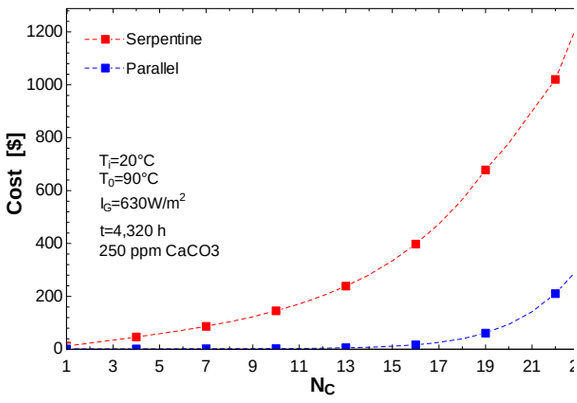

Figure 8

Cost comparison based on the number of connected collectors for each technology

Source: Own Elaboration

2.2 Comparison under Clean and Fouled Conditions

This section presents the results of the analysis for four solar collector configurations:

1. Spiral arrangement with 23 collectors under clean conditions (23s_S(NF))
2. Spiral arrangement with 23 collectors affected by fouling (23s_S(F))
3. Parallel arrangement with 20 collectors under clean conditions (20s_G(NF))
4. Parallel arrangement with 20 collectors affected by fouling (20s_G(F))

These configurations allow for a comparative assessment of thermal performance and system efficiency under varying operational conditions.

Box 9

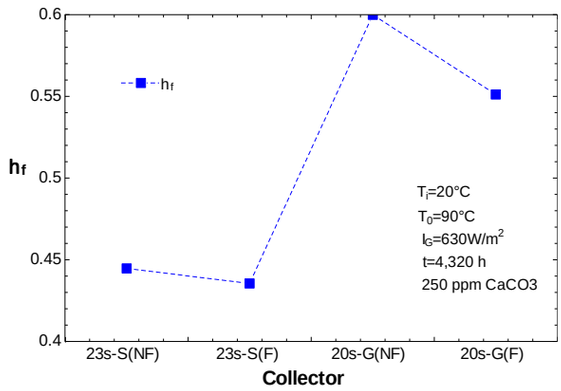

Figure 9

Efficiency comparison by collector type, under clean and scaled conditions

Source: Own Elaboration

From a thermal standpoint (Figure 9), the parallel configuration demonstrates higher efficiency in reaching the target temperature of 90 °C. Under clean conditions, spiral collectors reach an efficiency of 0.44, whereas the parallel arrangement achieves 0.60, an improvement of 36.4%. Although both configurations experience efficiency losses due to scaling, the impact is notably more severe in the spiral design.

Box 10

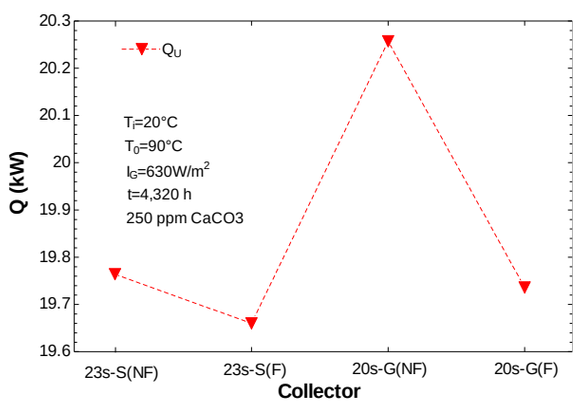

Figure 10

Instantaneous thermal load by collector type, under clean and scaled conditions.

Source: Own Elaboration

ISSN: 2523-6881
RENIECYT-SECIHTI: 1702902

Lugo-Granados, Hebert Gerardo, Canizalez-Dávalos, Lázaro and Picón-Núñez, Martín. [2025]. Análisis comparativo de colectores solares de placa plana evacuados bajo condiciones limpias y de ensuciamiento. Journal Renewable Energy. 9[21] 1-12: e10921112.
https://doi.org/10.35429/JRE.2025.9.21.2.1.12

Figure 10 presents the results for instantaneous thermal load, which follow the same trend observed in efficiency. The clean spiral setup (23s_S(NF)) delivers 19.78 kW, dropping slightly to 19.67 kW with fouling (23s_S(F)). In contrast, the clean parallel configuration (20s_G(NF)) reaches 20.25 kW, decreasing to 19.75 kW under fouled conditions (20s_G(F)). These results confirm that hydraulic design directly influences the recovery of useful energy, and that the parallel configuration is more resilient to the effects of scaling.

Box 11

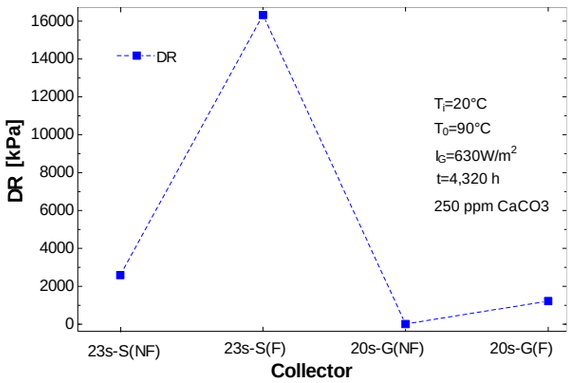

Figure 11

Pressure drop comparison by collector type, with and without scaling

Source: Own Elaboration

Figure 11 compares pressure drop (ΔP) across collector types, with and without fouling. In the clean spiral setup (23s_S(NF)), the pressure drop is 2,600 kPa, rising sharply to 16,000 kPa with scaling (23s_S(F)), a 515% increase. The parallel configuration shows much lower values: 300 kPa under clean conditions (20s_G(NF)) and 1,200 kPa when fouled (20s_G(F)), representing a 300% increase. This contrast highlights the hydraulic advantages of parallel design, particularly in scenarios involving mineral deposit accumulation.

Finally, Figure 12 presents the operating costs associated with both configurations. These follow a similar trend to the pressure drop, as pump energy consumption is directly linked to hydraulic resistance. In the presence of scaling (F), costs rise significantly. For the parallel setup (20s_G), the increase is 196%, while for the spiral configuration (23s_S), it reaches 500%.

Box 12

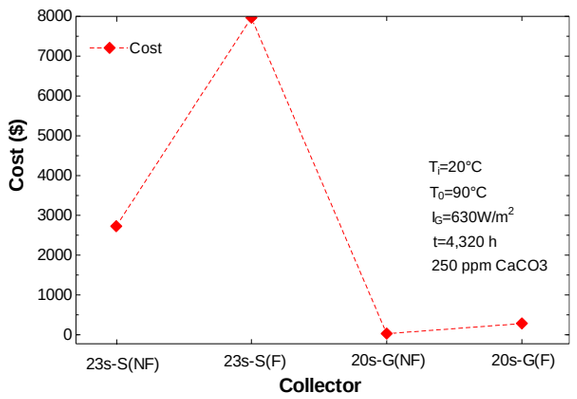

Figure 12

Cost comparison by collector type, with and without scaling

Source: Own Elaboration

Despite the percentage increase in operating costs due to scaling, collectors with parallel-tube configuration maintain significantly lower overall costs. Under clean conditions, the savings exceed $2,500, and in the presence of fouling, they can reach up to $7,500. This positions them as a more cost-effective and efficient alternative, both hydraulically and energetically.

3. Conclusions

The results of this study demonstrate that the evacuated flat-plate solar collector with parallel-tube configuration offers superior performance in terms of thermal efficiency, hydraulic behaviour, and operating costs when compared to the spiral-tube design. This technology performs reliably at low and medium temperatures and retains its efficiency even under scaling conditions, making it well-suited for long-term, real-world applications.

Its favourable performance is attributed to the multi-path parallel design, which promotes better fluid distribution and lower pressure drop, thereby enhancing heat transfer even under adverse conditions. In contrast, spiral configurations, with a single extended flow path, exhibit higher hydraulic resistance and are more vulnerable to performance losses due to scaling. For prolonged operation and in environments with high water hardness, the parallel-tube layout proves to be more efficient and dependable. Moreover, the higher thermal efficiency of the parallel design allows energy targets to be met with fewer modules, resulting reduced capital investment, and lower pumping requirements.

ISSN: 2523-6881
RENIECYT-SECIHTI: 1702902

Lugo-Granados, Hebert Gerardo, Canizalez-Dávalos, Lázaro and Picón-Núñez, Martín. [2025]. Análisis comparativo de colectores solares de placa plana evacuados bajo condiciones limpias y de ensuciamiento. Journal Renewable Energy. 9[21] 1-12: e10921112.
https://doi.org/10.35429/JRE.2025.9.21.2.1.12

The comparative analysis of spiral and parallel solar collector configurations, under both clean and scaled conditions (250 ppm $CaCO_3$), leads to the following specific conclusions:

- **Thermal Performance:** The parallel configuration without scaling (23s-G(NF)) achieved the highest thermal efficiency and useful load, reaching 20.25 kW, outperforming the spiral designs. Although scaling affected both configurations, the impact was more pronounced in the spiral collectors.

- **Hydraulic Performance:** Marked differences in pressure drop were observed. Spiral collectors reached up to 16,000 kPa under scaled conditions, a 515% increase compared to their clean state. In contrast, parallel collectors showed a much lower pressure drop (1,200 kPa), even with fouling, indicating a more favourable hydraulic response.

- **Economic Performance:** Operating cost variations were directly linked to pressure drop. Under scaling conditions, the spiral configuration's operating cost increased by up to 500%, while the parallel setup exhibit a rise of 196%. Nevertheless, parallel collectors maintained the lowest costs in both scenarios.

In summary, solar collectors with parallel-tube configuration offer clear advantages in thermal efficiency, hydraulic behaviour, and operating costs, even under scaling conditions. Their design supports better fluid distribution and reduced resistance, making them a more reliable and cost-effective option for extended use. Their implementation is recommended in settings with high water hardness, where spiral configurations face significant operational limitations.

Technical Recommendation

This study confirms that parallel-tube solar collectors provide notable benefits in thermal, hydraulic, and economic terms. They exhibit lower sensitivity to fouling and maintain stable, efficient performance over time.

For this reason, their use is advised in long-duration applications and in conditions prone to scaling. Additionally, the adoption of preventive cleaning schemes is recommended to preserve system performance.

Declarations

Conflict of interest

The authors declare no interest conflict. They have no known competing financial interests or personal relationships that could have appeared to influence the article reported in this article.

Author contribution

Lugo-Granados, Hebert Gerardo: Contributed to the research methodology and generation of results and writing of the manuscript.

Canizalez-Dávalos, Lázaro: Contributed to the research method and revision of the manuscript.

Picón-Núñez, Martín: Contributed to the project idea, research method, editing and revising of the manuscript.

Funding

This work has been funded by SECIHTI [grant number 2466286,487049].

Abbreviations

A_c	Collector area 2.506 (m^2)
A_s	Plate area (m^2)
C_1	Ca^{2+} concentration(kg/m^3),
C_2	CO_3^{2-} concentration(kg/m^3)
C_b	Thermal resistance between tube and plate (m^2 °C/W)
$Cost_a$	Annualised cost of solar collector ($/year)
$Cost_b$	Operating cost ($)
$Cost_t$	Total operating cost ($)
$cost_u$	Unit cost of electricity ($/kwh)
Cp	Water heat capacity (kJ/kg °C)
C_u	Commercial cost of a solar collector ($811.76 dollars)
d_0	Collector tube outer diameter (m).
d_i	Collector tube inner diameter (m)
d_s	Hydraulic diameter (m)
f	Friction factor
$F´$	Collector efficiency factor
F_A	Metal fin thermal efficiency
Ƒa	Annualization factor
F_R	Heat removal factor

ISSN: 2523-6881
RENIECYT-SECIHTI: 1702902

Lugo-Granados, Hebert Gerardo, Canizalez-Dávalos, Lázaro and Picón-Núñez, Martín. [2025]. Análisis comparativo de colectores solares de placa plana evacuados bajo condiciones limpias y de ensuciamiento. Journal Renewable Energy. 9[21] 1-12: e10921112.
https://doi.org/10.35429/JRE.2025.9.21.2.1.12

i	Interest rate (8%)
I_G	Solar radiation (W/m^2)
K_1	Friction resistance (kPa s^2/m^6)
K_2	Hydraulic resistance due to connections (kPa s^2/m^6)
k_b	Thermal conductivity (W/m °C)
k_r	Reaction constant (m^2/kg s)
k_f	Resistance factor
K_s	Thermal conductivity of plate (W/m °C)
K_{sp}	$CaCO_3$ solubility (kg^2/m^6)
L_t	Tube length (m)
$\dot{m}_d$	Mass flux (kg/m^2 s)
$\dot{m}_f$	Mass flow rate (kg/s)
$\dot{m}_r$	Mass flux removed (kg/m^2 s
Nc	Total number of collectors
Q	Process thermal load
Q_u	Useful heat (kW)
Q_T	Total heat load (kW)
Re	Reynolds number
R_h	Thermal resistance due to convection (m^2 °C/W)
R_s	Thermal resistance due to fouling (m^2 °C/W)
R_t	Thermal resistance due to conduction (m2 °C/W),
S	Distance between tubes (m)|
t	Operating time (h).
T_0	Outlet temperature (°C)
T_a	Ambient temperature (°C)
T_i	Inlet temperature (°C)
T_{pm}	Plate temperature (°C)
U_c	Overall heat transfer coefficient of losses (W/m^2°C)
W	Width (m)
x_f	Fouling layer thickness (m)
$\dot{V}$	Volumetric flow rate (m^3/s)
ΔP	Pressure drop (kPa)
$\dot{w}$	Pumping power
α	Deposition resistance factor
α_c	Plate absorbance
β	Mass transfer coefficient (m/s)
γ	Thickness between plate and tube (m)
δ	Plate thickness (m)
η_f	Collector thermal efficiency
η_b	Pump efficiency
ï	Annual interest rate
Λf	Thermal conductivity of $CaCO_3$ (W/m °C)
ρ	Density of water (kg/m^3)
ρf	Density of $CaCO_3$ (kg/m^3)
τ	Cover transmittance
ω	Collector lifespan of 20 years

References

Antecedents

Ayompe, L. M., Duffy, A., McCormack, S. J., McKeever, M., & Conlon, M. [2011]. Comparative field performance study of flat plate and heat pipe evacuated tube collectors (ETCs) for domestic water heating systems in a temperate climate. Energy. 3370–3378.

Kalair, A. R., Seyedmahmoudian, M., Saleem, M. S., Abas, N., Rauf, S., & Stojcevski, A. [2022]. A comparative thermal performance assessment of various solar collectors for domestic water heating. International Journal of Photoenergy. 9536772.

Kalogirou, S. A. [2004]. Solar thermal collectors and applications. Progress in Energy and Combustion Science. 231–295.

Basics

Deng, Y., & Zhao, Y. [2013]. Experimental investigation of performance for the novel flat-plate solar collector with micro-channel heat pipe array (MHPA-FPC). Applied Thermal Engineering. 440–449.

Gao, D., Gao, G., Cao, J., Zhong, S., Ren, X., Dabwan, Y. N., Hu, M., Jiao, D., Kwan, T. H., & Pei, G. [2020]. Experimental and numerical analysis of an efficiently optimized evacuated flat plate solar collector under medium temperature. Applied Energy. 115129.

Hassan, Z., Mahmood, M., Ahmed, N., Saeed, M. H., Khan, R., Abbas, M. M., Kalam, M. A., Almomani, F., & Abdelsalam, E. [2023]. Techno-economic assessment of evacuated flat-plate solar collector system for industrial process heat. Energy Science & Engineering. 2185–2201.

Pandey, K. M., & Chaurasiya, R. [2017]. A review on analysis and development of solar flat plate collector. Renewable and Sustainable Energy Reviews. 641–650.

Supports

Bott, T. R. (1995). Fouling of heat exchangers. Elsevier. Chemical Engineering Monographs. 97-135.

ISSN: 2523-6881
RENIECYT-SECIHTI: 1702902

Lugo-Granados, Hebert Gerardo, Canizalez-Dávalos, Lázaro and Picón-Núñez, Martín. [2025]. Análisis comparativo de colectores solares de placa plana evacuados bajo condiciones limpias y de ensuciamiento. Journal Renewable Energy. 9[21] 1-12: e10921112.
https://doi.org/10.35429/JRE.2025.9.21.2.1.12

Duffie, J. A., & Beckman, W. A. [2013]. Solar engineering of thermal processes. 4th edition. Wiley. 236-319.

Lugo-Granados, H., Picón Núñez M. [2018]. Modelling scaling growth in heat transfer surfaces and its application on the design of heat exchangers. Energy, 845-854.

Lugo-Granados, H. G., Canizalez-Dávalos L., Picón-Núñez Martín. [2023]. Thermohydraulic effects of scaling in flat plate solar collector networks. Chemical Engineering Transactions, 103, 421–426.

Lugo-Granados H. G., Picón-Núñez M., Canizalez-Dávalos L. [2024]. Flat plate solar collector networks: Design and retrofit considering fouling effects. Thermal Science and Engineering Progress. 102633.

Discussions

Bocanegra, J. A., Marchitto, A., & Misale, M. [2025]. Nanofluids in solar collectors: A comprehensive review focused on its sedimentation. Clean Technologies and Environmental Policy. 1753–1784.

Deshmukh, K. Bhausaheb, Nehe, S., Sargar, T., Benschwartz, R., Varkute, N., Vengadesan, E. and Karmare, S. [2025]. Heat Transfer, Friction Factor, and Performance Evaluation of U-Pipe Evacuated Tube Solar Thermal Collector with TiN Nanofluid and Twisted Tape Inserts. Journal of Renewable Energy and Environment. 40-59.

García-Rincón, M. A. & Flores-Prieto, J. J., [2024]. Nanofluids stability in flat-plate solar collectors: A review. Solar Energy Materials and Solar Cells. 112832.

ISSN: 2523-6881
RENIECYT-SECIHTI: 1702902

Lugo-Granados, Hebert Gerardo, Canizalez-Dávalos, Lázaro and Picón-Núñez, Martín. [2025]. Análisis comparativo de colectores solares de placa plana evacuados bajo condiciones limpias y de ensuciamiento. Journal Renewable Energy. 9[21] 1-12: e10921112.
https://doi.org/10.35429/JRE.2025.9.21.2.1.12

Journal Renewable Energy 9[21]1-11: e30921111
Article

Sizing parabolic trough solar thermal collector networks for Industrial Application – Case study

Dimensionamiento de redes termo solares de colectores parabólicos en aplicación Industrial – Caso de estudio

Lizárraga-Morazán, Juan-Ramón[a] & Picón-Núñez, Martín*[b]

[a] Universidad de Guanajuato • KXB-6991-2024 0000-0002-7733-5621 • 83138
[b] Universidad de Guanajuato • AHA-5481-2022 0000-0002-0793-192X • 12408

SECIHTI classification:

Area: Engineering
Field: Engineering
Discipline: Energy engineering
Subdiscipline: Solar energy

https://doi.org/10.35429/JRE.2025.9.21.3.1.11
Article History:
Received: June 20, 205
Accepted: December 10, 2025

* ✉ [picon@ugto.mx]

Abstract

Most studies currently available in the open literature on solar thermal network designs using parabolic trough collector (PTC) technology are highly specific and complex, making them difficult to apply for initial design assessments. This work proposes a simple and broadly applicable design methodology based on previously optimised networks. It enables the determination of the required surface area as a function of inlet temperature, the thermal load and temperature required by the process, and the solar fraction. Simple polynomial correlations between design variables are identified, validated with information from operating networks reported in open literature. An example application in an existing solar thermal plant is also presented. Comparing the results with operating systems shows that the proposed model yields network areas that are 40% to 81% smaller, while achieving solar fractions in the range of 1 to 1.2.

Resumen

Los estudios reportados hasta ahora en la literatura abierta sobre diseños de redes termo solares que operan con tecnología de concentradores de canal parabólico (PTC) resultan específicos y complejos, lo que dificulta su aplicación para una primera aproximación. En este trabajo se propone una metodología sencilla de diseño de amplia aplicación, basada en redes previamente optimizadas para la determinación del área superficial requerida como una función de la temperatura de entrada, de la temperatura y carga térmica requeridas por el proceso y la fracción solar. Se identifican correlaciones polinómicas sencillas entre variables de diseño, validadas con información de redes en operación reportadas en literatura abierta. Además, se desarrolla un ejemplo de aplicación en una planta termo solar existente. La comparación de los resultados con sistemas existentes en operación muestra que el modelo reporta redes con áreas menores entre un 40 y 81 %, cumpliendo con fracciones solares en el intervalo de 1 a 1.2.

Sizing Parabolic Trough Solar Thermal Collector Networks for Industrial Application – Case Study

Objectives	Methodology	Contribution
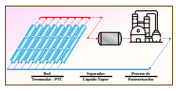	$Max\ Z = \left[\frac{PVLCES}{A}\right]$ s.t. $h(x) = 0$ $g(x) \leq 0$	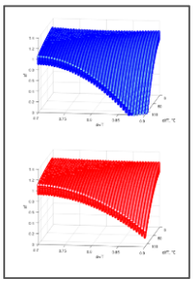

Dimensionamiento de Redes Termo Solares de Colectores Parabólicos en Aplicación Industrial – Caso de Estudio

Objetivos	Metodología	Contribución
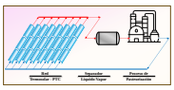	$Max\ Z = \left[\frac{PVLCES}{A}\right]$ s.t. $h(x) = 0$ $g(x) \leq 0$	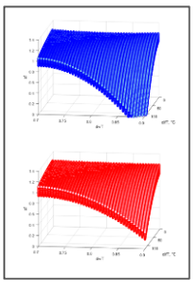

Solar, Fracción, Optimización, Energía, Industriales, Procesos.

Solar, fraction, optimization, Heat, Industrial, Processes

Area: Development of strategic leading-edge technologies and open innovation for social transformation

Citation: Lizárraga-Morazán, Juan-Ramón & Picón-Núñez, Martín. [2025]. Incorporation of Zinc Oxide Nanoparticles in Ceramic Materials. Sizing parabolic trough solar thermal collector networks for Industrial Application – Case study. Journal Renewable Energy. 9[21] 1-11: e30921111.

Introduction

The use of clean energy is becoming increasingly urgent. Fossil fuels have harmful effects on the environment and human health, and their prices continue to rise due to the costs of extraction (Khoo & Tan, 2006) and geopolitical events—such as conflicts in the Middle East—that create uncertainty in global supply and distribution. Solar energy stands out as one of the most promising options in the transition to clean energy, with the potential to meet up to 3,500 times the total energy demand projected for humanity in the year 2050 (IEA, 2018).

The industrial sector consumes between 32% to 35% of the total energy generated worldwide (IRENA, 2024). The thermal demand of industrial processes can be met by solar thermal systems known as SHIP (Solar Heat for Industrial Processes) which include technologies such as flat plate solar collectors (FPC), evacuated tube collectors (ETC), parabolic troughs (PTC), and compound parabolic concentrators (CPC) (Ituna-Yudonago et al., 2025). Among these, the most used technology today is the PTC type, representing 90% of the installed SHIP systems worldwide (REN21, 2023). Due to its high operational flexibility, with a wide temperature range from 50 to 400 °C (Kalogirou, 2009), the PTC collector offers opportunities in industrial heating, desalination, and hybrid energy systems (Mondal & Maji, 2025).

Optimisation is a tool commonly used in the design of equipment such as solar energy collectors and solar thermal networks. Some studies have proposed improvements to the internal design of solar energy collection systems. Rabienataj et al., 2025 conducted an optimisation study to determine the best geometry for receiver tubes, enhancing thermal performance using neural networks and numerical simulations. Yin et al., 2024 analyzed various configurations of the PTC collector, considering optical, economic, and thermodynamic factors. They concluded that a width of 8.2 m and a receiver tube diameter of 90 mm are the recommended design dimensions. Shaikh & Modi, 2025 proposed a hybrid solar plant combining PTC technology and Linear Fresnel Reflectors, with two thermal storage tanks to generate electricity via a Rankine steam power cycle.

The optimisation included a thermo-economic factor through parametric analysis. It minimised the levelized cost of electricity (LCOE). Their analysis increased the plant's capacity factor by 70% and reduced the LCOE by 20% compared to a conventional plant. Zeng et al., 2025 designed a Combined Cooling, Heating, and Power (CCHP) system powered by solar energy with thermal storage, to meet the energy demand of a 1000 m² building throughout the year.

The researchers improved efficiency by optimising inlet conditions and ammonia concentration before the turbine, achieving economic savings of up to $23,600 USD annually. Naaim et al., 2025 carried out an optimisation study in PTC systems using Monte Carlo Raytracing with a nanofluid containing 4% concentrations of Al_2O_3, Cu, and Ag in Therminol VP-1. Apart from increasing thermal conductivity, heat capacity, density, and viscosity, the nanoparticles improved optical performance and thermal flow distribution during operation. González-Mora & Durán-García, 2024 studied the optimal solar thermal configuration for direct steam power generation plants operating under identical conditions and geographic location.

They used PTC and Linear Fresnel Reflector (LFR) technologies. The optimisation aimed to maximise cycle efficiency. The researchers found that solar fields with 14 PTC loops performed better than those with 3 LFR loops, providing higher thermal efficiency and greater thermal storage capacity. Eskandari, 2023 designed a geothermal-solar power plant for electricity generation, heating, and cooling for the yeast industry.

The integrated system included a binary flash geothermal cycle, a PTC collector field, an auxiliary heater, a single-effect absorption chiller, and heat exchangers. Energy, exergy, and exergoeconomic analyses and parametric methods were applied. System optimisation was performed using a genetic algorithm. Under steady conditions, the energy and exergy efficiencies were 10.78% and 23.1%, respectively. The optimised exergy efficiency under ideal conditions reached 33.8%.

ISSN: 2523-6881
RENIECYT-SECIHTI: 1702902

Lizárraga-Morazán, Juan-Ramón & Picón-Núñez, Martín. [2025]. Incorporation of Zinc Oxide Nanoparticles in Ceramic Materials. Sizing parabolic trough solar thermal collector networks for Industrial Application – Case study. Journal Renewable Energy. 9[21] 1-11: e30921111.
https://doi.org/10.35429/JRE.2025.9.21.3.1.11

Other works have studied the inclusion of new systems or equipment into solar thermal networks using engineering software. Alghorayshi et al., 2024 studied and analysed different renewable sources for energy production in ASPEN Plus, including biomass and solar energy, to produce power, fuel (syngas – CO and H_2), and fresh water using a four-stage distillation system for seawater desalination. The solar thermal network designed with PTC technology covered an area of 38,908 m².

The authors concluded that combining solar and biomass resources is a viable option for meeting growing demand for water, electricity, and fuel. Contreras et al., 2023 developed a mathematical and numerical tool using SOLEEC software coded in MATLAB to evaluate a Direct Steam Generation (DSG) system with PTC technology in a combined power cycle. The model was based on a power plant in Mexico, showing that switching to DSG could reduce the solar field area by approximately 35%. Arias-Velasquez et al., 2024 proposed a methodology to design a 150 MW plant at the Arequipa solar park in Peru.

Their design included 7,399 cylindrical cavity HE54 heliostats in a tower reactor with molten salt (MS) thermal storage. The design featured two systems: one using PTC technology, and another integrating a heliostat thermal field. Energy, exergy, and economic analysis were performed using EES software. Results showed that exergy efficiency increased by around 6% in System 1 and 2% in System 2, with annual revenue of $34.87 million over a 20-year lifespan. Altiokka et al., 2023 investigated the design of a Solar Driven Absorption Cooling System (SACS) with thermal energy storage (TES) for operation under low solar radiation, addressing cooling demand for a 120 m² residence.

The study compared four collector technologies: PTC (parabolic trough), FPC (flat plate), ETC (evacuated tube), and CPC (compound parabolic). Their thermo-economic analysis found ETC to be the most cost-effective, while PTC was the most efficient. Cuce et al., 2024 conducted a study on Concentrating Solar Power (CSP) systems for cogeneration, finding that focal collectors such as Parabolic Dish Collectors (PDC) can reach higher process temperatures.

However, they are more expensive and require larger installation areas compared to linear-focus systems like PTC, which can reach temperatures up to 800 °C. Kessentini et al., 2023 described, developed, and operated a hybrid mini power plant with direct steam generation (DSG) using PTC technology in the southern Mediterranean region under the REECOOP (Renewable Electricity Cooperation) project. The plant was designed and tested under daily conditions, yielding valuable operational and control data for both conventional and hybrid modes. Zhao et al., 2024 studied two PTC systems: one ideal system using multiple concentration ratios (CR) across different sections, and a multi-section system applying practical CRs. They developed a two-dimensional thermal prediction model using the finite volume method. In the operating range of 293°C to 393 °C, the multi-section system achieved 6.7% higher optical efficiency and a 4.5% increase in thermal efficiency compared to the conventional system.

From the literature review, it is evident that the sizing of solar thermal plants using PTC technology for different applications remains an underexplored topic as in most applications, it is not established whether the designs are viable or if they meet the specific requirements of the processes. On the other hand, existing design methodologies tend to be complex, which limits their practical applicability in industrial settings that demand precise yet easily implementable solutions.

This study aims to present a simple and validated design methodology based on previously optimised network structures. The proposed approach enables the effective determination of the collector area, inlet temperature, and solar fraction of a PTC solar thermal network applied to industrial processes (SHIP), using only the process's target temperature and thermal load requirements as input parameters. Finally, a practical example is included to demonstrate the application of the proposed methodology.

Methodology

The methodology for obtaining operational and design data for optimised solar thermal networks in industrial processes is based on the work published by Lizárraga-Morazan & Picón-Núñez, 2024a.

ISSN: 2523-6881
RENIECYT-SECIHTI: 1702902

Lizárraga-Morazán, Juan-Ramón & Picón-Núñez, Martín. [2025]. Incorporation of Zinc Oxide Nanoparticles in Ceramic Materials. Sizing parabolic trough solar thermal collector networks for Industrial Application – Case study. Journal Renewable Energy. 9[21] 1-11: e30921111.
https://doi.org/10.35429/JRE.2025.9.21.3.1.11

A Particle Swarm Optimization (PSO) problem was solved using a transient thermo-hydraulic-economic model, validated under typical daily conditions in winter and summer, to determine the size (area) and structure (PTC geometry that defines the network) needed to meet a thermal load, given a mass flow rate and the type of heat transfer fluid (HTF). Sampling was carried out by varying the thermal load Q_p, the process's target temperature T_{obj}, and the inlet temperature T_{in} to generate a set of optimized points. The target temperature was set at seven values: 70°C, 125°C, 180°C, 235°C, 293°C, 345°C, and 400°C; the thermal load values chosen were: 400 kW, 1,600 kW, 2,800 kW, and 4,000 kW; and the different values of inlet temperature were related to the objective temperature as follows: 0.7, 0.8, and $0.9 \cdot T_{obj}$. Instantaneous daily environmental data were collected in the city of Guanajuato (21.0190° N, 101.2574° W). The optimisation problem was solved for each of the 84 variable combinations and for the typical days representing winter and summer seasons.

The solar fraction for each optimised point in both seasonal samples was obtained using the following expression:

$$sf = \frac{Q}{Q_p} \quad [1]$$

Where sf is the solar fraction, Q represents the useful thermal load generated by the optimised network during its operation, and Q_p is the thermal load required by the process. The mean optimised *sf* values for the winter and summer seasons, respectively are 1.05 ± 0.09 and 1.06 ± 0.08, with minimum and maximum values of 0.81 and 1.2, and 0.9 and 1.23 (Lizárraga-Morazán & Picón-Núñez, 2024b). To develop correlations based on these results that allow network design as a function of process variables, the solar fraction *sf* and the network area *A* were defined as independent variables. Additionally, the following independent variables were established: $d_{if}T = T_{obj} - T_{in}$; $d_{iv}T = \frac{T_{in}}{T_{obj}}$; and Q_p. Various fitting expressions were evaluated, with the best correlations obtained using polynomial equations. The relationships between the independent variables and the corresponding design variables from the highest-fitting correlations are presented below:

$$sf = sf\left(d_{if}T, d_{iv}T, Q_p\right)$$
$$A = A\left(sf, Q_p\right) \quad [2]$$

The validity of the resulting correlations was verified by comparing them to the areas of existing solar thermal networks. Finally, a representative case study was selected to demonstrate the practical application of the calculation methodology.

Results

The expression used to determine the solar fraction is as follows:

$$sf = sf(x_1, x_2, x_3) = w_1 + w_2x_1^2 + w_3x_1 + w_4x_2^2 + w_5x_2 + w_6x_1x_2 + w_7x_1x_2^2 + w_8x_2x_1^2 + w_9x_3 + w_{10}x_1x_3^2 + w_{11}x_2x_3^2 + w_{12}x_3x_1^2 \quad [3]$$

Where $x_1 = d_{if}T, x_2 = d_{iv}T, y\ x_3 = Q_p$. The correlation used to calculate the area of the solar thermal network is presented below:

$$A = A(x_1, x_2) = w_1 + w_2x_1^2 + w_3x_1 + w_4x_2^2 + w_5x_2 + w_6x_1x_2 + w_7x_1x_2^2 + w_8x_2x_1^2 \quad [4]$$

Where $x_1 = sf, x_2 = Q_p$

Tables 1 and 2 show the values of the correlation constants (weights) for equations [3] and [4], respectively.

Box 1

Table 1
Correlation [3] weights

w_i	Winter	Summer
1	4.381659035	2.702525781
2	0.0002618105	0.0001238720
3	-0.184758884	-0.101122509
4	4.94884E+00	2.18736E+00
5	-7.909089401	-3.545451963
6	0.4732791705	0.2639712102
7	-0.300857338	-0.171581734
8	-3.81988E-04	-1.85823E-04
9	-7.65424E-05	-0.000112347
10	3.887883E-11	2.876322E-11
11	8.312521E-09	1.605053E-08
12	-5.74657E-10	0.000000000

Source: Own elaboration.

ISSN: 2523-6881
RENIECYT-SECIHTI: 1702902

Box 2

Table 2

Correlation [4] weights

w_i	Winter	Summer
1	1698.522158	7725.614716
2	-940.0668403	5238.198464
3	-427.0328683	-12692.56241
4	8.642521E-04	2.746293E-04
5	0.185405954	-1.638407765
6	-0.922892605	4.5701634793
7	-0.000816573	-0.000277020
8	2.405315536	-1.467934015

Source: Own elaboration.

Table 3 summarizes the results of a statistical analysis for the correlations obtained for both the solar fraction and the area, across both seasons.

Box 3

Table 3

Multivariate polynomial regression statistics

	Winter		Summer	
	sf	***A***	***sf***	***A***
MSE	$1.9e^{-4}$	149.3	$9.0e^{-5}$	67.3
RMSE	$4.3e^{-2}$	12.2	$9.5e^{-3}$	8.2
R^2	0.98	1.00	0.99	1.00
R^2adj	0.97	1.00	0.99	1.00

Source: Own elaboration.

Figure 1 displays the graphical fit of the polynomial regression for the solar fraction during winter and summer.

Box 4

(a)

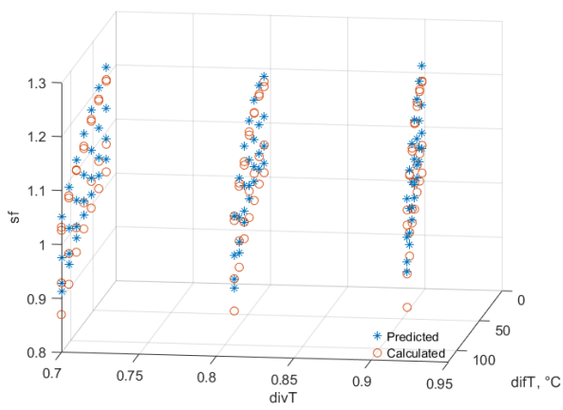

(b)

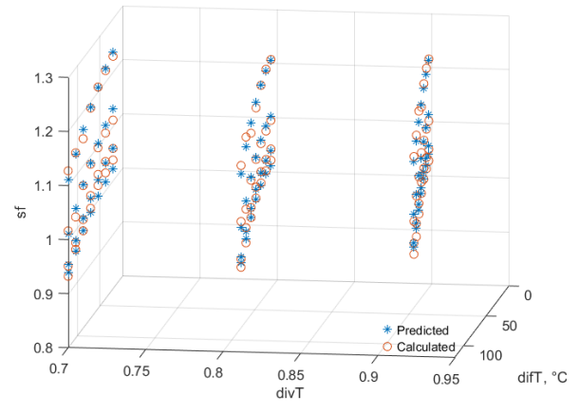

Figure 1

Fitness of the *sf-A* regression model: (a) winter and (b) summer.

Source: Own elaboration

Figure 2 presents the fit of the correlation used to determine the network area.

Box 5

(a)

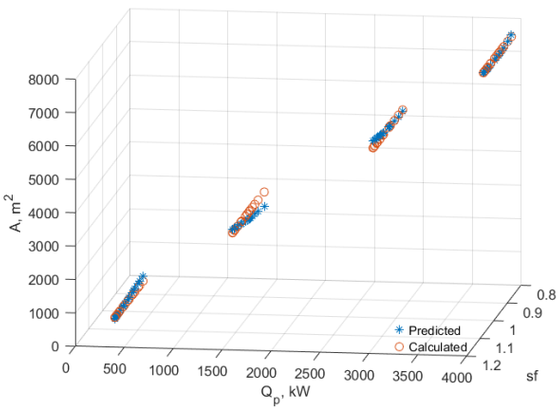

(b)

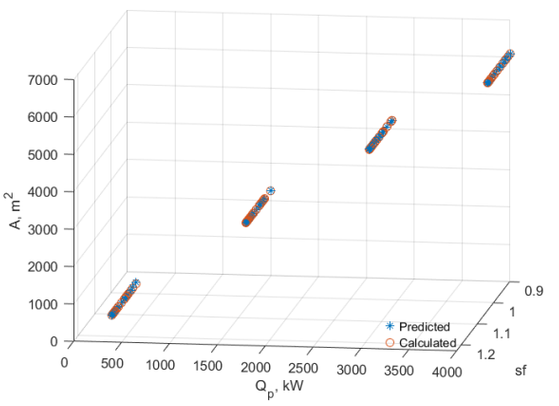

Figure 2

sf - A performance profile: (a) winter, and (b) summer.

Source: Own elaboration

ISSN: 2523-6881
RENIECYT-SECIHTI: 1702902

Lizárraga-Morazán, Juan-Ramón & Picón-Núñez, Martín. [2025]. Incorporation of Zinc Oxide Nanoparticles in Ceramic Materials. Sizing parabolic trough solar thermal collector networks for Industrial Application – Case study. Journal Renewable Energy. 9[21] 1-11: e30921111.
https://doi.org/10.35429/JRE.2025.9.21.3.1.11

Figure 3 illustrates the behavior of the solar fraction with respect to the independent variables $d_{if}T$ and $D_{iv}T$.

Box 6

(a)

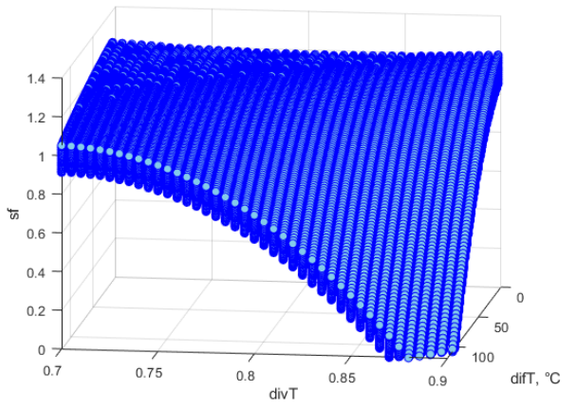

(b)

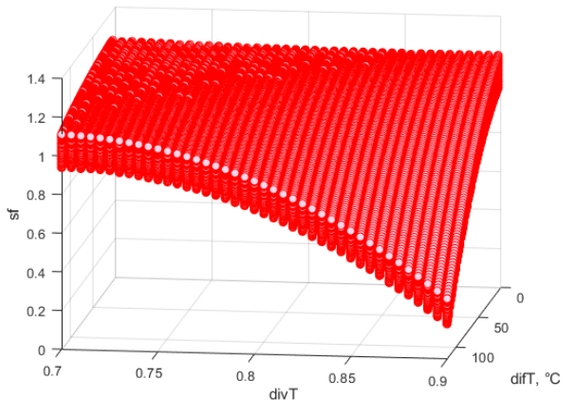

Figure 3

sf – $d_{iv}T$- $d_{if}T$ performance profile: (a) winter, and (b) summer.

Source: Own Elaboration

Figure 4 illustrates the behavior of the solar fraction with respect to the thermal load Q_p and the temperature gradient $d_{if}T$.

Box 7

(a)

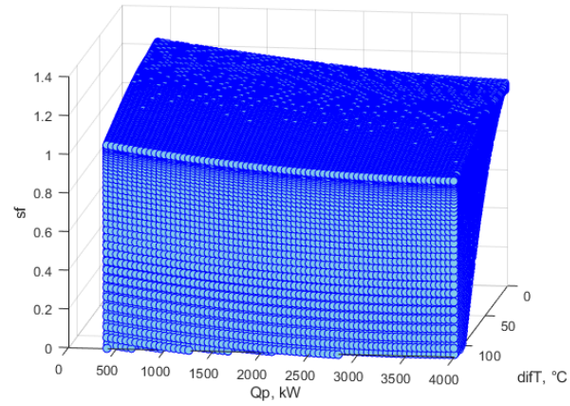

(b)

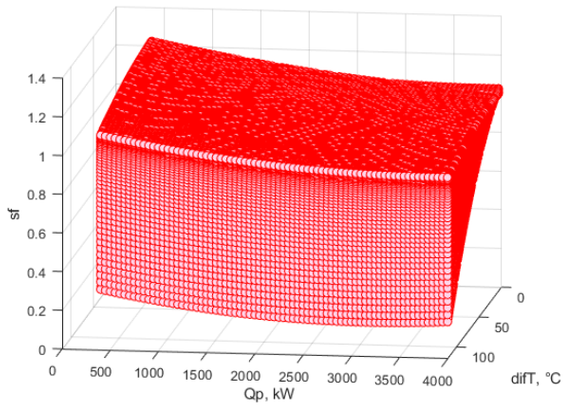

Figure 4

sf – Q_p – $d_{if}T$ performance profile: (a) winter, and (b) summer.

Source: Own Elaboration

Figure 5 shows the profile of the network area as a function of the thermal load and the solar fraction.

Box 8

(a)

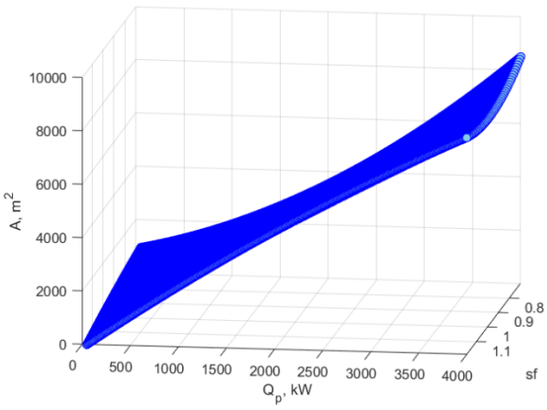

ISSN: 2523-6881
RENIECYT-SECIHTI: 1702902

Lizárraga-Morazán, Juan-Ramón & Picón-Núñez, Martín. [2025]. Incorporation of Zinc Oxide Nanoparticles in Ceramic Materials. Sizing parabolic trough solar thermal collector networks for Industrial Application – Case study. Journal Renewable Energy. 9[21] 1-11: e30921111.
https://doi.org/10.35429/JRE.2025.9.21.3.1.11

(b)

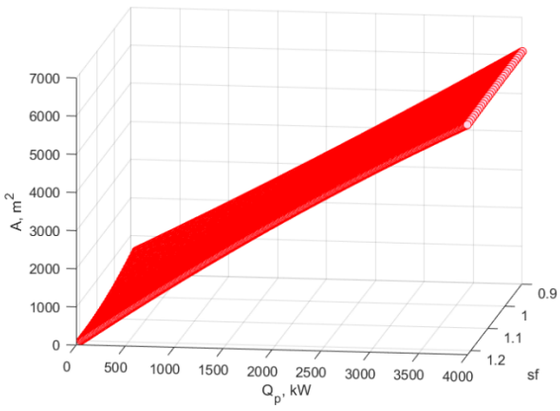

Figure 5

$A - Q_p - sf$ performance profile: (a) winter, and (b) summer.

Source: Own elaboration

The validation of the thermo-hydraulic model used to solve the network optimization problem was reported in the work by Lizárraga-Morazán & Picón-Núñez, 2024a. Table 4 presents a comparison between the installed area (A) and the average area (A_{calc}) obtained using correlations [3] and [4], for several solar thermal networks reported in the literature. The thermal load values fall within the range covered by the correlations. The networks referred to as Sello Rojo Lechera and Centro Cooperativo los Altos were reported by Rodríguez Rodrigo et al., 2024; Frito Lay by Schoeneberger et al., 2020; and Phoenix Correctional Institution by May et al., 2000. In these comparisons, the area calculated using the correlations was lower than the installed area, by a range of 46% to 81%.

Box 9

Table 4

SHIP´s installed area comparison

Entity	Location	A, m^2	Q kW	A_{calc}, m^2	%
Frito Lay	Modesto, California, USA	5,017	492	965	81
Sello Rojo Lechera	Guadalajara,Jal, Mx	1,641	240	429	74
Centro Lechero Cooperativo Los Altos	Arandas, Jal, Mx	422	94.5	136	68
Phoenix Federal Correctional Institution	Arizona, USA	1,584	440	858	46

Source: Own elaboration.

Table 5 presents a comparison of the installed area of industrial solar thermal networks using PTC technology currently in operation in Mexico (Ituna-Yudonago et al., 2025), against the area calculated using the proposed correlations. In this case, the calculated areas were lower by a range of 60% to 68%.

Box 10

Table 5

Mexican SHIP´s installed area comparison

Sector	Reported	Acalc	%
Food	A [m^2]	1,067	68
	3,366.83		
	60-120 °C		
	Q [kW]		
	541.51		
Dairy	A [m^2]	2,000	63
	5,508.40		
	60-120 °C		
	Q [kW]		
	1,010.60		
Agro-Industry	A [m^2]	1,503	60
	3,725.38		
	60-120 °C		
	Q [kW]		
	757.91		
Beverage	A [m^2]	685	66
	2,003.88		
	60-90 °C		
	Q [kW]		
	354.94		

Source: Own elaboration.

Case Study

The following section describes the design procedure of an industrial solar thermal plant. For comparison purposes, the data used is from a plant currently in operation. The network supplies hot water at a temperature of 78 °C to a milk pasteurization plant located in Guadalajara, Jalisco, Mexico (Figure 6). The installed area is 1,641 m², with a thermal load generation of 360.88 kW. The outlet temperature of the thermal fluid is 68 °C. The objective is to determine the optimised area of the solar thermal network and analyse the effect of varying the inlet temperature.

ISSN: 2523-6881
RENIECYT-SECIHTI: 1702902

Box 11

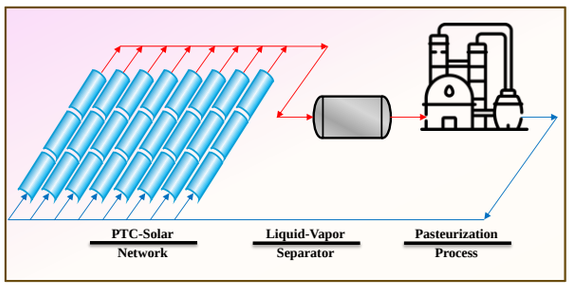

Figure 6

Plant Layout for case study.

Source: Own elaboration

The design data are summarised in Table 6.

Box 12

Table 6

Case Study data

Data	*Value*
T_{obj}, [° C]	78
T_{in}, [° C]	58
Q_p, [kW]	360.88
A, [m^2]	1,641

Source: Own Elaboration.

The temperature variables are $difT = 20$ °C and $divT = 0.743$. Using Equation [3], the solar fraction is determined for summer and winter seasons, resulting in 1.24 and 1.22, respectively. The network area is calculated using Equation [4], resulting in 669.6 m² and 716.3 m². The optimised areas for winter and summer are 59.2% and 72.8% lower than the reported value, respectively. A design area must be defined based on these results. Accordingly, the winter value (716.3 m²) is selected as the design area. A parametric analysis was conducted by varying the inlet temperature to determine its impact on the solar fraction and network area. The results are shown in Table 7.

Box 13

Table 7

Parametric analysis

T_{in}	*Summer*		*Winter*		$A_{summer} - A_{winter}$
[°C]	*sf*	*A* [m^2]	*sf*	*A* [m^2]	[m^2]
68	1.22	660.4	1.21	728.4	68.0
58	1.24	669.6	1.22	716.3	46.8
48	1.21	657.4	1.16	773.5	116.2
38	0.99	837.0	0.77	1,164.9	328.0
33	0.74	1,544	0.37	1,544.0	0

Source: Own elaboration.

From Table 7, an inlet temperature of $T_{in} = 58$ °C yields the maximum solar fraction for both seasons (1.24 for summer and 1.22 for winter). Figure 7 graphically represents the impact of T_{in} on both the network area and solar fraction in each season. Within the inlet temperature range of 50°C to 70 °C, the area and solar fraction remain relatively constant (see Figure 7).

The parametric analysis indicates that an inlet temperature of 58 °C is the most suitable, as it results in the highest solar fractions for both seasons and produces small and comparable design areas.

Box 14

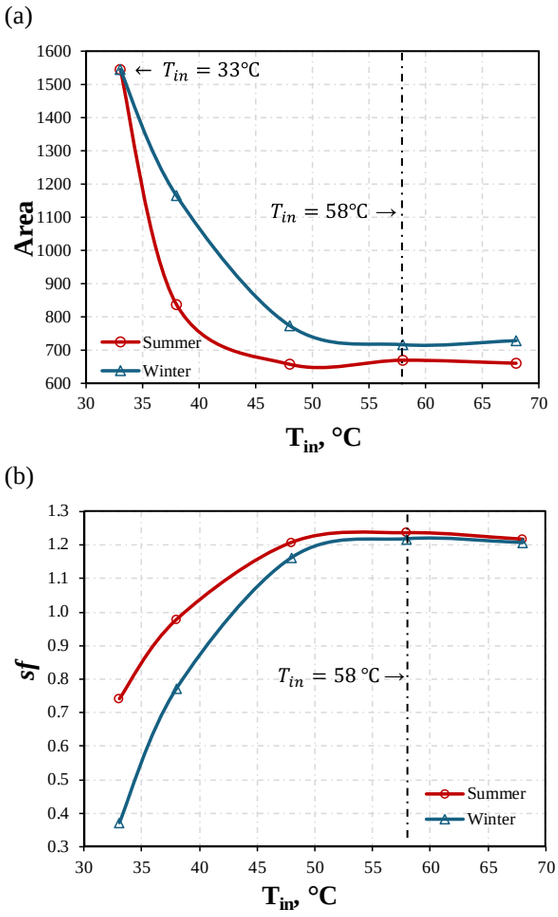

Figure 7.

Effect of T_{in} on (a) *sf* (b) *A.*

Source: Own elaboration

Conclusions

Based on the results of this work, the following conclusions are drawn:

ISSN: 2523-6881
RENIECYT-SECIHTI: 1702902

Lizárraga-Morazán, Juan-Ramón & Picón-Núñez, Martín. [2025]. Incorporation of Zinc Oxide Nanoparticles in Ceramic Materials. Sizing parabolic trough solar thermal collector networks for Industrial Application – Case study. Journal Renewable Energy. 9[21] 1-11: e30921111.
https://doi.org/10.35429/JRE.2025.9.21.3.1.11

1. The proposed expressions allow for the design of optimised SHIP plants based on three key variables: inlet temperature, objective process temperature, and required thermal load.
2. The solar thermal networks designed exhibit high flexibility, capable of maintaining elevated solar fractions across a wide range of inlet temperatures without modifying the collector area.
3. It is noteworthy that the network designs obtained are between 40% and 81% smaller compared to reported values, while maintaining superior solar fractions in the range of 1.1 to 1.2.
4. Inlet temperature and thermal load directly affect the required area and solar fraction: lower inlet temperatures or higher thermal loads lead to greater area requirements.
5. The polynomial regression models used enable effective prediction of the behavior of solar fraction and network area variables across different seasons.

Declarations

Conflict of interest

The authors declare no interest conflict. They have no known competing financial interests or personal relationships that could have appeared to influence the article reported in this article.

Authors' Contribution

Juan-Ramón Lizárraga-Morazán: Contributed to the research methodology and generation of results and writing of the manuscript.

Martín Picón-Núñez: Contributed to the project idea, research method, editing and revising of the manuscript.

Funding

No funding was received for the development of this research.

Acknowledgements

CONAHCYT is greatly acknowledged for the postdoctoral grant awarded to Dr. Juan-Ramón Lizárraga-Morazán.

Abbreviations

HTF	Heat transfer fluid
$SHIP$	Solar heat for industrial processess

Nomenclature

A	Network area, [m^2]
Q	Useful heat, [kW]
Q_p	Process heat, [kW]
sf	Solar fraction
T_{in}	HTF Inlet temperature, [°C]
T_{obj}	HTF target temperature, [°C]

References

Basics

IEA. (2018). *Clean and efficient heat for industry*. IEA, Paris. Accessed: Jul. 11, 2025. [Online]. Available: https://www.iea.org/commentaries/clean-and-efficient-heat-for-industry

IRENA. (2024). *RENEWABLE CAPACITY STATISTICS 2024*. [Online]. Available: https://www.irena.org/-/media/Files/IRENA/Agency/Publication/2024/Mar/IRENA_RE_Capacity_Statistics_2024.pdf

Differences

Alghorayshi, S. T. K., Imandoust, M., Hemmatzadeh, A., Abbasi, S., Javidfar, M., Seifollahi, M., Gitifar, S., & Zahedi, R. (2024). Design, simulation and investigation of the tri-generation process of fresh water, power and biogas using solar thermal energy and sewage sludge. *Chemical Engineering Research and Design*, *208*, 242–257. doi:10.1016/J.CHERD.2024.07.009

Arias-Velasquez, R. M. (2024). Methodology for the Design Solar Thermal Station: Case Study of 150 MW for Arequipa. *2024 IEEE ANDESCON*, 1–6. doi: 10.1109/ANDESCON61840.2024.10755776

Altiokka, G., Banu, A., Oğuz, A. (2023). Design and optimization of absorption cooling system operating under low solar radiation for residential use. Journal of Building Engineering, 73. https://doi.org/10.1016/J.JOBE.2023.106697

ISSN: 2523-6881
RENIECYT-SECIHTI: 1702902

Cuce, P. M., Guclu, T., & Cuce, E. (2024). Design, modelling, environmental, economic and performance analysis of parabolic trough solar collector (PTC) based cogeneration systems assisted by thermoelectric generators (TEGs). *Sustainable Energy Technologies and Assessments*, *64*, 103745. doi: 10.1016/J.SETA.2024.103745

Contreras, E., Saldaña, J. G. B., Alejo, J. de la C., Torres, C. D. C. G., Bernal, J. A. J., & Vazquez, M. B. A. (2023). A Feasibility Analysis of a Solar Power Plant with Direct Steam Generation System in Sonora, Mexico. *Energies*, *16*(11). doi: 10.3390/en16114388

Eskandari, A. (2023). Design, 3E scrutiny, and multi-criteria optimization of a trigeneration plant centered on geothermal and solar energy, using PTC and flash binary cycle. *Sustainable Energy Technologies and Assessments*, *55*, 102718. doi: 10.1016/J.SETA.2022.102718

González-Mora, E., & Durán-García, M. D. (2024). Assessing parabolic trough collectors and linear Fresnel reflectors direct steam generation solar power plants in Northwest México. *Renewable Energy*, *228*, 120375. doi:10.1016/J.RENENE.2024.120375

Ituna-Yudonago, J. F., García-Valladares, O., Ortiz-Rodríguez, N. M., Ibarra-Bahena, J., & Galindo-Luna, Y. R. (2025). Applications of solar thermal technologies in Mexican industries for heating processes and their contribution against global warming: An overview. *Solar Energy*, *291*, 113395. doi:10.1016/J.SOLENER.2025.113395

Kalogirou, S. (2009). Solar energy engineering: Process and systems. *London UK*, 49–89.
Kessentini, H., Ferchichi, S., & Bouden, C. (2023). Design, commissioning and operation of a mini hybrid parabolic trough solar thermal power plant for direct steam generation. *Solar Energy Advances*, *3*, 100039. doi:10.1016/J.SEJA.2023.100039

Khoo, H. H., & Tan, R. B. H. (2006). Environmental Impact Evaluation of Conventional Fossil Fuel Production (Oil and Natural Gas) and Enhanced Resource Recovery with Potential CO_2 Sequestration. *Energy & Fuels*, *20*(5), 1914–1924. doi:10.1021/ef060075+

Lizárraga-Morazan, J. R., & Picón-Núñez, M. (2024a). Harnessing solar power in industry: Heuristic optimisation design and transient thermal modelling of parabolic trough solar collector networks. *Chemical Engineering and Processing - Process Intensification*, *200*, 109776. doi:10.1016/J.CEP.2024.109776

Lizárraga-Morazán, J. R., & Picón-Núñez, M. (2024b). Determination of the solar fraction for optimized parabolic concentrator solar collector networks. *ECORFAN-Journal Democratic Republic of Congo*, *10*(18), 1–9. doi:10.35429/EJDRC.2024.10.18.1.9

Mondal, B., & Maji, A. (2025). A brief review on analysis and recent development of parabolic trough collector. *Energy Storage and Saving*, *4*(2), 123–132. doi:10.1016/J.ENSS.2024.12.003

Naaim, S., Ouhammou, B., El Merabet, Y., Aggour, M., Mihi, M., el Mers, E. M., & Daouchi, B. (2025). Optimization of Nanoparticle Concentration for Enhanced Performance of Therminol® VP-1-Based Nanofluids in Parabolic Trough Systems. *Results in Engineering*, *26*, 105051. doi:10.1016/j.rineng.2025.105051

Rabienataj Darzi, A. A., Razbin, M., Allahdadi, A., Mousavi, S. M., Taylor, R. A., & Li, M. (2025). Designing high-efficiency parabolic trough receiver tubes via AI-assisted simulation. *Renewable Energy*, *251*, 123366. doi:10.1016/J.RENENE.2025.123366

REN21. (2023). *RENEWABLES 2023 GLOBAL STATUS REPORT*. Renewables Now. [Online]. Available: https://www.ren21.net/wp-content/uploads/2019/05/GSR2023_GlobalOverview_Full_Report_with_endnotes_web.pdf

Shaikh, I., & Modi, A. (2025). A novel concentrating solar plant configuration with multiple solar fields and thermal energy storage to reduce energy production costs. *Case Studies in Thermal Engineering*, *71*, 106185. doi:10.1016/J.CSITE.2025.106185

Yin, H., Sun, Y., Zhang, J., Che, S., Zhang, X., & Xing, Y. (2024). Engineering optics and thermodynamics design of parabolic trough solar collector. *Journal of Physics: Conference Series*, *2782*, 12038. doi:10.1088/1742-6596/2782/1/012038

ISSN: 2523-6881
RENIECYT-SECIHTI: 1702902

Lizárraga-Morazán, Juan-Ramón & Picón-Núñez, Martín. [2025]. Incorporation of Zinc Oxide Nanoparticles in Ceramic Materials. Sizing parabolic trough solar thermal collector networks for Industrial Application – Case study. Journal Renewable Energy. 9[21] 1-11: e30921111.
https://doi.org/10.35429/JRE.2025.9.21.3.1.11

Zeng, J., Yin, S., Tong, L., Liu, C., Wang, L., & Wu, C. Y. (2025). Design and evaluation of an integrated CCHP system based on solar thermal supplementary heating and off-peak electrical thermal storage heating. *Energy*, *328*, 136505. doi: 10.1016/J.ENERGY.2025.136505

Zhao, K., Wang, X., Gai, Z., Qin, Y., Li, Y., & Jin, H. (2024). Enhancing the efficiency of solar parabolic trough collector systems via cascaded multiple concentration ratios. *Journal of Cleaner Production*, *437*, 140665. doi: 10.1016/J.JCLEPRO.2024.140665

Discussions

Rodríguez Rodrigo, R., Díaz Martín, R., Baranda Fernández, M., Román Gallego, J. Á., & Mayo del Río, C. (2024). Technical and economic study of solar energy concentration technologies (linear Fresnel and parabolic trough collectors) to generate process heat at medium temperature for the dairy industry of Spain. *Solar Energy*, *271*, 112420. doi:10.1016/J.SOLENER.2024.112420

Schoeneberger, C. A., McMillan, C. A., Kurup, P., Akar, S., Margolis, R., & Masanet, E. (2020). Solar for industrial process heat: A review of technologies, analysis approaches, and potential applications in the United States. *Energy*, *206*, 118083. doi:10.1016/J.ENERGY.2020.118083

May, K., Barker, G., Hancock, E., Walker, A., Dominick, J., & Westby, B. (2000). Performance of a Large Parabolic Trough Solar Water Heating System at Phoenix Federal Correctional Institution. *Journal of Solar Energy Engineering*, *122*(4), 165–169. doi:10.1115/1.1331288

ISSN: 2523-6881
RENIECYT-SECIHTI: 1702902

Journal Renewable Energy 9[21]1-8: e40921108
Article

Efectos de sistemas fotovoltaicos en la calidad de energía y el factor de potencia en la industria, simulación y validación experimental en México

Effects of photovoltaic systems on power quality and power factor in industry, simulation and experimental validation in Mexico

Tellez-Hernandez, Felipe*[a], Pineda-Piñón, Jorge[b], Sánchez-Vega, Guadalupe O.[c] and Mota-Del Carpio, Jimena[d]

[a] Instituto Politécnico Nacional-CICATA • 0000-0002-5890-6548 • 940533
[b] Instituto Politécnico Nacional-CICATA • 0000-0003-1392-6534 • 91313
[c] Uco Mondragón • 0000-0001-5709-4325 • 502821
[d] Instituto Politécnico Nacional-CICATA • 0009-0006-9523-3836 • 12437

SECIHTI classification:

Area: Engineering
Field: Energy engineering
Discipline: Energy Engineering
Subdiscipline: Solar energy

https://doi.org/10.35429/JRE.2025.9.21.4.1.8
Article History:
Received: June 20, 2025
Accepted: December 31, 2025

* ✉ [ftellez2400@alumno.ipn.mx]

Abstract

The rapid growth of photovoltaic generation in Mexico poses electrical challenges related to power factor and power quality. This study evaluates the impact of PV systems on harmonic distortion and power factor reduction in a company with critical equipment, considering the (DOF, 2017)-(CRE, 2020) and the (IEEE, 2009). Through electrical simulation and experimental measurement, losses of information and possible economic penalties were identified according to CFE data, the results show high agreement between simulations and measurements, evidencing that incorporating SFV without prior analysis can decrease the power factor and compromise stability. Hybrid and reactive compensation solutions are proposed, highlighting the importance of previous technical studies for an efficient and safe energy transition.

Objetive	Methodology	Contribution
Evaluate the impact of photovoltaic systems on power quality and power factor in industrial installations, through electrical simulation and experimental validation in Mexico	The electrical system was modeled in ETAP, and field measurements were carried out using power analyzers, comparing simulated and actual results under the NOM-EM-007-CRE-2017 and IEEE 519-2014 standards.	The study demonstrates the reduction of power factor caused by PV systems without reactive compensation and proposes hybrid solutions to optimize power quality and comply with regulatory standards.

Photovoltaic energy, power factor, energy quality.

Resumen

El rápido crecimiento de la generación fotovoltaica en México plantea retos eléctricos relacionados con el factor de potencia y la calidad de energía. Este estudio evalúa el impacto de sistemas FV en la distorsión armónica y la reducción del factor de potencia en una empresa con equipos críticos, considerando la (DOF, 2017)-(CRE, 2020) y el (IEEE, 2009). Mediante simulación eléctrica y medición experimental, se identificaron pérdidas de información y posibles penalizaciones económicas según datos de CFE, los resultados muestran alta concordancia entre simulaciones y mediciones, evidenciando que incorporar SFV sin análisis previo puede disminuir el factor de potencia y comprometer la estabilidad. Se proponen soluciones híbridas y de compensación reactiva, resaltando la importancia de estudios técnicos previos para una transición energética eficiente y segura.

Objetivo	Metodología	Contribución
Evaluar el impacto de los sistemas fotovoltaicos en la calidad de energía y el factor de potencia en instalaciones industriales, mediante simulación eléctrica y validación experimental en México.	Se modeló el sistema eléctrico en ETAP y se realizaron mediciones en campo con analizadores de red, comparando resultados simulados y reales bajo normas NOM-EM-007-CRE-2017 e IEEE 519-2014.	El estudio demuestra la disminución del factor de potencia por sistemas FV sin compensación reactiva y propone soluciones híbridas para optimizar la calidad de energía y cumplir con estándares regulatorios.

Energía fotovoltaica, factor de potencia, calidad de la energía

Area: Advocacy and attention to national problems

Citation: Tellez-Hernandez, Felipe, Pineda-Piñón, Jorge, Sánchez-Vega, Guadalupe O. and Mota-Del Carpio, Jimena. [2025]. Efectos de sistemas fotovoltaicos en la calidad de energía y el factor de potencia en la industria, simulación y validación experimental en México. Journal Renewable Energy. 9[21] 1-8: e40921108.

Introduction

In the last decade, Mexico has experienced a remarkable growth in the adoption of photovoltaic (PV) solar energy, driven by public policies, technological advances, and the need to diversify the national energy matrix (SENER, 2024), (CENACE,2025) Electricity generation through PV systems has shown annual increases of over 25%, consolidating this technology as one of the most promising renewable energy sources in the country SENER,2024),(CENACE,2025). This progress directly contributes to fulfilling international commitments on climate change mitigation and the United Nations Sustainable Development Goals (SDGs) (IRENA, 2024).

Most PV installations in Mexico operate under grid-connected (on-grid) schemes, offering significant economic and environmental benefits. However, this model also faces technical challenges related to power quality, such as low power factor, total harmonic distortion (THD), phase imbalance, voltage fluctuations, and reactive power variations (Ahsan et al., 2021);(Li, 2018). Regulations such as (DOF, 2017) and the Grid Code 2.0 require maintaining a minimum power factor of 0.90 to avoid economic penalties, which represents a challenge for installations whose inverters lack adequate reactive compensation mechanisms (CRE, 2021).

Recent studies show that, in the absence of capacitor banks or active filters, harmonic distortion levels can exceed 10%, potentially affecting the lifespan of transformers, motors, and other sensitive loads (Hernández-Mayoral et al., 2024). In addition, research in various Latin American countries indicates that high PV penetration can cause overload losses, increase harmonics, and create current imbalance, while moderate integration with compensation strategies can improve the quality of the power supply (Anny et al., 2025);(Gandhi et al., 2020). A 160 kW PV system connected to an internal grid, associated with a 225 kVA transformer and a main 750 kVA transformer, was analyzed to evaluate power quality (HUAWEI, 2023); (FLUKE, 2012); (METREL, 2023). The analysis revealed significant problems, including a low average power factor (0.69), excessive harmonics (TDD up to 11.76%), and current imbalance (up to 77.82%), exceeding national and international standards (IEEE, 2009)

These findings highlight the need for corrective measures such as automatic capacitor banks, harmonic filters, and load balancing to ensure efficient operation and regulatory compliance.

Therefore, this study seeks to comprehensively evaluate the interaction between the PV system and the internal grid, identifying the main technical challenges and proposing solutions to improve power quality, optimize operational efficiency, and maximize the benefits of photovoltaic generation in critical environments with high demand.

Methodology

The study was carried out at the facilities of a national company located in the municipality of El Marques, Queretaro, Mexico, located at 20° 38' 54" north latitude and 100° 17' 38" west longitude, at an altitude of 1 908 meters above sea level. The area has an average annual solar radiation of 5.3 $kWh \cdot m^{-2} \cdot day^{-1}$ (SENER, 2024), a favorable condition for the use of photovoltaic energy.

The evaluated photovoltaic system has four Huawei SUN2000-40KTL-M3 inverters (40 kW each) operating at 440 Vac, connected to a 225 kVA (440/220-127 V) dry transformer, which is integrated into the 750 kVA main transformer (Delta-Star, 5.48% impedance), responsible for powering critical loads such as server systems and production equipment. The methodology used consisted of three main stages, complemented by a validation procedure:

1. Normative analysis

Existing standards and regulations were revised to define evaluation criteria and compliance limits:

- NOM-EM-007-CRE-2017: minimum power factor of 0.90.
- IEEE 519-2014: Maximum allowable total harmonic distortion (THD) of 5%.
- CFE G0100-04: Operating limits of active and reactive power.

This review made it possible to establish the technical parameters that would be used as a reference throughout the study.

ISSN: 2523-6881
RENIECYT-SECIHTI: 1702902

Tellez-Hernandez, Felipe, Pineda-Piñón, Jorge, Sánchez-Vega, Guadalupe O. and Mota-Del Carpio, Jimena. [2025]. Efectos de sistemas fotovoltaicos en la calidad de energía y el factor de potencia en la industria, simulación y validación experimental en México. Journal Renewable Energy. 9[21] 1-8: e40921108.
https://doi.org/10.35429/JRE.2025.9.21.4.1.8

2. Modeling the electrical system

The ETAP software was used to simulate the electrical behavior before and after the photovoltaic integration, replicating the same measurement points used in the experimental monitoring to ensure direct comparability.

The model included:

- 750 kVA main transformer (Delta-Star, 5.48% impedance).
- Photovoltaic system of 160 kW nominal (360 modules).
- 225 kVA dry transformer for inverter coupling.
- Critical loads with hourly consumption profiles.
- 4 Huawei SUN2000-40KTL-M3 inverters
- Lines and internal protections of the plant.
- Critical loads (servers and production equipment).

The simulations evaluated power factor, active power, reactive power and THD in different operating scenarios:

- Normal conditions with maximum solar radiation.
- Periods of low or no photovoltaic generation.
- SFV disconnect scenarios.

3. Experimental measurement

For field measurement, three power grid analyzers were installed simultaneously for seven consecutive days, configured to record data every 20 seconds:

1. Fluke 435-II installed on the 750-kVA transformer low-voltage main board (CFE grid interconnection point).

2. Metrel MI 2892 installed in the secondary of the 225-kVA dry transformer, at the output of the photovoltaic system.

3. Metrel MI 2892 installed directly at the output of the PV inverters.

The following variables were measured at all points:

- Active power (kW).
- Reactive power (kVAr).
- Apparent power (kVA).
- Power factor (PF).
- Three-phase voltage and current.
- THD voltage and current.

The data were stored in the internal memory of the equipment for subsequent processing and comparative analysis with the simulation results.

4. Validation procedure

The results obtained in DWTP were contrasted with the experimentally measured data, verifying the coherence between both sources and evaluating the discrepancies. This process made it possible to quantify the real impact of the photovoltaic system on the power factor and power quality, as well as to identify the contribution of inductive loads to the deterioration of electrical indicators in periods of low or no solar generation.

Results

The simulated results were verified with the measured data to validate the behavior and determine the real magnitude of the electrical affectation due to the installed photovoltaic system which covers approximately 75% of the consumption of the place, the active power was approximately 5.69 kW, while the reactive power was -23.3 kVAr according to the simulation carried out in ETAP(Figure 1). These data allowed us to determine an approximate power factor of 0.237, according to the formula described below:

$$Fp = \frac{P}{\sqrt{P^2+Q^2}}$$

where:

P is the active power in Watts
Q is the reactive power Var
FP is the power factor (dimensionless)

Then:

$$0.237 = \frac{5.69k}{\sqrt{(5.69k)^2+(-23.3k)^2}}$$

ISSN: 2523-6881
RENIECYT-SECIHTI: 1702902

Tellez-Hernandez, Felipe, Pineda-Piñón, Jorge, Sánchez-Vega, Guadalupe O. and Mota-Del Carpio, Jimena. [2025]. Efectos de sistemas fotovoltaicos en la calidad de energía y el factor de potencia en la industria, simulación y validación experimental en México. Journal Renewable Energy. 9[21] 1-8: e40921108.
https://doi.org/10.35429/JRE.2025.9.21.4.1.8

The values obtained in the simulation (Figure 1) show a significant decrease with respect to the minimum thresholds established by national regulations (NOM-EM-007-CRE-2017) and international standards (IEEE 519-2014), so the results indicate a high prevalence of negative inductive reactive power from the inverter when the photovoltaic modules and the T2 are connected to the electricity grid. which could generate economic penalties and a decrease in energy efficiency due to the low power factor that is generated, on the other hand when disconnecting the photovoltaic system in the ETAP simulation software – specifically the T2 transformer (Figure 2) – a notable change was observed in the power triangle, with a significant improvement in the power factor, reaching a value of 0.985 when applying the data in the corresponding formula.

Box 1

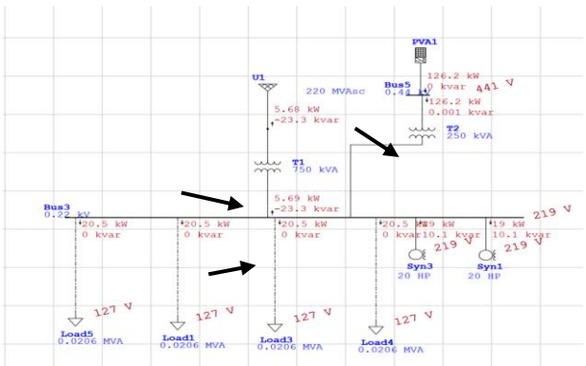

Figure 1

Simulation of a photovoltaic system interconnected to the grid

Source Generated using ETAP

Box 2

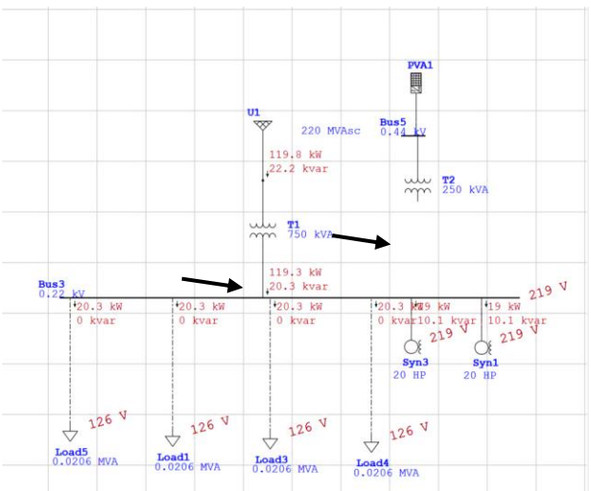

Figure 2

Simulation of electrical system with FP at 0.985 and transformer disconnected

Source Generated using ETAP

ISSN: 2523-6881
RENIECYT-SECIHTI: 1702902

These results coincide with the historical records of the CFE before and after the installation of the photovoltaic modules, where it is observed that the FP starts is 97.81% in June 2024, which indicates a well-compensated electrical system, while as of July, the FP falls to 86.09% and in August-September it reaches 79.44% just one month after the photovoltaic system (PVS) was installed, reflecting an increase in the demand for reactive power, in November 2024, the FP rises to 85.36%. In December 2024 (80.51%), with the PV system already in operation, there is no evidence of a clear improvement in the FP.

This suggests that investors are injecting active power, but not reactive offset. In the month of January, FP reached 89.44%. The PF was reduced after June 2024, reflecting an increase in reactive power due to the fact that PV inverters only generate real power (kW) and not reactive power (kVAR). As it does not produce reagents, the demand for this power continues to depend on the CFE grid, which keeps the reactive power consumed constant while the actual power injected by the photovoltaic system increases.

This imbalance increases the angle of the power triangle, which in turn decreases the power factor. In graphic terms, when the base of the triangle is reduced (real power) and the height (reactive power) is maintained, the relationship between the two causes a worsening of the power factor, generating lower values, this decrease in PF is due to the fact that photovoltaic inverters only generate active power (kW) and not reactive power (kVAr). As it does not produce reagents, the demand for this power continues to depend on the CFE network, keeping the reactive power consumed constant while the actual power injected by the PV system increases.

This imbalance increases the angle of the power triangle, reducing the ratio of active to reactive power, and worsening the power factor. To support these findings, the results of the measurements made in the main low-voltage panel of the 750 kVA T1 transformer (13200 V primary / 220/127 V secondary) are presented, where the variation of Phase to Neutral Voltage and the voltages between phases show a stable trend, consistent with the system configuration. However, abrupt voltage drops were recorded at specific times, indicating possible transient events, network failures or momentary disconnections. (Figure 3).

Tellez-Hernandez, Felipe, Pineda-Piñón, Jorge, Sánchez-Vega, Guadalupe O. and Mota-Del Carpio, Jimena. [2025]. Efectos de sistemas fotovoltaicos en la calidad de energía y el factor de potencia en la industria, simulación y validación experimental en México. Journal Renewable Energy. 9[21] 1-8: e40921108.
https://doi.org/10.35429/JRE.2025.9.21.4.1.8

Box 3

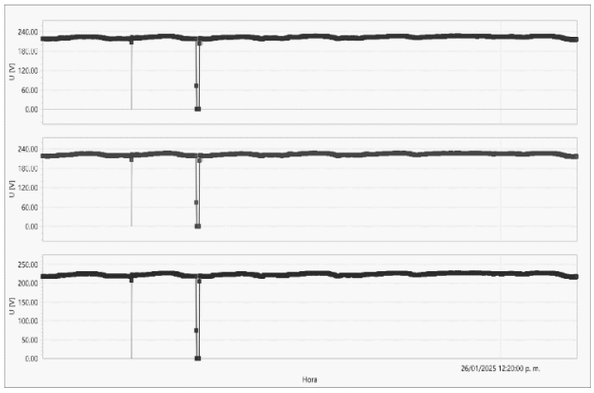

Figure 3
Voltage Variation Between Phases
Source Generated using Power Quality Analyser

Although the voltages do not present visible problems, as shown in Figure 3, it is observed that it complies with the provisions of IEEE STD 1159-2009, on the other hand, the study distinguishes a particular behavior in the power triangle of the 750 kVA T1 transformer (13200 V primary / 220/127 V secondary) due to the fact that the active power (kW) shows a cyclical pattern, with peaks during the day and reduced values at night, reflecting the interaction between the grid and solar generation (Figure 4).

Box 4

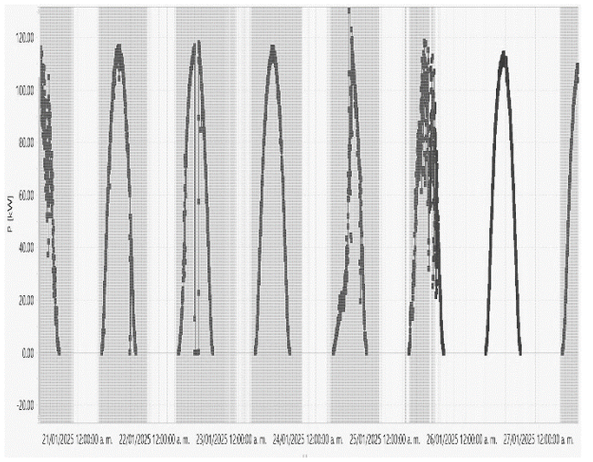

Figura 4
Variation in active power
Source Generated using Power Quality Analyser

On the other hand, the reactive power (kVAr) presents maximums during the day and decreases near zero at night, which indicates the operation of inductive loads and the partial compensation of the photovoltaic inverters, as a consequence of these variations, the apparent power (kVA) exhibits a cyclical behavior with daily peaks of up to 120 kVA, reflecting total demand (Figure 5)

Box 5

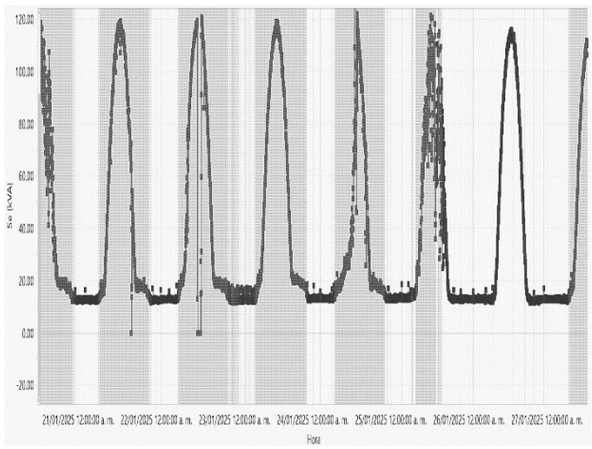

Figure 5
Apparent power variation
Source Generated using Power Quality Analyser

So a particular behavior is confirmed in the power triangle, directly affecting the PF that varies clearly between day and night, reaching values close to 1.0 during PV generation and decreasing outside that period, this indicates that the photovoltaic system does not improve the PF while operating, since the PF falls below 0.9 as the production of photovoltaic energy increases, regularizing the PF when there is little energy produced by the panels (Figure 6).

Box 6

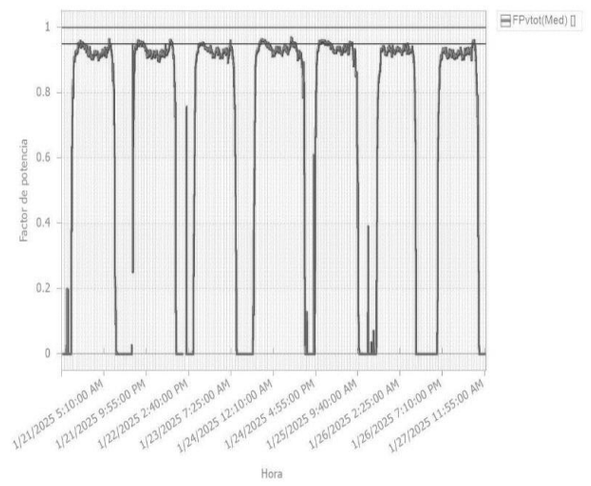

Figure 6
Power factor variation
Source Generated using Power Quality Analyser

Regarding the results of the network analyzers connected to the solar panel panel, it was found that the currents in phases A, B and C show a daily cyclical pattern with peaks greater than 200 A, reflecting the fluctuating demand of load and the start-up of transient equipment,

ISSN: 2523-6881
RENIECYT-SECIHTI: 1702902

Tellez-Hernandez, Felipe, Pineda-Piñón, Jorge, Sánchez-Vega, Guadalupe O. and Mota-Del Carpio, Jimena. [2025]. Efectos de sistemas fotovoltaicos en la calidad de energía y el factor de potencia en la industria, simulación y validación experimental en México. Journal Renewable Energy. 9[21] 1-8: e40921108.
https://doi.org/10.35429/JRE.2025.9.21.4.1.8

these variations show the influence of photovoltaic generation and the changes in the connected load with respect to the potencias, la activa sigue un diurnal behavior with peaks of up to 104.8 kW, while reactive behavior varies between 15 and 30 kVAr, presenting at times values close to zero or even negative, which indicates a partial compensation of reagents by investors (Figures 7).

Box 7

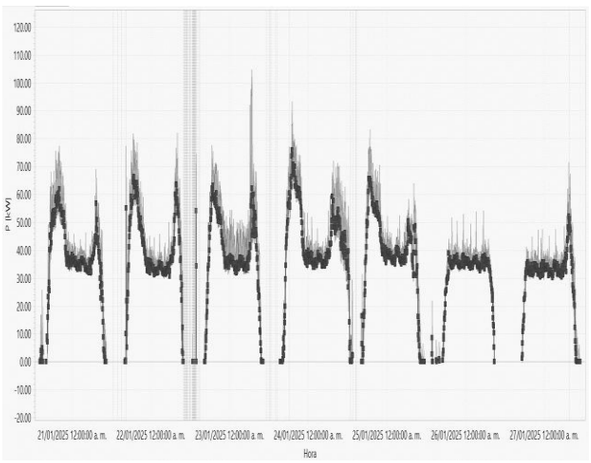

Figure 7

Active power variation in the photovoltaic system

Source Generated using Power Quality Analyser

The apparent power reaches up to 151.5 kVA, clearly showing the interaction between photovoltaic generation and energy demand (Figure 8). The power factor, on the other hand, presents high variability, with periods below the regulatory threshold of 0.9, reflecting fluctuations in the demand for reactive power and insufficient compensation from investors at certain times. In addition, current harmonics were recorded above the established limits, with a TDD of up to 11.76%, in breach of the RED 2.0 regulation. and a current imbalance that reached up to 77.82%, also outside the permitted limits.

Box

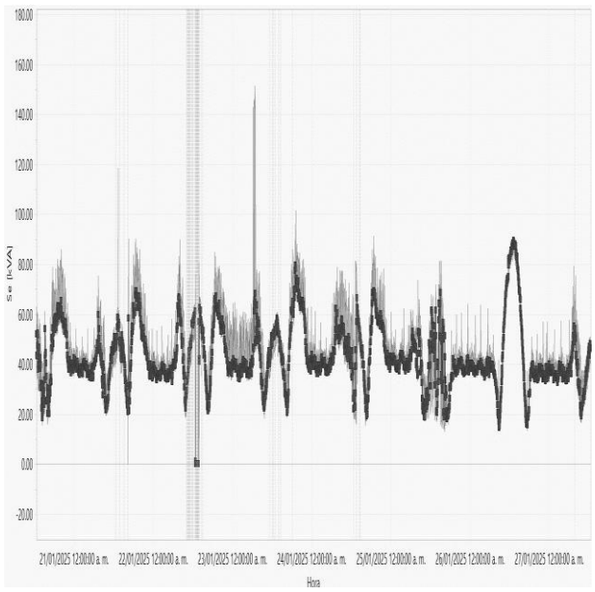

Figure 8

Apparent power variation in the photovoltaic system

Source Generated using Power Quality Analyser

Conclusions

The power quality analysis carried out revealed three problems that compromise the efficiency and reliability of a photovoltaic system (PVS) and the internal grid. First, the power factor presented an average of 0.69, a value significantly lower than the regulatory minimum of 0.90, which generates inefficiencies and cost overruns in electricity billing. Secondly, an excess of harmonics was identified, particularly in orders 3 and 5, failing to comply with the standards established in the Network Code and affecting the quality of the electricity supply. Finally, a current imbalance of more than 15% was observed, a situation that can cause overheating and reduce the useful life of transformers and critical equipment.

Declarations

Conflict of interest

The authors declare that there is no conflict of interest. They have no known competitive financial interests or personal relationships that could have influenced the work reported in this article.

Conflict of interest

The authors declare no interest conflict. They have no known competing financial interests or personal relationships that could have appeared to influence the article reported in this article.

ISSN: 2523-6881
RENIECYT-SECIHTI: 1702902

Tellez-Hernandez, Felipe, Pineda-Piñón, Jorge, Sánchez-Vega, Guadalupe O. and Mota-Del Carpio, Jimena. [2025]. Efectos de sistemas fotovoltaicos en la calidad de energía y el factor de potencia en la industria, simulación y validación experimental en México. Journal Renewable Energy. 9[21] 1-8: e40921108.
https://doi.org/10.35429/JRE.2025.9.21.4.1.8

Authors' contribution

Tellez-Hernández, Felipe: Conceptualization of research, development of simulations in DWTP, data collection with power quality analyzers, writing of the original draft and validation of results.

Pineda-Piñón, Jorge: Supervision of the experimental stage, guide in the application of international standards (IEEE 519-2014, IEEE 1547-2018, NOM-EM-007-CRE-2017) and critical review of the methodology.

Sánchez-Vega, Guadalupe O.: Contributed to data analysis, measurement processing of the Fluke 435-II and Metrel MI 2892 equipment, preparation of tables and figures.

*Mota-Del Carpio, Jimena***:** Supported the experimental stage, assisting in equipment configuration, field data acquisition, and verification of system performance.

Availability of data and materials

The datasets generated and/or analyzed during this study are available upon request from the corresponding author. The raw measurement files of the Fluke 435-II and Metrel MI 2892 analyzers, as well as the ETAP simulation files, have been archived and can be shared for academic purposes.

Funding

This work has been funded by SECHITI [NA]; PRODEP [NA].

Thanks

The authors wish to thank the National Polytechnic Institute (CICATA-IPN Querétaro) for the academic support, and the collaborating industrial company for allowing access to its facilities and operational data.

Abbreviations

FP – Power Factor
CFE - Federal Electricity Commission
FP - Power Factor
kVA - Kilovolt-ampereo
kVAr - Reactive Kilovolt-ampere
kW – Kilowatt
PV – Photovoltaic
PVGIS - Photovoltaic Geographic Information System
SFV - Photovoltaic System
THD - Total Harmonic Distortion

References

Antecedents

Anny, H. R., Agustin, I. R., & Ricardo, C. H. (2025). Increasing photovoltaic hosting capacity in distribution networks in Puerto Rico: Seasonal and technical characteristics analysis and solutions. *Energy Reports*, *14*, 867–885.

CENACE. (2025). *Centro Nacional de Control de Energia Estadistica de la Energia Generada Liquidada Agregada (MWh) Intermitente y Firme por Tipo de Tecnologia*.

Gandhi, O., Kumar, D. S., Rodríguez-Gallegos, C. D., & Srinivasan, D. (2020). Review of power system impacts at high PV penetration Part I: Factors limiting PV penetration. *Solar Energy*, *210*, 181–201.

IRENA. (2024). *World Energy Transitions Outlook 2024: 1.5°C pathway*.

Li, C. (2018). Comparative performance analysis of grid-connected PV power systems with different PV technologies in the hot summer and cold winter zone. *International Journal of Photoenergy*, *2018*.

SENER. (2024). *Programa Sectorial de Energía 2020-2024*.

Basics

CRE. (2020). *NOM-001-CRE/SCFI-2019*.

CRE. (2021). *MANUAL DE REQUERIMIENTOS TÉCNICOS PARA LA INTERCONEXIÓN DE CENTRALES ELÉCTRICAS AL SISTEMA ELÉCTRICO NACIONAL 2 CONTENIDO*.

DOF. (2017). NOM-EM-007-CRE-2017. *DOF*.

FLUKE. (2012). *Fluke 434-II/435-II/437-II Analizador trifásico de energía y calidad de la energía eléctrica*.

HUAWEI. (2023). *Efficiency Curve Circuit Diagram Reliable Smart Safe*.

ISSN: 2523-6881
RENIECYT-SECIHTI: 1702902

Tellez-Hernandez, Felipe, Pineda-Piñón, Jorge, Sánchez-Vega, Guadalupe O. and Mota-Del Carpio, Jimena. [2025]. Efectos de sistemas fotovoltaicos en la calidad de energía y el factor de potencia en la industria, simulación y validación experimental en México. Journal Renewable Energy. 9[21] 1-8: e40921108.
https://doi.org/10.35429/JRE.2025.9.21.4.1.8

IEEE. (2009). *Monitoring Electric Power Quality maquinas electricas fime (Escuela Superior de Ingeniería Mecánica y Eléctrica Unidad Culhuacan).*

METREL. (2023). *Analizadores de calidad de energía MI 2892 Power Master*.

Supports

Ahsan, S. M., Khan, H. A., Hussain, A., Tariq, S., & Zaffar, N. A. (2021). Harmonic analysis of grid-connected solar PV systems with nonlinear household loads in low-voltage distribution networks. *Sustainability (Switzerland)*, *13*(7).

Hernández-Mayoral, E., Jiménez-Román, C. R., Enriquez-Santiago, J. A., López-López, A., González-Domínguez, R. A., Ramírez-Torres, J. A., Rodríguez-Romero, J. D., & Jaramillo, O. A. (2024). Power Quality Analysis of a Microgrid-Based on Renewable Energy Sources: A Simulation-Based Approach. *Computation*, *12*(11).

ISSN: 2523-6881
RENIECYT-SECIHTI: 1702902

Tellez-Hernandez, Felipe, Pineda-Piñón, Jorge, Sánchez-Vega, Guadalupe O. and Mota-Del Carpio, Jimena. [2025]. Efectos de sistemas fotovoltaicos en la calidad de energía y el factor de potencia en la industria, simulación y validación experimental en México. Journal Renewable Energy. 9[21] 1-8: e40921108.
https://doi.org/10.35429/JRE.2025.9.21.4.1.8

Journal Renewable Energy 9[21]1-9: e50921109
Article

SOLNIDO: Un modelo innovador de incubadora solar para la producción sostenible de pollos

SOLNIDO: A novel solar-powered incubator model for advancing sustainable poultry farming

Marroquín-De Jesús, Ángel[a], Castillo-Martínez, Luz Carmen[b], Soto-Álvarez, Sandra[c] and Olivares-Ramírez, Juan Manuel[d]

[a] Universidad Tecnológica de San Juan del Río • 0000-0001-7425-0625 • 81204
[b] Universidad Tecnológica de San Juan del Río • 0000-0001-7953-0431
[c] Universidad Tecnológica de San Juan del Río • 0009-0002-8604-1577
[d] Universidad Tecnológica de San Juan del Río • 0000-0003-2427-6936

SECIHTI classification:

Area: Engineering
Field: Engineering
Discipline: Energy engineering
Subdiscipline: Solar energy

https://doi.org/10.35429/JRE.2025.9.21.5.1.9
Article History:
Received: June 20, 2025
Accepted: December 31, 2025

* ✉ [dr.ramirorb96@gmail.com]

Abstract

This article presents SolNido, an innovative solar incubator model designed to promote sustainable poultry production in rural and urban communities. The prototype integrates photovoltaic energy, an autonomous electrical storage system, and automatic control of temperature and humidity to ensure optimal incubation conditions. Field tests conducted in San Juan del Río, Querétaro, validated its feasibility, maintaining stable conditions (37.5 ± 0.5 °C and 50–55% relative humidity) and achieving a 20% hatching rate using non-certified eggs. Although preliminary, projections indicate that success rates could exceed 70% when employing certified fertile batches. Beyond its technical performance, SolNido provides strategic advantages such as a 95% reduction in grid energy dependence, significant annual savings in operating costs, and environmental benefits equivalent to preventing 0.14 tons of CO_2 emissions per year. This development underscores the potential of renewable energy innovation in agriculture as a viable pathway to create sustainable, resilient, and socially impactful production systems.

Resumen

Este artículo presenta SolNido, un modelo innovador de incubadora solar diseñado para impulsar la producción avícola sostenible en comunidades rurales y urbanas. El prototipo integra energía fotovoltaica, un sistema autónomo de almacenamiento eléctrico y control automático de temperatura y humedad para asegurar condiciones óptimas de incubación. Las pruebas de campo realizadas en San Juan del Río, Querétaro, validaron su factibilidad, manteniendo condiciones estables (37.5 ± 0.5 °C y 50–55% de humedad relativa) y alcanzando una tasa de eclosión del 20% con huevos no certificados. Aunque preliminares, las proyecciones indican que el éxito podría superar el 70% al emplear lotes fértiles certificados. Más allá de su desempeño técnico, SolNido ofrece ventajas estratégicas como una reducción del 95% en la dependencia de la red eléctrica, ahorros anuales significativos en costos de operación y beneficios ambientales equivalentes a evitar la emisión de 0.14 toneladas de CO_2 por año. Este desarrollo subraya el potencial de la innovación en energías renovables aplicada a la agricultura como vía viable hacia sistemas productivos sostenibles, resilientes y de alto impacto social.

Solar energy, poultry incubation, sustainability

Energía solar, incubación avícola, sostenibilidad

Area: Development of strategic leading-edge technologies and open innovation for social transformation

Citation: Marroquín-De Jesús, Ángel, Castillo-Martínez, Luz Carmen, Soto-Álvarez, Sandra and Olivares-Ramírez, Juan Manuel. [2025]. SOLNIDO: Un modelo innovador de incubadora solar para la producción sostenible de pollos. Journal Renewable Energy. 9[21] 1-9: e50921109.

Introduction

Poultry farming is one of the strategic sectors of food production worldwide. Mexico ranks high in chicken and egg consumption, accounting for more than 37% of the national livestock GDP. However, the incubation process, a key stage for productivity, depends largely on conventional electric incubators that require high energy consumption and, in many cases, generate dependence on fossil fuels.

In 2023-2024, the poultry sector in Querétaro generated a production value of more than 16.203 billion pesos, consolidating itself as a strategic pillar of the local economy, with the municipalities of Tequisquiapan, Ezequiel Montes and Colón as the main contributors (Elsitio Avícola; OEM).

At the national level, Querétaro ranks among the top five producers of chicken meat, along with states such as Veracruz, Jalisco, and Aguascalientes (Unión Nacional de Avicultores; Elsitio Avícola).

The Mexican poultry industry accounts for almost 37% of the national livestock GDP, underscoring its role as one of the most dynamic livestock activities in the country. The state of Querétaro contributes significantly to this dynamic (National Union of Poultry Farmers).

At the local level, there are farms located in rural areas of Querétaro that are advancing with a technological vision, such as the Huevo Santiago company, which is committed to regional development and strengthening the local poultry industry (Huevo Santiago).

Climate change, energy price volatility and the need for autonomy in rural communities make the development of clean, accessible and replicable technologies essential.

Mexico has exceptional solar potential, with average irradiation levels exceeding 5 kWh/m² per day in most of the country, positioning it as one of the countries with the greatest comparative advantages for the use of solar energy. In states such as Querétaro, annual irradiation favours the development of photovoltaic projects and decentralised applications, enabling innovative solutions in productive sectors such as poultry farming.

This availability of solar resources makes photovoltaic energy a viable and sustainable alternative for promoting energy autonomy and reducing dependence on fossil fuels in rural communities.

Box 1

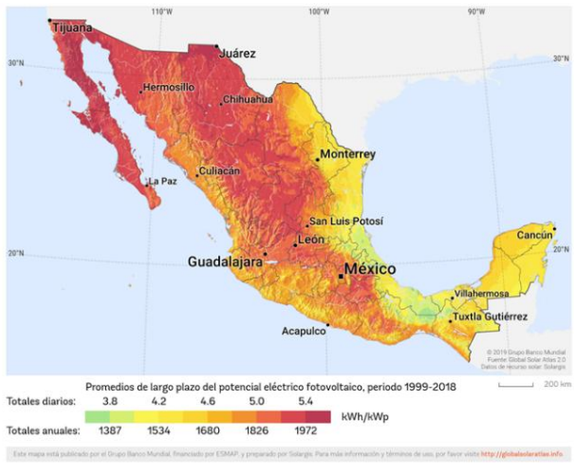

Figure 1

Solarama. (n.d.). Solar radiation in Mexico *https://solarama.mx/blog/radiacion-solar-en-mexico/*

In this context, SolNido emerges: an innovative solar incubator that combines sustainability, efficiency and low operating costs, offering a viable alternative for small and medium-sized producers.

2. Background

The first studies on solar incubators date back to Rubio Picó (1979), who proposed the use of solar thermal panels to replace electric heating in incubators, achieving thermal stability and reducing energy costs. Decades later, García-Hierro Navas (2016) developed a system based on solar thermal collectors applied to the incubation of red-legged partridges, also incorporating smart sensors to monitor biological activity, which allowed for more precise control of temperature and humidity with lower electricity consumption.

In 2019, Corzo Hernández designed and built a low-cost automated incubator at the Technological Institute of Tuxtla Gutiérrez, with a capacity for 30 eggs and controlled by Arduino, which improved incubation efficiency and guaranteed the availability of national spare parts, as well as contributing to the preservation of wild species in UMAs.

ISSN: 2523-6881
RENIECYT-SECIHTI: 1702902

Marroquín-De Jesús, Ángel, Castillo-Martínez, Luz Carmen, Soto-Álvarez, Sandra and Olivares-Ramírez, Juan Manuel. [2025]. SOLNIDO: Un modelo innovador de incubadora solar para la producción sostenible de pollos. Journal Renewable Energy. 9[21] 1-9: e50921109
https://doi.org/10.35429/JRE.2025.9.21.5.1.9

Subsequently, Monta Toapanta (2020) presented a fuzzy control and monitoring system for poultry farms, using solar-powered underfloor heating, which provided an innovative vision of intelligent automation and energy efficiency in poultry production.

Along the same lines, Yerovi Parra (2021) implemented a monitoring and control system with IoT technology applied to chicken incubators in Ecuador, enabling remote supervision of critical parameters and optimisation of the incubation process through digital platforms.

A year later, Franco Sánchez (2022) designed a semi-automatic artisanal incubator for Creole eggs in Ecuador, highlighting the relevance of low-cost solutions adapted to the rural context. In this context, SolNido emerges: an innovative solar incubator that combines sustainability, efficiency and low operating costs, offering a viable alternative for small and medium-sized producers.

Box 2

2. Background

The first studies on solar incubators date back to Rubio Picó (1979), who proposed the use of solar thermal panels to replace electric heating in incubators, achieving thermal stability and reducing energy costs.

Decades later, García-Hierro Navas (2016) developed a system based on solar thermal collectors applied to the incubation of red-legged partridges, also incorporating smart sensors to monitor biological activity, which allowed for more precise control of temperature and humidity with lower electricity consumption.

In 2019, Corzo Hernández designed and built a low-cost automated incubator at the Technological Institute of Tuxtla Gutiérrez, with a capacity for 30 eggs and controlled by Arduino, which improved incubation efficiency and guaranteed the availability of national spare parts, as well as contributing to the preservation of wild species in UMAs. Subsequently, Monta Toapanta (2020) presented a fuzzy control and monitoring system for poultry farms, using solar-powered underfloor heating, which provided an innovative vision of intelligent automation and energy efficiency in poultry production.

Along the same lines, Yerovi Parra (2021) implemented a monitoring and control system with IoT technology applied to chicken incubators in Ecuador, enabling remote supervision of critical parameters and optimisation of the incubation process through digital platforms. A year later, Franco Sánchez (2022) designed a semi-automatic artisanal incubator for Creole eggs in Ecuador, highlighting the relevance of low-cost solutions adapted to the rural context

Complementarily, Hernández Elizondo (2023) addressed the breeding and management of laying hens with a sustainable approach, highlighting responsible production practices that strengthen food security and economic resilience in rural communities. More recently, Romero Pisco, Pérez Cubillos, Pardo Pedraza and Quiñonez Puentes (2025) developed a solar photovoltaic poultry incubator focused on mitigating the effects of power outages, ensuring the continuity of the production process in rural communities in Colombia.

This evolution shows that the application of renewable energies, intelligent automation, sustainable practices, and digital technologies in poultry incubation is technically and socially viable, with different approaches: from solar thermal energy, through digitisation via IoT and low-cost artisanal solutions, to comprehensive models of sustainable production. In this context, SolNido (2025) represents an innovative leap forward by integrating photovoltaic energy, automated control and electrical storage, offering greater autonomy, scalability and replicability in rural areas with limited access to electricity, thereby strengthening food security and productive sustainability.

ISSN: 2523-6881
RENIECYT-SECIHTI: 1702902

Marroquín-De Jesús, Ángel, Castillo-Martínez, Luz Carmen, Soto-Álvarez, Sandra and Olivares-Ramírez, Juan Manuel. [2025]. SOLNIDO: Un modelo innovador de incubadora solar para la producción sostenible de pollos. Journal Renewable Energy. 9[21] 1-9: e50921109
https://doi.org/10.35429/JRE.2025.9.21.5.1.9

3. Methodology

The research was carried out using an applied experimental approach, divided into four phases:

1. Conceptual design: incubation requirements were established (37.5 °C, 50–55% relative humidity, automatic turning every 2 hours).

2. Energy sizing: calculation of the incubator's electricity consumption (35 W, 24 hours/day, 48 hours of autonomy).

The energy balance was calculated as:

$$Ed = Pc \times t = 35W \times 24h = 840\ Wh/day$$

For photovoltaic sizing:

$$Npv = (Ed/(HSP \times Pmod \times \eta)) = ((840/(5 \times 100 \times 0.8)) \approx 2.1\ modules$$

The initial prototype was operated with 1 module (100 W) and a 110 Ah battery, validating minimum viability.

3. Prototype construction: integration of automatic temperature and humidity control systems, thermally insulated incubation chamber, ventilation system, and turning mechanisms.

4. Experimental testing: incubation of 20 eggs in the UTSJR renewable energy laboratory, with temperature, humidity, and ovoscopy monitoring.

Fig. 2. Electrical diagram of the photovoltaic system implemented in the SolNido prototype. Source: Own elaboration, 2024.

Commercial components that are easily accessible on the domestic market were used in the construction of the SolNido prototype. The charge control system consisted of a generic PWM solar controller with an integrated LCD screen, 5 V USB outputs and basic protection functions (microprocessor control, voltage adjustment, built-in timer and total protection). This device enabled the management of energy flow between the photovoltaic panel, the battery and the incubator, ensuring a stable and secure supply.

An Epcom Power Line sealed deep cycle battery, model PL-110B-12, with a capacity of 110 Ah at 12 V DC, was used for energy storage. This component provided the energy autonomy required during periods without solar radiation, ensuring the continuity of the incubation process for up to 48 hours.

Box 3

Figure 3

SolNido solar incubator prototype

Source: Own Elaboration.

The incubation system was implemented using a YUNJAS automatic incubator, with a nominal power of 35 W and the capacity to operate on alternating current (110 VAC, 50–60 Hz) and direct current (12 VDC). The incubator is equipped with an LED panel that allows for the configuration and monitoring of temperature and humidity, as well as a backup system that automatically switches from the mains (110 VAC) to battery power (12 VDC) in the event of power outages, ensuring.

Box 4

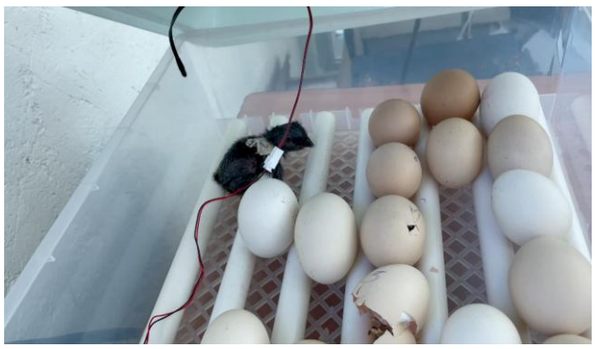

Figure 4

SolNido solar incubator prototype undergoing field testing at the Technological University of San Juan del Río

Source: Own Work

ISSN: 2523-6881
RENIECYT-SECIHTI: 1702902

4. Results

The prototype maintained an average temperature of 37.5 ± 0.5 °C and relative humidity in the range of 50–55%, conditions that remained stable throughout the incubation cycle and confirm the adequate performance of the control system. To maintain humidity, it was necessary to manually add approximately two litres of water to the incubator's reservoir every three or four days, as the prototype did not have an automatic supply system.

The hatch rate was 20%, a result conditioned by the nature of the eggs used, as they were provided without fertility certification. It is important to note that there was no certainty that all the eggs had been fertilised by a rooster; that is, some may have been fertile eggs, while others were probably only unfertilised laying eggs. In this context, it is projected that the system could achieve hatch rates of over 70% when using selected and verified fertile batches.

Likewise, the prototype recorded a 95% reduction in dependence on the electrical grid, as it was powered most of the time by direct current voltage from a solar-charged battery. This operating scheme resulted in an estimated environmental benefit of 0.14 tonnes of CO_2 avoided per year, directly contributing to the mitigation of emissions associated with the use of conventional electricity.

Box 5

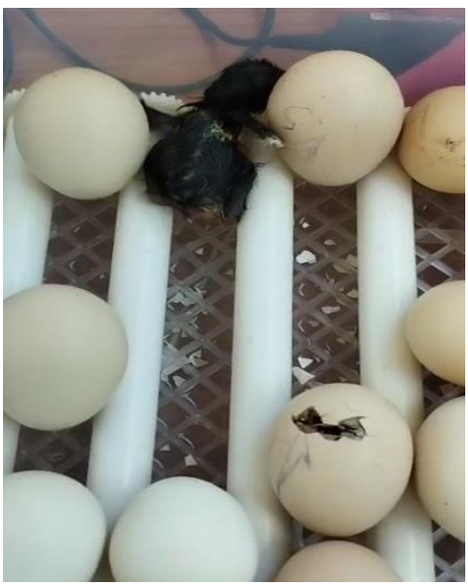

Figure 5

Chicks hatched during the experimental phase of the SolNido prototype

Source: Own Work

Ovoscopy is a technique used to observe the inside of an egg during the incubation process, using a light source to check fertility and embryonic development. Figure X shows an egg placed in the incubator's integrated ovoscope, where light passes through the shell and reveals its internal state. This procedure is essential for identifying fertile eggs (fertilised and developing), as well as for discarding unfertilised or unviable eggs that could affect the process if they remain in the incubator. In tests carried out with the SolNido prototype, candling confirmed that some of the eggs introduced were only unfertilised laying eggs, which largely explains the limited hatching rate of 20% recorded in this first experimental stage.

Box 6

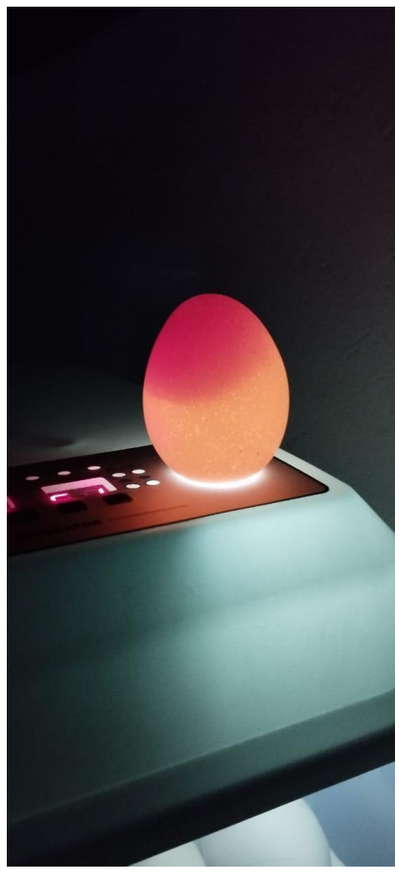

Figure 6

Egg candling, different stages of embryonic development during testing with SolNido

Source: Own Work

5. Comparison with commercial incubators

SolNido was compared with a conventional 100-egg incubator and a commercial 500-egg incubator:

ISSN: 2523-6881
RENIECYT-SECIHTI: 1702902

Box 7

Table 1
Comparison between different incubators

Indicator	Conventional (100)	Commercial (500)	SunNest (20)
Monthly energy consumption	45 kWh ($270 MXN)	225 kWh ($1350)	2 kWh ($12)
Annual electricity cost	$3,240 MXN	$16,200 MXN	$144 MXN
CO_2 emissions (kg/year)	235	1,176	12
Autonomy during power cuts	0 h	0 h	48 h
Initial equipment cost	$12,000 MXN	$65,000 MXN	$6,500 MXN

The brooder box is an essential device for the initial housing of chicks after hatching, as it ensures shelter, warmth and well-being from the first day of life. It is made of corrugated cardboard and has a bed of sawdust at the bottom, which helps to keep the space dry, clean and comfortable. Heat is provided by a 60-watt Philips incandescent lamp, powered by 110 volts of alternating current, which guarantees a suitable temperature for the chicks' development. Instinctively, the chicks move closer to or further away from the lamp according to their thermal needs, thus regulating their comfort. The box is also equipped with water and feed dispensers, which cover the basic nutrition and hydration requirements during the first days of life.

Box 8

Figure 7
Corrugated cardboard brooder box with newly hatched chicks, equipped with a 60 W Philips incandescent lamp, sawdust on the bottom, and feed and water dispensers
Source: Own Elaboration

Box 9

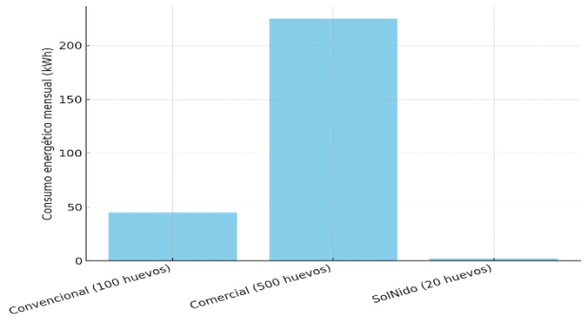

Figure 8
Comparison of annual energy consumption between a conventional incubator, a commercial incubator and the SolNido prototype. Source: own elaboration with experimental and manufacturer data, 2024
Source: Own Elaboration

Twenty-one days after hatching, the chicks show visible development in their morphology and behaviour. Their plumage has changed from an initial state of soft tufts to a denser covering, predominantly black in colour, with uniform growth on the wings, back and neck. A differentiation in the length and strength of the limbs can be observed, with well-formed legs and defined scales, allowing for greater mobility and stability. Body weight has increased significantly since birth, estimated to be in the range of 250 to 300 grams, depending on genetics and nutrition. Their behaviour reflects greater autonomy: they actively explore the brooder box, feed independently from the dispensers and display gregarious behaviour typical of the species. The breeding box is made of corrugated cardboard with a sawdust base and equipped with water and balanced feed dispensers, ensuring adequate hygiene and nutrition for this stage of growth.

Box 10

Figure 9
Chickens 21 days after hatching, showing plumage development and limb strength
Source: authors, 2024

ISSN: 2523-6881
RENIECYT-SECIHTI: 1702902

Figure 10 shows the Governor of the State of Querétaro, Mauricio Kuri González, accompanied by the Rector of the Technological University of San Juan del Río, Fernando Ferrusca Ortíz; the Secretary of Education, Dr Martha Elena Obregón Soto; Dr Ángel Marroquín de Jesús, professor of Renewable Energy; and Dr. Juan Manuel Olivares Ramírez, Director of the Chemistry and Renewable Energy Division, during the Citizens' Conference held on 23 July 2023 in the city of San Juan del Río, Querétaro. At this event, the SolNido project was presented as an example of technological innovation with social and productive impact.

Box 1 1

Figure 10

From left to right and in the foreground, the Governor of the State of Querétaro, Mauricio Kuri González, Rector of the Technological University of San Juan del Río, Fernando Ferrusca Ortíz, Secretary of Education, Martha Elena Obregón Soto, Ángel Marroquín de Jesús, and Juan Manuel Olivares Ramírez.

The economic and social impact of the SolNido prototype is particularly significant when analysing its projections in terms of savings, income and sustainability. At the household level, savings in electricity consumption reach approximately £2,000 per year, allowing the initial investment to be recovered in an estimated period of two years, generating net profits thereafter. Furthermore, considering a projected hatch rate of 70% with fertile eggs, each family could earn up to an additional £7,560 per year through the sale of chickens, providing a source of self-employment and productive diversification.

From a regional perspective, if the model were adopted by 100 rural families, the impact would multiply considerably: collective savings of more than £2,000 per year would be achieved, a reduction of approximately 22 tonnes of CO_2 per year and an estimated production of 8,400 chickens, directly contributing to food security and strengthening the local economy.

To put this environmental benefit into perspective, the reduction in emissions is equivalent to planting around 1,000 trees or avoiding the consumption of more than 9,000 litres of petrol in a year, which reinforces the relevance of SolNido as a sustainable solution.

These results demonstrate that SolNido is not only a technological prototype, but also a strategic tool capable of improving quality of life, generating sustainable income, and promoting more equitable and resilient rural development.

6. Discussion

The results obtained with SolNido confirm that the integration of renewable energies in poultry incubation is technically and socially viable, showing that it is possible to achieve stable temperature and humidity conditions with minimal energy consumption and high autonomy from the electricity grid.

Compared to early attempts at solar incubation based on thermal collectors (Rubio Picó, 1979; García-Hierro Navas, 2016), SolNido represents a significant advance by integrating photovoltaic energy, automatic control and electrical storage, which provides total independence from the grid.

Compared to low-cost proposals such as that of Corzo Hernández (2019), which used Arduino as a control system, this project stands out for offering a comprehensive solution that combines technological accessibility, operational reliability and environmental sustainability.

The fuzzy control system proposed by Monta Toapanta (2020) demonstrated the importance of advanced automation, although its complexity may limit replication in rural areas. In contrast, SolNido prioritises operational simplicity and scalability, making it more suitable for small and medium-sized producers who require robust but easy-to-operate systems.

ISSN: 2523-6881
RENIECYT-SECIHTI: 1702902

Similarly, the semi-automatic incubators developed in Ecuador (Franco Sánchez, 2022) and the sustainable production guidelines (Hernández Elizondo, 2023) find a point of convergence in this model, which ensures both productive efficiency and environmental responsibility. At the regional level, the experience of Romero Pisco et al. (2025) in Colombia reinforces the need for solar incubators as an energy resilience strategy in the face of power outages. In this context, SolNido responds to the Mexican context and has the potential for technology transfer to rural communities seeking sustainable production alternatives. Finally, the path towards digitalisation, proposed by Yerovi Parra (2021), opens up the possibility for future versions to incorporate remote monitoring through IoT, strengthening the traceability, control and efficiency of the process.

However, certain limitations observed in this first experimental phase should be noted. The initial hatching rate (20%) was conditioned by the lack of certainty regarding the fertility of the eggs used, as they were provided without prior certification or verification. As a result, both potentially fertilised eggs and unfertilised laying eggs were incubated, which reduced the success rate. Furthermore, the prototype depends on seasonal solar availability and still requires additional scalability testing, as its current capacity is limited. Overcoming these limitations will involve the use of verified batches of fertile eggs, the incorporation of automatic humidification systems, and the development of higher-capacity models that consolidate the productive and social impact of the proposal.

7. Conclusions

The development of the SolNido prototype confirms the technical feasibility of using photovoltaic solar energy in poultry incubation processes, demonstrating that it is possible to maintain stable temperature (37.5 ± 0.5 °C) and relative humidity (50–55%) conditions with a reduction of more than 90% in energy costs compared to conventional incubators. This performance validates the potential of integrating clean and accessible technologies into a strategic sector such as poultry farming, contributing directly to the reduction of CO_2 emissions and the strengthening of agricultural sustainability in rural and peri-urban contexts.

The results obtained in this experimental phase, although preliminary, show a hatching rate of 20% with non-certified eggs, which was conditioned by the lack of certainty regarding the fertility of the eggs used. However, it is projected that, by using verified fertile batches, the system could achieve hatch rates of over 70%, confirming its potential for scaling up to versions with a capacity of 200 to 500 eggs, while maintaining the principle of autonomous and sustainable operation.

Beyond its technical achievements, SolNido should be understood as an innovative proposal with high social impact, capable of improving the quality of life of families through the generation of self-employment, productive diversification, and the strengthening of food security. Its implementation opens up the possibility of developing community solar farms, operating under a maquila scheme in which different producers can access controlled, homogeneous and low-cost incubation processes, promoting productive equity and local cooperation.

In short, SolNido transcends the status of an experimental prototype to establish itself as a technological vision of the future, characterised by its replicability, social relevance and contribution to the energy transition of the agricultural sector. Its eventual mass adoption could constitute a transformative strategy for poultry farming in Mexico and Latin America, by articulating energy innovation, productive efficiency and environmental responsibility as pillars of a more just, resilient and sustainable rural development model.

8. Future projections

The SolNido project has the potential to evolve into higher-capacity versions, with incubators for between 200 and 500 eggs, integrating more efficient ventilation systems and optimised heating. Likewise, the incorporation of hybrid solar energy and electricity grid schemes is planned, guaranteeing the continuity of the process even in seasons of low solar radiation. Digitisation through smart sensors and integration with IoT technologies will enable real-time remote monitoring and traceability of the process, providing greater reliability and efficiency.

ISSN: 2523-6881
RENIECYT-SECIHTI: 1702902

Marroquín-De Jesús, Ángel, Castillo-Martínez, Luz Carmen, Soto-Álvarez, Sandra and Olivares-Ramírez, Juan Manuel. [2025]. SOLNIDO: Un modelo innovador de incubadora solar para la producción sostenible de pollos. Journal Renewable Energy. 9[21] 1-9: e50921109
https://doi.org/10.35429/JRE.2025.9.21.5.1.9

At the social level, the proposal could take the form of a community solar farm model that functions as a maquila for local producers, where eggs are incubated in controlled and homogeneous conditions at low cost. Similarly, its inclusion in rural extension programmes and government projects would strengthen food security, self-employment and the economic resilience of vulnerable communities. Finally, diversification into other species and analysis of the environmental impact throughout its life cycle will consolidate SolNido as a replicable, sustainable technology with a high social impact in Mexico and Latin America.

9. Acknowledgements

The authors would like to thank the Technological University of San Juan del Río (UTSJR) for its institutional support, the members of the renewable energy academic body who contributed to the improvement of this work with their comments, the students of the ER01SM23 group of the Renewable Energy degree programme who participated in the testing and development of the SolNido prototype, Miguel Angel Ramírez Colin, for the tests carried out, and Verónica García Huerta for providing the eggs for this study.

10. References

Admin. (2023). *Incubación de pollos*. Actualidad Avícola.

Alfonso, R. (2024). *Inversores de onda pura en sistemas fotovoltaicos aislados*. Documento técnico.

Corzo Hernández, S. (2019). *Diseño y construcción de una incubadora para mejorar la eficiencia del proceso productivo de incubación de huevos de aves de corral* (Informe final). TecNM – IT Tuxtla Gutiérrez.

EnergyBatt. (2021). *Baterías de ciclo profundo en aplicaciones solares*. Documento técnico.

Franco Sánchez, P. A. (2022). *Implementación de una incubadora artesanal semi automática para la incubación de huevos criollos*. UNESUM.

García-Hierro Navas, J. (2016). *Aplicación de la energía solar térmica en una incubadora comercial de perdiz roja y supervisión de la actividad biológica mediante sensores inteligentes* (Tesis doctoral). UPM.

Hernández Elizondo, M. J. (2023). *Crianza, reproducción y manejo de la gallina de postura con enfoque sustentable* (Tesis). UAQ.

Monta Toapanta, C. F. (2020). *Sistema de control difuso y monitoreo para granjas avícolas utilizando suelo radiante con energía solar*. UTA.

Planas, J. (2016). *Controladores solares: funciones y aplicaciones*. Documento técnico.

Redacciones. (2019). *Energía solar y su aplicación en sistemas autónomos*. Revista técnica.

Rodríguez Colín, M. (2024). *Prototipo de una incubadora solar* (Trabajo de titulación). UTSJR.

Romero Pisco, C. J., Pérez Cubillos, E. V., Pardo Pedraza, N. X., & Quiñonez Puentes, R. S. (2025). *Incubadora avícola solar: solución energética para la continuidad de la producción ante apagones*. Universidad EAN.

Rubio Picó, J. J. (1979). Aplicación de la energía solar en incubación. *Selaví: Revista Española de Avicultura*, (257), 257–260.

Unión Nacional de Avicultores. (2024). *Industria avícola mexicana: una industria de altos vuelos*. UNA.

Yerovi Parra, G. A. (2021). *Implementación de un sistema de monitorización y control de una incubadora de pollos con tecnología IoT para la empresa privada Incucampos*. ESPOCH.

ISSN: 2523-6881
RENIECYT-SECIHTI: 1702902

Journal Renewable Energy 9[21]1-12: e60921112
Article

Analysis of the ultraviolet radiation profile based on measurements from the UTVM-UNAM solarimetric station and its effects on health

Análisis del perfil de radiación ultravioleta basado en mediciones de la estación solarimétrica UTVM-UNAM y sus efectos sobre la salud

Demillón-Pascual, Rufino*[a], López-Mendoza, Israel[b], Trejo-Leal, Huber Baltazar[c] and Callejas-Mejía, Miriam[d]

[a] Universidad Tecnológica del Valle del Mezquital • RID118250 • 0000-0001-5914-0970 • 412117
[b] Universidad Tecnológica del Valle del Mezquital • RID116099 • 0000-0001-6144-2070 • 466060
[c] Universidad Tecnológica del Valle del Mezquital • RID116098 • 0009-0000-8881-4305 • 167584
[d] Universidad Tecnológica del Valle del Mezquital • RID116094 • 0009-0000-1197-006X • 1344752

SECIHTI classification:

Area: Engineering
Field: Engineering
Discipline: Energy
Subdiscipline: Renewable Energy

https://doi.org/10.35429/JRE.2025.9.21.6.1.12
Article History:
Received: June 20, 2025
Accepted: December 31, 2025

* ✉ [rdemillon@utvm.edu.mx]

Abstract

The need to understand solar energy drives the analysis of solarimetric and meteorological data, as mentioned by (Frederick & Lubin, 1988), who contributed significantly to understanding the effects of UV-B on the Earth's surface and its relationship to the ozone column, as also stated by asegura (Modronich, 1993) in his atmospheric studies. Direct, in-situ measurement of UV-B radiation is essential to establish models and methodologies for its estimation, laying the foundation for more detailed analysis. This research focuses on the dissemination and universal access to science and addresses a study centered on the analysis of the solar ultraviolet type B radiation profile in Ixmiquilpan, Hidalgo, Mexico, based on minute-by-minute measurements at the Ixmiquilpan solarimetric station. The fundamental purpose of this research is to interpret its temporal and spectral profile, obtaining a characteristic curve for each month, as well as annual averages and maximum values in MED/h and UVB index.

Objetives	Methodology	Contribution
To determine the UV-B solar radiation profile based on direct measurements at the RESOLMEX solar radiation monitoring station in Ixmiquilpan, Hidalgo, Mexico.	Bibliographic documentation Measurement of UVB radiation over one year Downloading and processing minute-by-minute data Data analysis and results	To obtain surface measurement data as a reference for the Mezquital Valley region; To determine the critical points of UVB radiation during typical hours and months of the year.

Radiation, UV-B, Solar

Resumen

La necesidad de comprender la energía solar, impulsa el análisis de datos solarimétricos y meteorológicos, como lo menciona (Frederick & Lubin, 1988), quienes contribuyeron significativamente a la comprensión de los efectos de la UV-B en la superficie terrestre y su relación en la columna de ozono, así como también lo asegura (Modronich, 1993) con su estudio de la atmosfera. La medición directa en sitio radiación UV-B es fundamental para establecer modelos y metodologías para su estimación, sentando bases para su análisis más detallado. La investigación se enfoca a la Difusión y acceso universal a la ciencia y aborda un estudio centrado en el análisis del perfil de la radiación ultravioleta solar tipo B en Ixmiquilpan, Hidalgo México, a partir mediciones realizadas cada minuto en la estación solarimétrica Ixmiquilpan. El propósito fundamental de esta investigación es interpretar el perfil temporal y espectral de la misma, obteniendo una curva característica de cada mes, los promedios y máximos anuales en MED/hr e índice UVB.

Objetivos	Metodologíaa	Contribución
Determinar el perfil de Radiación Solar UV-B a partir de mediciones directas en la estación solarimétrica de Ixmiquilpan, Hgo, de la RESOLMEX	Documetacion bibliográfica Medición de la radiacion UV de un año Descarga y procesamientode datos minutales Analisis de datos y resultados	Disponer de una referencia de mediciones en superficie en la zona del Valle del Mezquital Determinar los puntos criticos de la radiacion UVb en horas y meses tipicos de un año

Radiación, UV-B, Solar

Area: Promotion of frontier research and basic science in all fields of knowledge

Citation: Demillón-Pascual, Rufino, López-Mendoza, Israel, Trejo-Leal, Huber Baltazar and Callejas-Mejía, Miriam. [2025]. Analysis of the ultraviolet radiation profile based on measurements from the UTVM-UNAM solarimetric station and its effects on health. Journal Renewable Energy. 9[21] 1-12: e40921112.

Introduction

This work presents an analysis of UV-B radiation, aligned with the dissemination and universal access to science. UV-B radiation is a portion of the solar electromagnetic spectrum with wavelengths generally between 290 and 320 nanometers, although some sources define it in the range of 280 to 315 nm (Modronich, 1993). This research seeks to identify patterns, variations, and, crucially, critical points where radiation presents atypical profiles or values of interest.

The results actively contribute to the scientific community by providing a UV-B radiation profile from on-site measurements, promoting new research lines in solar energy, its applications, and implications. In addition, this work contributes to the efforts of other members of the Mexican Solarimetric Network (RESOLMEX), aiming to develop local action plans that may also contribute to global research efforts. Recommendations are proposed in response to adverse UV-B radiation values. The intensity of UV-B radiation reaching the Earth's surface depends on the time of day, altitude, atmospheric conditions such as ozone and clouds, and the amount of aerosols (OMS, 2003).

The magnitude of this radiation affects material durability and has biological importance due to its ability to interact with living organisms, potentially causing cellular damage (uvb.nrel.colostate.edu, 2025), However, it is also essential for vitamin D production in human skin (FDA, 2025). Extreme values prompt preventive measures to avoid health risks.

1.- Ultraviolet Radiation and the Electromagnetic Spectrum

Ultraviolet radiation has shorter wavelengths than visible light and ranges from 10 nm to 400 nm (Lazara & Perez, 2022); Lázara & Pérez Below 200 nm, this radiation is toxic to living beings. Ultraviolet radiation is classified into three categories: UVA (315–400 nm), UVB (280–315 nm), and UVC (100–280 nm) (Lazara & Perez, 2022).

The Sun emits radiant energy in all directions, including large explosions that cause solar wind affecting our planet.

The Earth's atmosphere filters and sustains life, allowing UV radiation near 300 nm to pass through (Modronich, 1993), Radiation from 10 to 120 nm is highly energetic but absorbed by the atmosphere, which is beneficial because it increases thermal energy and atmospheric ionization. This study found that filtered radiation levels are lower than expected, revealing higher values—an important finding for deeper analysis.

Figure 1 shows a simulation of ultraviolet radiation observed from outer space

Box 1

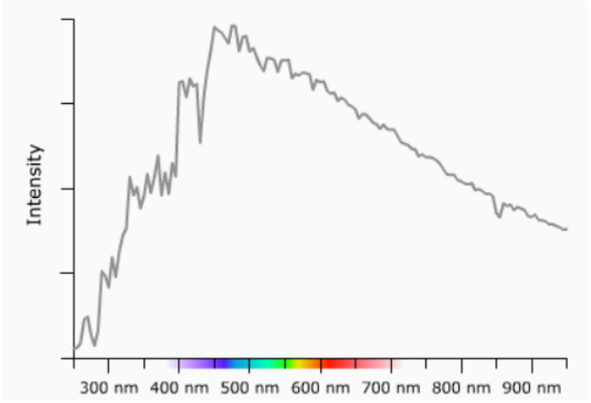

Figure 1

Simulation of the solar spectrum observed from outer space

Source: Nebraska Astronomy Applet Project (NAAP), 2020

2.-Understanding Ultraviolet B (UVB) Radiation

UVB radiation is characterized by its wavelength range, which is between 290 and 320 nanometers, according to the most commonly accepted definition (Modronich, 1993). It is important to note a slight variation in this range, as some sources place it between 280 and 315 nm (Modronich, 1993). Compared to Ultraviolet A (UVA) radiation, which has longer wavelengths, UVB possesses shorter wavelengths and, therefore, higher energy levels. This higher energy of UVB photons is a key factor in its biological effects (Modronich, 1993). A distinctive feature of UVB radiation is its interaction with the Earth's atmosphere. Unlike UVA, which is practically not absorbed by the ozone layer, and Ultraviolet C (UVC), which is completely filtered by the atmosphere, UVB is partially absorbed by the stratospheric ozone layer (Modronich, 1993).

ISSN: 2523-6881
RENIECYT-SECIHTI: 1702902

Demillón-Pascual, Rufino, López-Mendoza, Israel, Trejo-Leal, Huber Baltazar and Callejas-Mejía, Miriam. [2025]. Analysis of the ultraviolet radiation profile based on measurements from the UTVM-UNAM solarimetric station and its effects on health. Journal Renewable Energy. 9[21] 1-12: e40921112
https://doi.org/10.35429/JRE.2025.9.21.6.1.12

This partial absorption means that a fraction of the solar UVB radiation manages to reach the Earth's surface. According to the WHO, the majority of ultraviolet radiation remains in the atmosphere (90%); additionally, this radiation increases by 4% every 300 meters in altitude (OMS, 2003), In this investigation, it is observed that this does not align with what is described by the OMS, as it increases more than what is considered for the monitoring point's altitude. According to the observed data, this means the UV-B radiation levels are higher and, consequently, more harmful to the health of living beings.

3.- The Effects of UVB Radiation on the Skin

The biological effects of UVB radiation are significant. It is well known that UVB is the primary cause of sunburn (NEDA - Northeast Dermatology Associates, 2025) and mainly affects the outer layers of the skin, known as the epidermis (Diffey, 1991).

However, UVB radiation also plays a crucial role in the skin's synthesis of vitamin D (Ultraviolet (UV) radiation, 2025) an essential process for bone and muscle health (FDA, 2025). It also has the ability to directly damage the DNA in skin cells, which in the long term can increase the risk of developing skin cancer, including melanoma (Diffey, 1991). It is crucial to know that the permissible level of sun exposure depends on the skin pigmentation type, from light to dark (see Table 1). As can be observed, it has less impact on people with dark skin.

Box 2

Table 1
Skin type classification

Fototipo de piel	Color de piel	Sensibilidad a la radiación	Descripción
I	Blanca (deficiente en melanina)	Muy sensible	Siempre se quema con facilidad tras la exposición al Sol, raramente se broncea.
II	Blanca (deficiente en melanina)	Muy Sensible	Habitualmente se quema tras la exposición al Sol, algunas veces se broncea.
III	Blanca (con melanina suficiente)	Sensible	Algunas veces se quema tras la exposición al Sol, habitualmente se broncea de manera gradual y uniforme, (café claro).
IV	Café Clara (con melanina suficiente)	Moderadamente sensible	Raramente se quema tras la exposición al Sol, siempre se broncea bien. (café moderado).
V	Café (con protección melanica)	Mínimamente sensible	Rara vez se quema. Se broncea intensamente (café oscuro).
VI	Café oscuro o negro (con protección melanica)	Insensible o mínimamente sensible	Nunca se quema. Se broncea intensamente (café oscuro o negro).

Source: Global Solar UV Index, Practical Guide. OMS, OMM, PNUMA y el ICNIRP. 2003

Knowing skin pigmentation and the UV index, there are studies that show the maximum recommended time for direct exposure to solar radiation in order to avoid adverse health effects (see Figure 2).

Box 3

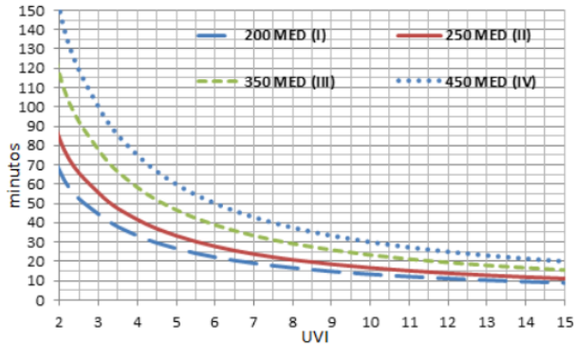

Figure 2
Exposure time in minutes associated with UVI according to skin type
Source: Technical Note N° 002-2016 SENAMHI, pag. 59

As shown in Figure 2, the effect on the skin will depend on the exposure time, the magnitude of UVB radiation, and skin pigmentation. It visualizes the time in minutes necessary to accumulate a 1 MED dose as a function of the UVI and skin type, serving as a guide to take precautions and not exceed the permissible time. Ignoring this can cause erythema, or sensitive skin reddening, for different UVI levels and for each skin type (OMS, 2003), This research shows that the maximum exposure a human being with type IV skin can have in the region of analysis, with a UVI index of 12, is no more than 25 minutes of direct exposure.

Exposure to solar ultraviolet UVB radiation beyond the permissible limit will cause harmful effects on the organism, such as immediate injuries ranging from minor skin reddening to actual burns, or delayed injuries like photoaging, photosensitivity, actinic keratosis, skin cancer, and cataracts. (Diffey, 1991) and (OMS, 2003).

4. Radiaton Intensity UV-B

Figure 3. Shows the factors that influence UV-B radiation levels. The intensity of solar radiation varies due to diverse factors, depending on the situation; according to the time of day and the season of year. Outside of tropical zones, the highest UV radiation intensities occur when the sun reaches its maximum altitude, around solar noon during the summer months (Diffey, 1991) and (OMS, 2003).

The factors to consider regarding intensity are:

ISSN: 2523-6881
RENIECYT-SECIHTI: 1702902

Latitude: The closer to the equator, the more intense the UV radiation (OMS, 2003).

Cloud cover: UV radiation intensity is highest when there are no clouds, but it can be high even with cloud cover. Scattering can produce the same effect as reflection from different surfaces, increasing the total UV radiation intensity (OMS, 2003).

Altitude: At higher altitudes, the atmosphere is thinner and absorbs a smaller proportion of UV radiation. With every 1000-meter increase in altitude, UV radiation intensity increases by 10% to 12% (OMS, 2003).

Ozone: Ozone absorbs part of the UV radiation that would otherwise reach the Earth's surface. Ozone concentration varies throughout the year and even throughout the day (OMS, 2003).

Ground reflection: Different types of surfaces reflect or scatter UV radiation to varying degrees; for example, fresh snow can reflect up to 80% of UV radiation; dry beach sand, around 15%; and sea foam, around 25% (OMS, 2003).

Box 4

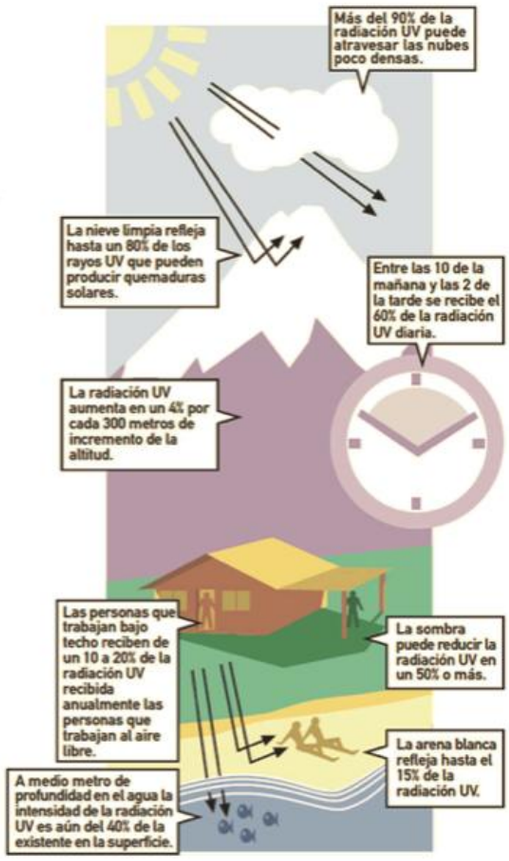

Figure 3
Some factors modify the levels radiations UV-B
Source: OMS, OMM, PNUMA y el ICNIRP

5. Influence of Solar Angle and Atmospheric Path at 2000 masl

At an altitude of 2000 masl, the effect of the sun's daily cycle on UVB intensity is accentuated due to the lower atmospheric density. During the central hours of the day, when the solar angle is high and the path of light through the atmosphere is shorter, the UVB intensity will be even greater at 2000 masl than at sea level under the same solar angle. This is because the lesser amount of atmosphere present offers fewer opportunities for the absorption and scattering of radiation (OMS, 2003) and (Blumthaler & Ambach, 1990).

On the other hand, during the early morning and late afternoon hours, although the general UVB intensity is lower, the reduction compared to the midday peak could be proportionally similar to that observed at sea level. However, the absolute UVB intensity values will still be higher at 2000 masl compared to sea level for the same solar angle (OMS, 2003) and (Blumthaler & Ambach, 1990).

It is important to consider that the ratio between UVA and UVB radiation intensity varies throughout the day. Generally, this ratio is higher in the morning and afternoon, and lower at midday (LearnSkin, 2025). While UVA intensity tends to remain relatively constant during daylight hours, UVB intensity experiences more significant fluctuations based on the solar angle (LearnSkin, 2025). At 2000 masl, this daily variation in the UVA/UVB ratio could have different implications for skin damage and vitamin D synthesis compared to sea level, although the information provided does not specifically detail this aspect, as the altitude in this case is not 2000 masl but is very close.

6. Atmospheric Scattering and Absorption of UVB Radiation

The Earth's atmosphere contains various components that interact with solar radiation, including UVB, through scattering and absorption processes. Ozone (O3) is one of the primary absorbers of UVB radiation in the stratosphere (uvb.nrel.colostate.edu, 2025). Furthermore, air molecules, mainly nitrogen and oxygen, are responsible for the Rayleigh scattering of UV radiation (NOAA Antarctic UV Monitoring Network, 2025).

ISSN: 2523-6881
RENIECYT-SECIHTI: 1702902

Aerosols and dust particles present in the atmosphere also contribute to the scattering and absorption of radiation (Solar and ultraviolet radiation - NCBI, 2025)

At an altitude of 2000 masl, the concentration of these atmospheric components is lower compared to lower altitudes. This lower concentration results in less absorption and scattering of UVB radiation. Therefore, a greater amount of incident UVB manages to reach the surface at this altitud (OMS, 2003) and (Blumthaler & Ambach, 1990).

The solar radiation that reaches the Earth's surface is composed of a direct part, which comes directly from the sun, and a diffuse part, which is the radiation that has been scattered by the atmosphere. (Solar and ultraviolet radiation - NCBI, 2025). It is estimated that a significant portion of UVB, around 70% at a wavelength of 300 nm, corresponds to the diffuse component (Solar and ultraviolet radiation - NCBI, 2025).

At high altitudes, with a thinner atmosphere, the proportion between direct and diffuse UVB radiation could differ from that observed at sea level, which could influence how UVB interacts with surfaces and living organisms. Nonetheless, the consulted documents do not offer specific data on this proportion at 2000 masl, so this is considered another finding.

7. Modification of UVB Patterns by Cloud Cover and Other Atmospheric Conditions

The presence of clouds can significantly alter the amount of UVB radiation that reaches the Earth's surface (UVA vs. UVB Rays: What's the Difference - Healthline, 2025). In general, clouds tend to reduce UVB through absorption and reflection processes (Stratosphere: UV Index: Effects of Clouds - Climate Prediction Center, 2025). However, the magnitude of this effect depends on the type, thickness, and density of the clouds. Thin or scattered clouds may have a minimal effect, and even dense clouds do not completely block UVB (UVA vs. UVB Rays: What's the Difference - Healthline, 2025). Studies indicate that up to 80% of UV rays can pass through clouds (NEDA - Northeast Dermatology Associates, 2025)

It is crucial to highlight the "partly cloudy sky effect," where scattered clouds can even increase UVB radiation due to reflection and scattering (Can Harmful UV Rays Get Through the Clouds, 2025)] Increases of up to 25% or even higher have been reported under these conditions (Stratosphere: UV Index: Effects of Clouds - Climate Prediction Center, 2025). Furthermore, clouds are generally more effective at blocking visible light than UV radiation.

Other atmospheric conditions, such as weather, dust, and air pollution, can scatter UVB radiation, which could reduce the amount that reaches the surface (American Scientist , 2025,) However, the specific impact of these factors at 2000 masl could be different due to the lower overall concentrations compared to lower altitudes.

8. The Daily Cycle of the Sun and UVB Radiation Intensity

The intensity of UVB radiation reaching the Earth's surface is strongly conditioned by the sun's angle relative to the horizon, known as the solar elevation angle (LearnSkin, 2025). Throughout the day, this angle undergoes significant variations. The sun is at its lowest point on the horizon during sunrise and sunset, reaching its maximum elevation around solar noon (Sunwise Toolkit and Samples, 2025).

This variation in the solar angle has a direct impact on the distance that sunlight must travel through the Earth's atmosphere. When the sun is at a high angle, near the zenith, the light passes through a smaller portion of the atmosphere (UVA vs. UVB Rays: What's the Difference - Healthline, 2025). Conversely, in the early morning and late afternoon hours, the sun is at lower angles, which means the sunlight must travel a longer path through the atmosphere (UVA vs. UVB Rays: What's the Difference - Healthline, 2025). As a result of this difference in the atmospheric path, UVB radiation intensity is typically highest around solar noon, the time when the sun reaches its maximum height in the sky (LearnSkin, 2025). Various sources agree that the period of maximum UVB intensity usually occurs between 10 a.m. and 4 p.m. (UVA vs. UVB Rays: What's the Difference - Healthline, 2025), with a more pronounced peak between 11:30 a.m. and 1:30 p.m. (UVA and UVB in sunlight, Optimal Utilization of UV rays in Sunlight for phototherapy, 2025).

ISSN: 2523-6881
RENIECYT-SECIHTI: 1702902

Demillón-Pascual, Rufino, López-Mendoza, Israel, Trejo-Leal, Huber Baltazar and Callejas-Mejía, Miriam. [2025]. Analysis of the ultraviolet radiation profile based on measurements from the UTVM-UNAM solarimetric station and its effects on health. Journal Renewable Energy. 9[21] 1-12: e40921112
https://doi.org/10.35429/JRE.2025.9.21.6.1.12

A practical rule for estimating UVB intensity is to observe the length of an object's or person's shadow. The shadow rule states that the intensity of UVB rays is lower when the shadow is longer than the object's height, which occurs during the morning and afternoon. In contrast, the intensity is highest when the shadow is shorter than the height, a situation that occurs around midday. (LearnSkin, 2025).

9. Impact of Altitude (2000 masl) on UVB Radiation

Altitude is a determining factor in the intensity of UVB radiation that reaches the Earth's surface. As altitude increases, the atmosphere becomes less dense and thinner (Cancer Council NSW, 2025). This lower atmospheric density implies a smaller quantity of molecules capable of absorbing and scattering UV radiation, including UVB (Cancer Council NSW, 2025).

As a direct consequence, the intensity of UVB radiation increases with altitude (UVA vs. UVB Rays: What's the Difference - Healthline, 2025). Various studies have attempted to quantify this increase. It is estimated that for every 1000-meter increase in altitude, UVB radiation levels can increase by 10% to 12% (Cancer Council NSW, 2025), or approximately 12% (Hong Kong Observatory, 2025). Other research suggests an increase of around 7% per kilometer of altitude (The Relationship between Ultraviolet Radiation Exposure and Vitamin D Status - PMC, 2025), while a specific study found an increase of 19% per 1000 meter (Applied and Environmental Microbiology - ASM Journals, 2025).

Considering this data, at an altitude of 2000 masl, a significant increase in UVB radiation intensity would be expected compared to sea level. Based on the 7% to 12% increase range per 1000 meters, UVB intensity at 2000 masl ranges from 14% to 24% higher than at sea level. The 19% per 1000 meters figure suggests an even greater increase of 38%. It is evident that people at this altitude are exposed to considerably higher levels of UVB radiation. (Applied and Environmental Microbiology - ASM Journals, 2025).

Box 5

Table 2

Percentage increase in UV-B intensity per 1000 meters above sea level according to various sources

Source	Percentage Increase per 1000 meters
(Cancer Council NSW, 2025)	10-12%
(Hong Kong Observatory, 2025)	approximately 12%
(The Relationship between Ultraviolet Radiation Exposure and Vitamin D Status - PMC, 2025)	Around 7%
(Applied and Environmental Microbiology - ASM Journals, 2025) 0	19%

Source: Compiled from the sources mentioned

8.- Equivalence of Ultraviolet Radiation to Exposure Category

It is imperative to know the factor level of the radiation that the Earth's crust receives and that impacts living beings. Below, data obtained from NASA (see Table 3) focused on the Mezquital Valley Region are shown.

Box 6

Table 3

Ultraviolet Radiation en mW/m^2

LAT	LON	YEAR	ALLSKY_SFC_UVA
19.5	-102.5	2023	280
19.5	-101.5	2023	260
19.5	-100.5	2023	270
19.5	-99.5	2023	240
19.5	-98.5	2023	260
20.5	-102.5	2023	270
20.5	-101.5	2023	250

Source: NASA Data Base

According to (apogee, 2024) the relationship between the UV index and UV radiation can be approximated by dividing it by 5.7. Figure 4 shows the W/m2 vs. UV index relationship

ISSN: 2523-6881
RENIECYT-SECIHTI: 1702902

Demillón-Pascual, Rufino, López-Mendoza, Israel, Trejo-Leal, Huber Baltazar and Callejas-Mejía, Miriam. [2025]. Analysis of the ultraviolet radiation profile based on measurements from the UTVM-UNAM solarimetric station and its effects on health. Journal Renewable Energy. 9[21] 1-12: e40921112
https://doi.org/10.35429/JRE.2025.9.21.6.1.12

Box 7

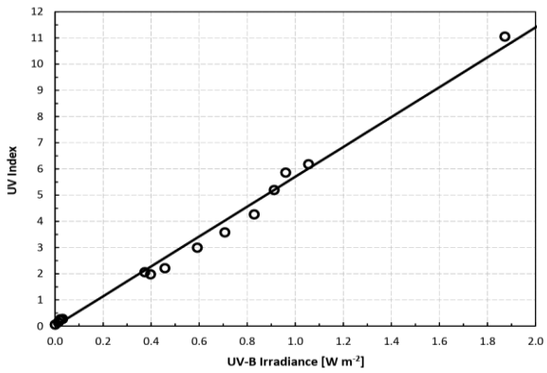

Figure 4
UV index conversion UV chart
Source: Apogee 2024

According to the NASA database, the lowest value recorded in 2023 is 0.05 Wm-2 and the maximum was 0.53 Wm-2. This data indicates that the UV index in the region of analysis ranges between 0 and 21.5, and according to the WHO, the exposure is moderate to high.

UVB Radiation Levels in Ixmiquilpan and its Measurement

As is known by the scientific community, UV radiation levels are not the same everywhere on planet Earth. As specified by (Cortez, y otros, 2011) factors such as: solar elevation, altitude, longitude, latitude, and cloud cover, among others, limit its intensity. It should be noted that the instruments used in this research are located in Ixmiquilpan, Hidalgo; Mexico, at the geographic coordinates: 20.4951° North, -99.1804° West, with an altitude of 1,700 masl. In Figure 5, the Universidad Tecnológica del Valle del Mezquital can be seen.

Box 8

Figure 5
Universidad Tecnológica del Valle del Mezquital
Source: googlemaps, 2025

To know the levels, on-site measurements are required using appropriate equipment, as in this case, a Solar Light Model 501 Biometer.

To know the levels, on-site measurements are required using appropriate equipment, as in this case, a Solar Light Model 501 Biometer.

The measurements are carried out in units of MED/hour, and the UV index, which has a scale from 1 to 15, is commonly used. The system has the capability to display, via the digital monitoring console, the UV radiation intensity in MED/Hour units. Since Ultraviolet Index (UVI) units are normally used in various places, a conversion factor of 2.332 [(MED/Hour * 2.332 = 1 UVI] (02-UVI-Calculations-2-7, 2006), is used, which is the same one employed in this study.

Data acquisition and preprocessing help obtain the solar radiation profile in Ixmiquilpan. The solar radiation profile analysis allows for the identification of the UV-B Radiation level through a critical point analysis and the periods in which they occur.

Table 4 presents the MED/hour equivalent for the 15 UV Index values.

Box 9

Table 4
Equivalentes en MED/hora los 15 valores del IUV

Indice UV	med/Hr
0	0
1	0.43
2	0.86
3	1.29
4	1.72
5	2.14
6	2.57
7	3
8	3.43
9	3.86
10	4.29
11	4.72
12	5.15
13	5.57
14	6
15	6.43

Source: using a conversion factor of 2.332

ISSN: 2523-6881
RENIECYT-SECIHTI: 1702902

Recommendations

Given the higher intensity of UVB radiation at 1700 masl, it is crucial to adopt protective measures, even on cloudy days. It is important to note that the potential [for exposure] increases when reflective surfaces are present, such as snow, whitish soil like that of the Mezquital Valley, or water, which can be more common in high-altitude environments.

Daily UV index forecasts, which are often available, should be consulted and can be useful for planning outdoor activities.

Considering that the soil type in the Mezquital Valley area is limestone (whitish) or predominantly "tepetate" [a hard, light-colored soil], this implies it has a high reflectance of UVB radiation, increasing the intensity of exposure for people.

The most important recommendations to reduce risks are:

- Reduce exposure during the central hours of the day.
- Seek out areas where there is shade.
- Use protective clothing. (Even very thin fabric helps drastically reduce UVB intensity on the skin.)
- Use a wide-brimmed hat to protect the eyes, face, and neck. We should resume the good habits of our parents and grandparents, where wearing a hat was common, and reduce the use of baseball caps, as they cover less and reduce protection from solar radiation.
- Protect the eyes with wrap-around sunglasses or those with side panels.
- Use a broad-spectrum sunscreen with a sun protection factor (SPF) of 15+, applying it generously and as often as needed.
- Avoid tanning beds.

It is particularly important to protect babies and young children.

It would be very helpful for local media to issue alerts to the community when UVB Index values are very high, so that preventive actions can be taken.

Methodology

Given that the research is exploratory in nature, with its specific objectives, the method used for this field study is broken down as follows.

A Solar Light Model 501 Biometer is used, with a spectral range of 280-320nm and a measurement range of 0-10 MED/Hr, for permanent outdoor use. The equipment is a radiometer for solar radiation measurement systems used in meteorological stations and observatories in various parts of the world, with reproducibility for each unit (Solar Light Co. Inc., 2006), It is a high-precision instrument with instantaneous results and non-volatile memory.

This measurement is transferred via fiber optics to a data storage system on a computer using a CR3000 data acquisition system.

The information was downloaded in monthly periods for one year, where, under optimal system operation conditions, one data point per minute is continuously available.

The measurement units for UVB radiation are given in MED/hr in the database, which contains an average of 43,200 data points per month.

The information was analyzed in units of Minimum Erythemal Dose per Hour (MED/Hr). Sixty data points per hour were grouped and averaged for each hour, and then sorted by 24-hour days.

Each hour was grouped by month to calculate the average for hours 1 through 24 from the days contained in each month, in order to obtain a 24-hour monthly average profile in MED/hour units (See Table 6).

The conversion factor was applied to obtain the Ultraviolet Index (UVI), which is the most standardized value, in order to understand its effects in various areas, such as public health.

Through this analysis, the results are graphed to establish a monthly average profile and, finally, the annual profile.

The equivalent for each day per monthly period was obtained, to subsequently calculate a mean daily average for the month, which is the most important final result presented in this work.

ISSN: 2523-6881
RENIECYT-SECIHTI: 1702902

Subsequently, the critical hours and months of maximum radiation are identified to provide a crucial basis for public health decision-making and citizen awareness in the Valle del Mezquital.

Results

After processing a database in the range of 500,000 samples per year to analyze UVB radiation behavior, it was possible to obtain the results shown in Figure 6 and Figure 7.

It is important to mention that the graphs of the on-site measurements will allow for comparison in future stages with other indirect information sources, such as via software or other platforms like NASA's, which has information obtained from satellites.

Box 10

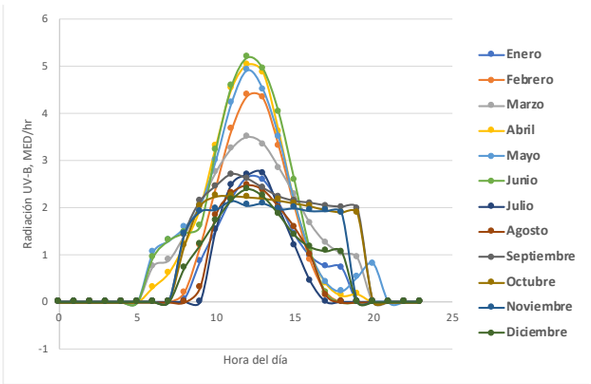

Figure 6

Average daily radiation profile UV-B, MED/Hr

Source: Own Elaboration

Box 11

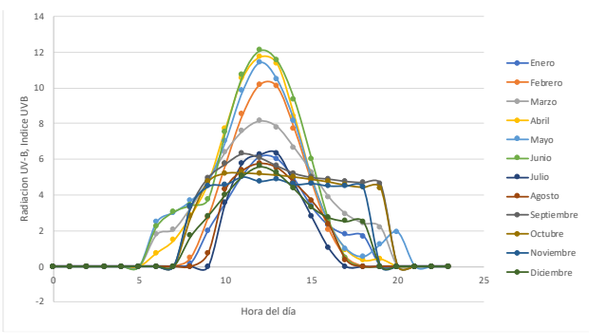

Figure 7

Average daily UV-B radiation profile, UVB INDEX

Source: Own Elaboration

In Figure 7, it can be seen that there are UVB radiation peaks of up to 12 UVI in the month of June, which corresponds with the warmest periods in the Mezquital Valley region. Likewise, it can be observed that the months with the highest intensity were from February to June; in the remaining months, it decreases. This is justified by the planet's tilt relative to the sun, as the radiation arrives at a steeper angle relative to the horizon in the northern latitude, and by the onset of the rainy seasons and the arrival of winter in Mexico.

Therefore, the period from February to June is when the population should be urged to be careful during periods of direct sun exposure. Critical Hours: The period of greatest UV-B intensity is typically found between 10:00 a.m. and 2:00 p.m.

Box 12

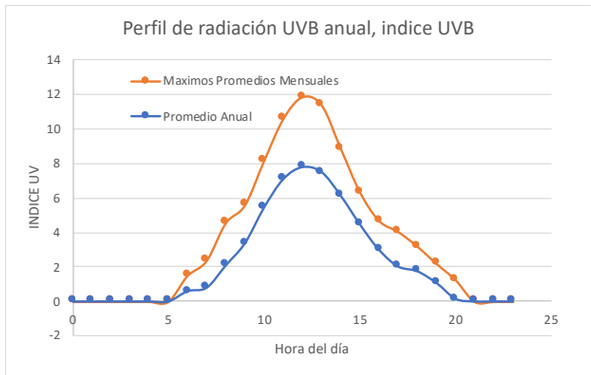

Figure 8

Annual average daily profile of UV-B radiation, average and maximums, UV INDEX

Source: Own Elaboration

Analyzing the final graph of the average and maximums, it can be observed that there are periods of the year with UVB radiation indices of 12, making it possible that, on particular days, these values are exceeded, which represents a greater risk during prolonged sun exposure. Considering Table 5, in the region in question, we are experiencing UVB intensities considered extremely high according to the OMS.

ISSN: 2523-6881
RENIECYT-SECIHTI: 1702902

Demillón-Pascual, Rufino, López-Mendoza, Israel, Trejo-Leal, Huber Baltazar and Callejas-Mejía, Miriam. [2025]. Analysis of the ultraviolet radiation profile based on measurements from the UTVM-UNAM solarimetric station and its effects on health. Journal Renewable Energy. 9[21] 1-12: e40921112
https://doi.org/10.35429/JRE.2025.9.21.6.1.12

Box 13

Table 5

UVB Intensity, Color Scale, and International Exposure Category

CATEGORÍA DE EXPOSICIÓN	INTERVALO DE VALORES DEL IUV
BAJA	<2
MODERADA	3 A 5
ALTA	6 A 7
MUY ALTA	8 A 10
EXTREMADAMENTE ALTA	11 +

Source: IndiceUV Solar Mundial: Guía práctica de la OMS Organización Meteorológica Mundial (PNUMA y Comisión Internacional de Proteccion contra Radiación no ionizante, 2003

Conclusions

The behavior of UVB radiation at an altitude of 1700 masl during the day is characterized by a daily cycle with an intensity peak around solar noon. Due to the lower atmospheric density at this altitude, UVB levels are significantly higher compared to sea level during all hours of the day. The solar angle influences UVB intensity, with shorter atmospheric paths resulting in higher levels. The presence of clouds can modify this pattern, generally reducing the intensity.

Other atmospheric factors can also have an impact. Understanding these patterns is fundamental for taking appropriate precautions and protecting the health of the population at high altitudes, especially during the hours of 10 a.m. to 2 p.m. and the most intense months detected (February to June), where UVB indices are on the order of 12, which is considered extremely high.

In sum, the study provides the first reference of in-situ measurements for this area, establishing that exposure during peak hours and months of highest intensity demands the implementation of urgent preventive measures. It is recommended that local health authorities and media outlets disseminate early warnings about the UVI and promote the adoption of essential protective measures, such as the use of sunscreen, hats, sunglasses, and the reduction of exposure during the highest-risk hours.

It should be noted that these profiles can change due to atypical years; therefore, subsequent years must continue to be characterized to see how this variable evolves over time, and so that in the future the data can be compared with other RESOLMEX stations to quantify its variation due to altitude differences.

Annexes

The 60-minute-per-hour data was averaged to provide one data point per hour, daily, which is equivalent to 720 average data points per month. This was grouped into daily hours to obtain Table 6, which means there are 12 equivalent tables

Box 14

Table 6

Promedios horarios en MED/hora

	Dias									
HORA	1	2	3	4	5	6	7	8	.....	30
0	0.80893	0.80872	0.80318	0.76142	0.79182	0.77322	1.08292	1.11933	.....	-0.00425
1	0.81933	0.81452	0.81042	0.76827	0.80393	0.78998	1.07223	1.13488	.....	-0.00433
2	0.82112	0.81512	0.80968	0.76797	0.80938	0.79427	1.11293	0.09462	.....	-0.00418
3	0.83578	0.82705	0.83355	0.78402	0.81452	0.78685	0.07440	0.04528	.....	-0.00323
4	0.85090	0.84065	0.83705	0.79285	0.81805	0.80092	0.23395	0.06427	.....	-0.00472
5	0.86263	0.84983	0.84635	0.81125	0.83468	0.79922	-0.13273	0.12640	.....	-0.00403
6	0.88173	0.86730	0.86548	0.83940	0.84712	0.81953	-0.10040	0.27395	.....	0.02133
7	1.00455	1.04508	1.09905	1.64623	0.69147	0.86672	0.87760	0.53597	.....	0.26757
8	1.84108	2.06615	2.03642	1.96612	0.80248	1.68078	1.41680	1.55297	.....	1.01485
9	2.24687	2.20767	2.25388	2.06828	2.08808	1.76175	1.83388	1.74938	.....	2.32625
10	2.20018	2.12630	3.98213	3.92277	3.67967	1.82122	3.18508	2.45782	.....	3.94463
11	2.17787	2.10905	5.32670	5.31717	4.94948	1.96853	4.43337	4.49458	.....	5.24030
12	2.04608	2.07723	6.08578	5.78190	5.54367	4.64890	5.11420	5.23518	.....	5.84265
13	2.05728	2.17175	5.48185	5.51860	5.27247	4.82027	5.10850	5.12245	.....	5.53930
14	2.07108	2.13088	3.97613	4.45230	4.13595	3.90778	3.89037	1.68842	.....	4.21790
15	1.98072	1.93103	2.45373	2.82017	2.56305	2.49282	2.29805	1.74682	.....	2.53335
16	1.87345	1.98313	1.25465	1.25747	1.12660	1.05910	1.17377	1.03223	.....	0.98430
17	1.67858	1.75760	0.30727	0.32530	0.83605	0.30930	0.30510	0.28228	.....	0.30750
18	0.79808	0.87580	0.02903	0.21467	0.68537	-0.06048	0.02600	0.02687	.....	0.03493
19	0.76408	0.76060	0.56177	0.63278	0.66053	0.00060	0.00410	-0.00390	.....	-0.00213
20	0.75695	0.77355	0.77320	0.68472	0.76585	0.35963	1.03263	-0.00463	.....	-0.00297
21	0.78907	0.79885	0.76725	0.78523	0.77223	1.03790	1.13632	-0.00500	.....	-0.00322
22	0.79997	0.79458	0.75770	0.79020	0.76990	1.25108	0.86955	0.06672	.....	-0.00345
23	0.80037	0.79407	0.75893	0.80152	0.76918	1.00352	1.02397	0.45018	.....	-0.00315

Source: based on data from the Ixmquilpan, Hgo. solarimetric station

Declarations

Conflict of interest

The authors declare no conflicts of interest. No financial interests or personal relationships exist that could have influenced the content of this article.

Author contribution

Demillón Pascual Rufino, is the Researcher and technical manager responsible for providing technical maintenance for the solarimetric station, downloading data, organizing the information downloaded over a year, and processing it month by month.

ISSN: 2523-6881
RENIECYT-SECIHTI: 1702902

López Mendoza, Israel; Collaborates on the documentation for the development of the theoretical framework and the study design.

Callejas Mejía, Miriam: collaborates by reviewing the graphs obtained from the UV-B radiation and analyzing the profiles.

Trejo Leal, Huber Baltazar: Collaborates in reviewing the structural writing of the scientific article.

Availability of data and materials

The data belong to the Mexican Solarimetric Network (RESOLMEX) and its members, of which we are a part as the Ixmiquilpan solarimetric station, which is in collaboration with the Universidad Tecnológica del Valle del Mezquital (UTVM) and 12 additional (HEIs [Higher Education Institutions] and Research Centers) institutions at the national level.

Funding

The arrangement of all sensors and their installation at the solarimetric station was financed by another part of the Mexican Center for Innovation in Solar Energy (CEMIESOL) project, through sub-project P16 - “National Inventory of Solar Resource (Solar Resource Map)” in coordination with the Institute of Geophysics of UNAM. UTVM collaborates through a commodate agreement for the land and financed all the civil infrastructure.

Acknowledgements

We thank CEMIESOL, through sub-project P16, for funding the sensor of interest and the commissioning of the monitoring system.

We thank the IG of UNAM for its role in coordinating RESOLMEX and for advancing the improvement process for monitoring schemes to obtain higher-quality data.

We thank UTVM for providing the facilities and the funding to present this research work on one variable of interest (out of the 14 available at this time) from the solarimetric station

Abbreviations

CEMIESOL	Centro Mexicano de Innovación en Energía Solar
IG-UNAM	Instituto de Geofisica de la Universidad Nacional Autonoma de México
masl	meters above sea level
MED	Minimal Erithemal Dose
RESOLMEX	Red Solarimetrica Mexicana
UVB	Radiación Ultravioleta B
UTVM	Universidad Tecnológica del Valle del Mezquital
UVI	Indice Ultravioleta

References

Basic

02-UVI-Calculations-2-7. (2006). *CULCyT//Septiembre–Diciembre, 2006, Año 3, No 16-17 , pag. 12,* . Obtenido de http://meteo.lcd.lu/uvi_calculator/02-UVI-Calculations-2-7.PDF

Diffey, B. L. (1991). *Solar ultraviolet radiation effects on biological systems*. *Physics in Medicine and Biology, 36(3), 299–328. 1*.

Frederick, J. E., & Lubin, D. (1988). Te bugdet of biologically active ultraviolet radiation in the hear-atmosphere system. Journal of Geographysical Researh: Atmospheres, 93(D3), 3825-3832

Lazara, A., & Perez, M. (2022). *La radiación ultravioleta y su impacto ambiental*. Editorial Solar.

Modronich, S. (1993). *La otmosfera y la radiación UV-B a nivel de suelo. MTevini (Ed), Radiación UV-B y agotamiento de Ozono: Efectos sobre los humanos, animales, plantas, microorganismos y materiales (pp. 1-39)*. CRC Press.

NEDA - Northeast Dermatology Associates. (4 de abril de 2025). *What You Need to Know About UV Radiation*.

Solar and ultraviolet radiation - *NCBI*. (2025 de Abril de 2025).

uvb.nrel.colostate.edu. (4 de Abril de 2025).

ISSN: 2523-6881
RENIECYT-SECIHTI: 1702902

Support

American Scientist . (4 de abril de 2025,). *Sunshine on a Cloudy Day*.

Applied and Environmental Microbiology - ASM Journals. (04 de abril de 2025). *Diverse Responses to UV-B Radiation and Repair Mechanisms of Bacteria Isolated from High-Altitude Aquatic Environments*.

apogee, i. (20 de junio de 2024). *ULTRAVIOLET INDEX* . Obtenido de ULTRAVIOLET-B SENSOR: chrome-extension://efaidnbmnnnibpcajpcglclefindmkaj/

Can Harmful UV Rays Get Through the Clouds. (4 de abril de 2025).

Cancer Council NSW. (4 de abril de 2025). *Factors that affect UV radiation levels*.

Cortez, A., Enciso , J., Reyes, C., Arriaga, E., Romero, C., Ribes, J., . . . Hernández, M. (2011). El índice ultravioleta en el ámbito laboral: un instrumento educativo. *Medicina y Seguridad del Trabajo, 57*(225), 319-330. doi:https://dx.doi.org/10.4321/S0465-546X2011000400006

LearnSkin. (4 de abril de 2025). *UVA/UVB Rays & Sun Exposure & Change Ratio*.

OMS. (10 de junio de 2003). *Índice UV Solar Mundial*. Obtenido de Guía práctica: chrome-extension://efaidnbmnnnibpcajpcglclefindmkaj/

Solar Light Co. Inc. (2006). Manual del usuario, . *UV - BIOMETER* . Philadelphia. , USA: Copyright 2006.

Stratosphere: UV Index: Effects of Clouds - Climate Prediction Center. (4 de Abril de 2025).

Sunwise Toolkit and Samples. (4 de abril de 2025).

The Relationship between Ultraviolet Radiation Exposure and Vitamin D Status - PMC. (04 de abril de 2025).

Ultraviolet (UV) radiation. (4 de abril de 2025).

UVA and UVB in sunlight, Optimal Utilization of UV rays in Sunlight for phototherapy. (4 de abril de 2025).

Differences

Blumthaler, M., & Ambach, W. (1990). *Indication of increasing solar ultraviolet-B radiation flux in alpine regions. Science, 248(4952), 206–208*.

FDA. (04 de abril de 2025). *Ultraviolet (UV) Radiation*.

Hong Kong Observatory. (4 de abril de 2025). *Ultraviolet radiation at high altitude*.

NOAA Antarctic UV Monitoring Network. (4 de abril de 2025).

UVA vs. UVB Rays: What's the Difference - Healthline. (4 de abril de 2025). Obtenido de

(uvb.nrel.colostate.edu, 2025)

ISSN: 2523-6881
RENIECYT-SECIHTI: 1702902

Demillón-Pascual, Rufino, López-Mendoza, Israel, Trejo-Leal, Huber Baltazar and Callejas-Mejía, Miriam. [2025]. Analysis of the ultraviolet radiation profile based on measurements from the UTVM-UNAM solarimetric station and its effects on health. Journal Renewable Energy. 9[21] 1-12: e40921112
https://doi.org/10.35429/JRE.2025.9.21.6.1.12

Journal Renewable Energy 9[21]1-8: e70921108
Article

Sweet sustainability: Comparative study of solar and electric cooking in the production of crystallized orange peel candy

Dulce sostenibilidad: Estudio comparativo de la cocción solar y eléctrica en la elaboración de dulce cristalizado de cáscara de naranja

Castillo-Martínez, Luz-Carmen[a], Marroquín-De Jesús, Ángel[b]*, Alonso-Arroyo, Juana[c] and Olivares-Ramírez, Juan Manuel[d]

[a] Universidad Tecnológica de San Juan del Río • 0000-0001-7953-0431
[b] Universidad Tecnológica de San Juan del Río • 0000-0001-7425-0625 • 81204
[c] Universidad Tecnológica de San Juan del Río
[d] Universidad Tecnológica de San Juan del Río • 0000-0003-2427-6936

SECIHTI classification:

Area: Engineering
Field: Engineering
Discipline: Energy engineering
Subdiscipline: Solar energy

https://doi.org/10.35429/JRE.2025.9.21.7.1.8
Article History:
Received: June 20, 2025
Accepted: December 31, 2025

* ✉ [dr.ramirorb96@gmail.com]

Abstract

Food waste represents one of the most pressing global challenges for sustainability. Among the most abundant by-products of the food industry is orange peel, whose potential applications remain underexploited. This study explores the elaboration of crystallized orange peel candy using two different cooking methods: an electric stove and a parabolic solar stove. The objective was to compare their efficiency, preparation times, and the sensory quality of the final product through attributes such as color, aroma, flavor, and texture. Experimental results revealed that the solar stove achieved competitive cooking performance, reaching adequate temperatures to ensure food safety and acceptable sensory characteristics, while reducing energy consumption and greenhouse gas emissions. In comparison with the electric stove, the solar method demonstrated longer preparation times but offered a cleaner and more sustainable alternative. Overall, the findings highlight solar cooking as a viable strategy that contributes to renewable energy use, circular economy, and sustainable food practices.

Orange peel, solar stove, crystallized candy, renewable energy, sustainability

Resumen

El desperdicio de alimentos constituye uno de los mayores retos globales para la sostenibilidad. Entre los subproductos más abundantes de la industria alimentaria se encuentra la cáscara de naranja, cuyo aprovechamiento sigue siendo limitado. Este estudio presenta la elaboración de dulce cristalizado de cáscara de naranja utilizando dos métodos de cocción: una parrilla eléctrica y una estufa solar parabólica. El objetivo fue comparar su eficiencia, los tiempos de preparación y la calidad sensorial del producto final en atributos como color, aroma, sabor y textura. Los resultados experimentales mostraron que la estufa solar alcanzó temperaturas suficientes para garantizar inocuidad y características sensoriales aceptables, reduciendo al mismo tiempo el consumo energético y las emisiones asociadas. En comparación con la parrilla eléctrica, el método solar requirió mayor tiempo de cocción, pero demostró ser una alternativa más limpia y sostenible. En conjunto, los hallazgos confirman a la cocción solar como estrategia viable que impulsa la economía circular y el uso de energías renovables.

Cáscara de naranja, estufa solar, dulce cristalizado, energía renovable, sostenibilidad

Area: Development of strategic leading-edge technologies and open innovation for social transformation

Citation: Castillo-Martínez, Luz-Carmen, Marroquín-De Jesús, Ángel, Alonso-Arroyo, Juana and Olivares-Ramírez, Juan Manuel. [2025]. Sweet sustainability: Comparative study of solar and electric cooking in the production of crystallized orange peel candy. Journal Renewable Energy. 9[21] 1-8: e70921108.

Introduction

The citrus agroindustry is a strategic sector in Mexico and Latin America, but nearly 40% of an orange is peel, which is usually discarded, generating negative environmental impacts. Several studies highlight its nutraceutical value due to the presence of flavonoids, essential oils and vitamin C, with applications in the food, cosmetics and pharmaceutical industries (Rolffy & Araujo, 2023; Dongre et al., 2023). Its use in bioenergy to produce biogas and bioethanol has also been demonstrated (Gonzabay & Suárez, 2016).

In food, Basurto, Limongi and Muñoz (2025) confirmed that orange peel flour can improve the nutritional properties of biscuits, while Barrero et al. (2024) proposed its use in the sustainable extraction of essential oils with social and economic impact. At the same time, the Mexican tradition of crystallised sweets (Vázquez, 2020; Del Carmen, 2020; Balboa, 2024) constitutes a cultural heritage that can be linked to clean technologies such as solar cooking, documented in bread making and fruit drying (Ceviz et al., 2024; Basurto, 2021; Cogollo, 2022). Ramírez, Jaramillo and Dorantes (2015) validated the viability of parabolic solar cookers, reaching over 100 °C under direct irradiation, which supports their application in new processes. In this context, the present study aimed to produce crystallised orange peel sweet using a parabolic solar cooker and compare it with the electric method, evaluating its technical, sensory and environmental viability.

2. Theoretical basis

The performance analysis of a parabolic solar cooker is based on the principles of optical concentration and heat transfer.

2.1 Concentrator aperture area

where D is the diameter of the parabolic (m). This expression is the classic formulation for circular concentration collectors

2.2 Incident solar power

The theoretical solar power available in the concentrator is given by:

where:
G is the incident solar irradiance (W/m^2)
Aap=Aap is the aperture area (m^2)
η is the optical efficiency, product of the reflectance of the material, transmittance of the covering and absorptance of the receiver.

2.3 Energy and useful power absorbed by the food

The energy absorbed by the food product is estimated using the calorimetric equation:

where:
m is the mass of the food (kg),
c is the specific heat (J/kg·°C),
ΔT is the temperature increase of the food (°C).

The useful power (Pútil) is determined as:

where t is the cooking time (s).

2.4 Comparison with electric cooking

The power of the electric grill was determined from its energy consumption, calculated as:

where E corresponds to the electricity consumption (kWh) in a given cooking period.

2.5 Thermal efficiency (η) measures the fraction of captured solar energy that is actually used in the food (sweet in this case). The most commonly used formula (Duffie & Beckman, 2013; Kalogirou, 2009) is:

η=Qu/Qs
Qu = Useful energy absorbed by the product [J]
Qs = Solar energy incident on the opening area of the stove [J]

Methodology

The research was carried out in San Juan del Río, Querétaro, Mexico (20°23′N, 100°00′W, 1,920 m above sea level) on 8 July this year, during a sunny day with maximum irradiance of 1123 W/m². A 1.5 m diameter parabolic solar cooker and a 1500 W electric grill were used. The instruments included a pyranometer, digital thermometer, scale, and stopwatch.

The study was conducted using a comparative experimental design, in which batches of crystallised orange peel candy were produced using two cooking methods: electric grill and parabolic solar cooker.

ISSN: 2523-6881
RENIECYT-SECIHTI: 1702902

Castillo-Martínez, Luz-Carmen, Marroquín-De Jesús, Ángel, Alonso-Arroyo, Juana and Olivares-Ramírez, Juan Manuel. [2025]. Sweet sustainability: Comparative study of solar and electric cooking in the production of crystallized orange peel candy. Journal Renewable Energy. 9[21] 1-8: e70921108
https://doi.org/10.35429/JRE.2025.9.21.7.1.8

The aim was to evaluate differences in cooking time, environmental parameters and sensory quality of the final product.

3.1. Raw materials and materials

Raw material: fresh oranges (Citrus sinensis) at commercial maturity.

Utensils and equipment: stainless steel knives, cutting boards, plastic containers. Four main pieces of equipment were used for the experimental development. First, an Ohaus triple-beam balance (maximum capacity 610 g, accuracy ±0.1 g) was used to accurately determine the initial mass of the orange peel in each test. Secondly, a laboratory electric grill (127 V power supply, 1,500 W nominal power, temperature control by electrical resistance), which allowed conventional cooking of the jam and served as a reference for comparing times and energy consumption. Thirdly, a compact infrared thermometer model 42510A-121 (measuring range −50 °C to 500 °C, accuracy ±2 %, resolution 0.1 °C, distance-to-spot ratio 12:1, adjustable emissivity) was used to monitor the temperature of the product during the cooking process. The instruments ensured that reliable and comparable data were obtained for the two cooking methods evaluated. Auxiliary ingredients: food-grade salt (NaCl) and refined sugar.

3.2. Initial preparation (common to both methods)

1. Washing and disinfecting the oranges with 2% sodium hypochlorite.
2. Removing the peel, taking care to remove as much of the albedo as possible.
3. Cut the peel into 2 cm wide strips.
4. Weigh 70 g of fresh peel per batch.
5. Initial soaking in salt water (5 g/L) for 15 minutes.

3.3. Blanching and reduction of bitterness

– **Electric grill:**
– First cycle: boil in water with 1 g of salt for 30 minutes.
– Second cycle: boil in unsalted water for 15 minutes.
– Repeat the process in clean water three more times.

– **Parabolic solar cooker:**
– First cycle: boil in water with 1 g of salt for 15 minutes.
– Second cycle: boil in unsalted water for 15 minutes.

Repeat the process in clean water three more times.

The cooker was manually adjusted to ensure maximum solar radiation capture.

3.4. Syrup preparation and cooking

The same formulation was used in both methods: 200 g of sugar dissolved in 500 mL of water.

– **Electric grill**:

The syrup was heated over low heat until completely dissolved; then the peels were added and cooked for 60 minutes at an average temperature of 90 to 95°C.

– **Parabolic solar cooker**:

The syrup was prepared directly with solar radiation. Once boiling point was reached, the peels were added and cooked for 60 minutes under irradiance of 820–1120 W/m². During the process, irradiance, relative humidity, ambient temperature and syrup temperature were recorded every 45 minutes.

3.5. Crystallisation and drying (common to both methods)

1. The peels were left to rest in the syrup for 24 hours.
2. They were then removed, drained and sprinkled with 3 g of sugar per batch.
3. Finally, they were dried at room temperature (25 ± 2 °C) until they obtained a firm, crystallised texture.

3.6. Sensory evaluation

A hedonic test was conducted with a panel of 20 untrained judges, who evaluated the attributes of colour, aroma, flavour and texture on a scale of 1 (very unpleasant) to 9 (very pleasant).

ISSN: 2523-6881
RENIECYT-SECIHTI: 1702902

Castillo-Martínez, Luz-Carmen, Marroquín-De Jesús, Ángel, Alonso-Arroyo, Juana and Olivares-Ramírez, Juan Manuel. [2025]. Sweet sustainability: Comparative study of solar and electric cooking in the production of crystallized orange peel candy. Journal Renewable Energy. 9[21] 1-8: e70921108
https://doi.org/10.35429/JRE.2025.9.21.7.1.8

4. Results

The results of the experiment were divided into three main blocks: environmental measurements, comparison of cooking methods, and sensory evaluation.

4.1. Measurements

The climatic variables corresponding to irradiance, relative humidity, and ambient temperature were recorded during solar cooking using data from https://www.wunderground.com/dashboard/pws/IQUERETA29. This provided real, verified data on local weather conditions.

Box 1

Figure 1
Preparation of orange peel sweet

Box 2

Table 1
Climate and process variables recorded during the preparation of crystallised sweets in a solar oven.

Time	Irradiance (W/m²)	Ambient temperature (°C)	Wind speed (km/h)	Sweet temperature (°C)	Relative humidity (%)
11:30	860	22.0	0.0	17.9	57
11:45	932	22.6	0.0	35.3	56
12:00	916	22.8	0.0	56.8	54
12:15	976	22.7	0.0	69.4	56
12:30	274	23.2	0.0	40.9	55
12:45	1116	23.1	0.0	48.5	57
13:00	1065	23.7	0.0	80.0	53
13:15	1085	23.9	0.0	21.8	52
13:30	1123	24.2	0.0	47.6	51
13:45	1083	24.3	0.0	56.7	50
14:00	1041	24.1	0.0	62.4	52
14:15	1079	24.0	0.0	70.0	51
14:30	323	24.0	0.0	69.8	49
14:45	346	24.4	0.0	68.8	46
15:00	1060	24.4	0.0	73.0	44
15:15	921	25.0	0.0	72.9	44

It was observed that irradiance peaked around 1:00–1:30 pm, with values exceeding 1100 W/m², which favours intense solar cooking. Relative humidity gradually decreased during the day, favouring transpiration and evaporation, which helped the jam to dry and crystallise. The ambient temperature remained between 22–25 °C °C, which helps prevent the jam from cooling too quickly while crystallising.

Figure 2. Temperature evolution of the jam in a solar oven vs. an electric grill.

4.2. Comparison between electric cooking and solar cooking

Here, the two methods were compared in terms of time, energy consumption, temperatures reached, and final product texture.

Box 3

Table 2
Comparison of technical and sensory parameters between the electric grill and the solar cooker

Method	Total time (min)	Energy consumption	Maximum temperature reached (°C))	Observed texture
Electric grill	~ 60	~ 1.5 kWh	~ 85	Firm, uniform, more golden colour
Solar greenhouse	~ 240	0 kWh	~ 80	Firm, crystallised, slightly lighter colour

Although solar cooking took approximately four times longer than electric cooking, it completely eliminated conventional energy consumption, which is a significant advantage in terms of sustainability.

ISSN: 2523-6881
RENIECYT-SECIHTI: 1702902

Castillo-Martínez, Luz-Carmen, Marroquín-De Jesús, Ángel, Alonso-Arroyo, Juana and Olivares-Ramírez, Juan Manuel. [2025]. Sweet sustainability: Comparative study of solar and electric cooking in the production of crystallized orange peel candy. Journal Renewable Energy. 9[21] 1-8: e70921108
https://doi.org/10.35429/JRE.2025.9.21.7.1.8

The maximum temperature in the solar cooker was close to 80 °C, high enough to caramelise and crystallise without burning, indicating that this method can achieve results comparable to electric cooking if the irradiance is optimised.

4.3. Sensory evaluation

A hedonic test was conducted with a panel of 20 untrained judges, evaluating the attributes: colour, aroma, flavour and texture. The average results indicate high acceptability for both methods, with slight differences favouring the solar method in some attributes:

Box 4

Table 3

Sensory evaluation of crystallised sweets made in an electric grill and a parabolic solar cooker

Attribute	Electric grill	Parabolic solar greenhouse
Colour	8.2 ± 0.5	8.5 ± 0.4
Aroma	7.8 ± 0.6	8.4 ± 0.5
Flavour	8.0 ± 0.5	8.6 ± 0.4
Texture	8.5 ± 0.4	8.2 ± 0.6
Promedio	**8.1 ± 0.5**	**8.4 ± 0.5**

The sweet prepared in the solar cooker was perceived as having a slightly superior colour and flavour, which is attributed to the gradual distribution of solar heat, which promotes a smoother and more uniform caramelisation. In contrast, the texture was more homogeneous in the electric cooking, attributed to the continuous and stable application of temperature provided by the electric grill.

4.4. Interpretation of trends and relevance

– The data collected from https://www.wunderground.com/dashboard/pws/IQUERETA29respaldan the reliability of the climate measurements during the solar test, which gives transparency to the experimental process.

– It is evident that, under high irradiance conditions (≥ 1000 W/m²), the solar cooker can come quite close in performance to the traditional electric method.

– Although solar cooking time limits its applicability in fast-paced production environments, it could be adjusted with more efficient cooker designs or hybrid assistance (solar + electric) for times of low radiation.

– In terms of practical impact, users can plan solar cooking based on local weather forecasts, optimising production periods.

Box 5

Table 4

Sensory comparison of orange peel jam prepared in a solar cooker and on an electric grill

Attribute	Solar greenhouse	Electric grill
Colour	Slightly more intense, with a uniform golden hue due to gradual caramelisation.	Less uniform colour, with slight variations in tone.
Flavour	More aromatic with mild sweet notes, attributable to slow, natural cooking.	Distinct flavour but less aromatic, tending to be more pronounced when cooked quickly.
Texture	It exhibits slight variations in consistency due to its dependence on solar radiation.	More consistent and firm, thanks to the stable temperature of the electrical equipment.
Aroma	Better preserves the essential oils in the peel, giving it a fresh, natural aroma..	Less intense aroma, with slight loss of volatile compounds during cooking..

5. Discussion

The calculation of the thermal efficiency of the parabolic solar oven yielded a value of 1.5%, lower than the range reported in the literature (5–15%), due to the high humidity of the mixture, thermal losses, and irradiance variability. As pointed out by Kalogirou (2009) and Ramírez, Jaramillo and Dorantes (2015), efficiency depends on the geometry of the concentrator, the reflectivity of the materials and the solar orientation, so improvements such as thermal storage and automatic tracking are required. In sensory terms, the solar sweet had a more uniform colour and a more aromatic flavour, which coincides with Ortiz Ballesteros (2007) regarding gentle caramelisation and the preservation of volatile compounds, while the electric grill offered greater homogeneity in texture, in line with Gómez (2019).

ISSN: 2523-6881
RENIECYT-SECIHTI: 1702902

Castillo-Martínez, Luz-Carmen, Marroquín-De Jesús, Ángel, Alonso-Arroyo, Juana and Olivares-Ramírez, Juan Manuel. [2025]. Sweet sustainability: Comparative study of solar and electric cooking in the production of crystallized orange peel candy. Journal Renewable Energy. 9[21] 1-8: e70921108
https://doi.org/10.35429/JRE.2025.9.21.7.1.8

The reuse of orange peel as a raw material is in line with Balboa (2016) and Cogollo Torres (2022), who highlight the circular economy in the food industry. Furthermore, the results agree with Barrero (2024), showing the viability of solar cooking for local enterprises that promote self-employment and decentralised production. Taken together, the findings reinforce their link to SDGs 12, 8 and 3, and confirm that this model is replicable for sustainable production projects with social, economic and environmental impact.

6. Conclusions

This study demonstrated the viability of producing crystallised orange peel using solar cooking as an alternative to electric cooking, comparing both methods in technical, sensory and environmental terms. From a technical point of view, the parabolic solar cooker reached temperatures above 70 °C, sufficient to guarantee cooking, although with a longer cooking time than the electric grill, in accordance with Ortiz Ballesteros (2007). Sensory analysis showed that the solar-cooked candy had a more uniform colour and a more aromatic flavour, results that coincide with those reported by Cogollo Torres (2022) on the preservation of volatile compounds, while the electric grill offered a more homogeneous texture, in line with Gómez (2019).

In environmental terms, solar cooking eliminated electricity consumption (0 kWh versus 1.5 kWh), representing a reduction of approximately 0.8 kg of CO_2 avoided for each batch of 70 g of processed peel, reinforcing the findings of Balboa (2016) and Barrero (2024) regarding the potential of solar energy in the circular economy.

From a socio-economic perspective, the use of orange peel, considered agro-industrial waste, opens up opportunities for added value and self-employment. In a scenario of community production of 100 kg of crystallised solar sweet per month, it is estimated that 2 to 3 direct jobs will be generated, with incomes of around MXN 15,000–20,000 per month depending on the selling price in local markets. In a semi-industrial scheme, the production of 1 tonne per month could avoid more than 100 kg of CO_2 equivalents, while consolidating micro-enterprises with the capacity to access green labels or fair trade certifications.

Thus, this study not only technically validates solar cooking in a traditional pastry product, but also demonstrates its potential as a driver of community development, improving quality of life, reducing agro-industrial waste, and strengthening SDGs 8, 12, and 3. The central strength of the study lies in integrating technical, environmental, social and cultural dimensions, showing that the combination of traditional knowledge and clean technologies constitutes a replicable and sustainable model with possibilities for productive scaling.

Box 6

Table 5

Hypothetical scenarios for scaling up the production of solar-powered orange peel sweets

Setting	Estimated production	Jobs created	Approximate income*	CO_2 avoided (kg/month)**	Expected impact
Domestic	1–2 kg/mes	0 (self-consumption)	—	2–3	Food safety, reducing household waste
Community	100 kg/ month	2–3 jobs	$15,000–20,000 MXN	80–100	Self-employment, local economy, strengthening gastronomic identity
Semi-industrial	1 tonne/month	8–10 jobs	$150,000–200,000 MXN	800–1,000	Consolidation of micro-enterprises, possibility of environmental and fair trade certifications, access to differentiated markets

7. Economic outlook

The study shows that solar cooking of orange peel has high socio-economic potential. In rural communities, workshops for the production of crystallised sweets could boost self-employment and strengthen local economies. In the educational sphere, the methodology offers a teaching tool for renewable energy, agribusiness, and the circular economy, fostering technical skills and environmental awareness. At the semi-industrial level, the use of parabolic solar cookers with hybrid electrical backup would allow for the production of value-added sweets with a sustainability label, aimed at differentiated markets. In addition, it opens up opportunities for environmental or fair trade certification, increasing regional competitiveness. Overall, this initiative not only reduces waste and promotes clean energy, but also contributes to economic and social development in line with SDGs 8, 12 and 13.

Figure 3 Socio-economic perspectives of solar cooking: community, education and semi-industrial production.

ISSN: 2523-6881
RENIECYT-SECIHTI: 1702902

Castillo-Martínez, Luz-Carmen, Marroquín-De Jesús, Ángel, Alonso-Arroyo, Juana and Olivares-Ramírez, Juan Manuel. [2025]. Sweet sustainability: Comparative study of solar and electric cooking in the production of crystallized orange peel candy. Journal Renewable Energy. 9[21] 1-8: e70921108
https://doi.org/10.35429/JRE.2025.9.21.7.1.8

Declarations

Contribution of the authors:

Ángel Marroquín de Jesús: Review of graphs and interpretation of experimental results and preparation of the manuscript.

Luz Carmen Castillo Martínez: Analysis and interpretation of results, as well as supervision of the sweet-making process.

Juana Alonso Arroyo: Search, compilation and systematisation of the literature review.

Juan Manuel Olivares Ramírez: General review of the manuscript and identification of areas for improvement.

Funding:

This work did not receive external funding. The research was carried out with our own resources and with the institutional support of the Technological University of San Juan del Río.

Conflict of interest:

The authors declare that there is no conflict of interest that could influence the results presented or the interpretation of the data.

Acknowledgements

The authors express their gratitude to the Technological University of San Juan del Río for its support during the course of this study. Special recognition is given to the institutional directors and members of the Renewable Energy Academic Body, whose observations and comments contributed significantly to the improvement of this work. We also thank the student volunteers who collaborated in the sensory test and experimental stages, contributing with enthusiasm and commitment to the development of the research must be high quality, not pixelated and should be noticeable even reducing image scale.

References

Antecedents

Balboa, L. (2016). La repostería conventual mexicana: tradición y vigencia. *Revista Tradiciones*, 12(18), 45-59.

Barrero, W. (2024). Modelo de aprovechamiento de residuos de cáscara de naranja en Chapinero, Bogotá. *Universidad EAN*.

Del Carmen, M. (2020). Los dulces tradicionales de convento en México. *Revista de Patrimonio Cultural*, 5(2), 33-47.

Vázquez, L. (2020). Los dulces cristalizados en la gastronomía mexicana: tradición y vigencia. *Revista Gastronómica de México*, 8(1), 15-27.

Gonzabay, J., & Suárez, M. (2016). Producción de biogás y bioetanol a partir de residuos de cítricos. *Revista Técnica Energía*, 14(2), 95-105.

Basics

Duffie, J. A., & Beckman, W. A. (2013). *Solar Engineering of Thermal Processes* (4th ed.). Wiley.

Kalogirou, S. A. (2009). *Solar Energy Engineering: Processes and Systems*. Academic Press. Disponible en

Kreith, F., & Kreider, J. F. (1978). *Principles of Solar Engineering*. Hemisphere Publishing. Disponible en

Ramírez, A., Jaramillo, O., & Dorantes, R. (2015). Cálculo y diseño de una estufa solar parabólica para la cocción de alimentos. *Universidad Tecnológica de Puebla*. Recuperado de

Ortiz Ballesteros, J. J. (2007). Cocción de alimentos con energía solar (Trabajo de grado). *Universidad Católica de Pereira*. Recuperado de

Supports

Basurto Intriago, Y., Limongi Luna, J. M., & Muñoz Murillo, J. P. (2025). Efecto de varios porcentajes de harina de cáscara de naranja (*Citrus sinensis*) sobre las propiedades fisicoquímicas, bromatológicas y sensoriales de galletas dulces. *Nutrición Clínica y Dietética Hospitalaria*, *45*(1).

ISSN: 2523-6881
RENIECYT-SECIHTI: 1702902

Ceviz, M. A., Aydın, H., & Yılmaz, M. (2024). Solar energy applications in food processing: A review. *Renewable Energy, 223*, 120-135.

Cogollo Torres, C. I. (2022). Evaluación de estufas solares parabólicas en la cocción de alimentos. *Revista Colombiana de Energías Renovables, 10*(3), 77-88. Recuperado de

Dongre, P., Gupta, A., & Singh, R. (2023). Phytochemical analysis and nutraceutical potential of citrus peel extracts. *Journal of Food Science and Technology, 60*(8), 2512–2520.

Rolffy, L., & Araujo, D. (2023). Valor nutracéutico de la cáscara de naranja y su aplicación en la industria alimentaria. *Food and Nutrition Journal, 12*(4), 233-245.
.

ISSN: 2523-6881
RENIECYT-SECIHTI: 1702902

Castillo-Martínez, Luz-Carmen, Marroquín-De Jesús, Ángel, Alonso-Arroyo, Juana and Olivares-Ramírez, Juan Manuel. [2025]. Sweet sustainability: Comparative study of solar and electric cooking in the production of crystallized orange peel candy. Journal Renewable Energy. 9[21] 1-8: e70921108
https://doi.org/10.35429/JRE.2025.9.21.7.1.8

[[Title in TNRoman and Bold No. 14 in English and Spanish]

Surname, Name 1st Author*[a], Surname, Name 1st Co-author[b], Surname, Name 2nd Co-author[c] and Surname, Name 3rd Co-author[d] [No.12 TNRoman]

[a] Affiliation institution, Researcher ID, ORC ID, SNI-SECIHTI ID or CVU PNPC [No.10 TNRoman]
[b] Affiliation institution, Researcher ID, ORC ID, SNI-SECIHTI ID or CVU PNPC [No.10 TNRoman]
[c] Affiliation institution, Researcher ID, ORC ID, SNI-SECIHTI ID or CVU PNPC [No.10 TNRoman]
[d] Affiliation institution, Researcher ID, ORC ID, SNI-SECIHTI ID or CVU PNPC [No.10 TNRoman]

All ROR-Clarivate-ORCID and SECIHTI profiles must be hyperlinked to your website.
Prot- University of South Australia • 7038-2013• 0000-0001-6442-4409 • 416112

SECIHTI classification:
https://marvid.org/research_areas.php [No.10 TNRoman]
Area:
Field:
Discipline:
Subdiscipline:

DOI: https://doi.org/
Article History:
Received: [Use Only ECORFAN]
Accepted: [Use Only ECORFAN]
Contact e-mail address:
* ✉ [example@example.org]

Abstract [In English]
Must contain up to 150 words
Graphical abstract [In English]

Authors must provide an original image that clearly represents the article described in the article. Graphical abstracts should be submitted as a separate file. Please note that, as well as each article must be unique. File type: the file types are MS Office files.No additional text, outline or synopsis should be included. Any text or captions must be part of the image file. Do not use unnecessary white space or a "graphic abstract" header within the image file.

Keywords [In English]
Indicate 3 keywords in TNRoman and Bold No. 10

Abstract [In Spanish]
Must contain up to 150 words
Graphical abstract [In Spanish]

Authors must provide an original image that clearly represents the article described in the article. Graphical abstracts should be submitted as a separate file. Please note that, as well as each article must be unique. File type: the file types are MS Office files.No additional text, outline or synopsis should be included. Any text or captions must be part of the image file. Do not use unnecessary white space or a "graphic abstract" header within the image file.

Keywords [In Spanish]
Indicate 3 keywords in TNRoman and Bold No. 10

Citation: Surname, Name 1st Author, Surname, Name 1st Co-author, Surname, Name 2nd Co-author and Surname, Name 3rd Co-author. Article Title. Journal Renewable Energy. Year. V-N: Pages [TN Roman No.10].

Introduction

Text in TNRoman No.12, single space.

General explanation of the subject and explain why it is important.

What is your added value with respect to other techniques?

Clearly focus each of its features.

Clearly explain the problem to be solved and the central hypothesis.

Explanation of sections Article.

Development of headings and subheadings of the article with subsequent numbers

[Title No.12 in TNRoman, single spaced and bold]

Products in development No.12 TNRoman, single spaced.

Including figures and tables-Editable

In the article content any table and figure should be editable formats that can change size, type and number of letter, for the purposes of edition, these must be high quality, not pixelated and should be noticeable even reducing image scale.

[Indicating the title at the bottom with No.10 and Times New Roman Bold]

Box

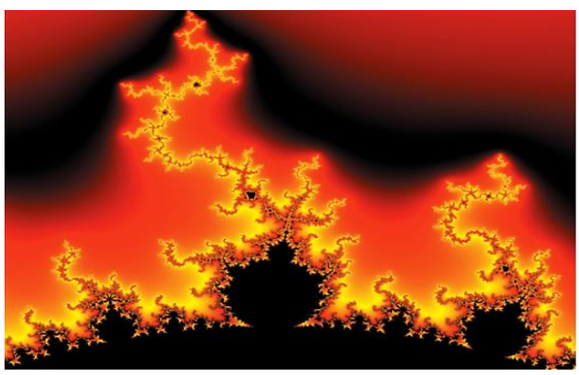

Figure 1

Title [Should not be images-everything must be editable]

Source [in italic]

Box

Table 1

Title [Should not be images-everything must be editable]

Source [in italic]

The maximum number of Boxes is 10 items

For the use of equations, noted as follows:

$$Y_{ij} = \alpha + \sum_{h=1}^{r} \beta_h X_{hij} + u_j + e_{ij} \quad [1]$$

Must be editable and number aligned on the right side.

Methodology

Develop give the meaning of the variables in linear writing and important is the comparison of the used criteria.

Results

The results shall be by section of the article.

Conclusions

Clearly explain the results and possibilities of improvement.

Annexes

Tables and adequate sources.

The international standard is 7 pages minimum and 14 pages maximum.

Declarations

Conflict of interest

The authors declare no interest conflict. They have no known competing financial interests or personal relationships that could have appeared to influence the article reported in this article.

ISSN: 2523-6881
RENIECYT-SECIHTI: 1702902

Surname, Name 1st Author, Surname, Name 1st Co-author, Surname, Name 2nd Co-author and Surname, Name 3rd Co-author. Article Title. Journal Renewable Energy. Year. V-N: Pages [Times New Roman No. 8].
https://doi.org/10.35429/

Author contribution

Specify the contribution of each researcher in each of the points developed in this research.

Prot-
Benoit-Pauleter, Gerard: Contributed to the project idea, research method and technique.

Availability of data and materials

Indicate the availability of the data obtained in this research.

Funding

Indicate if the research received some financing.

Acknowledgements

Indicate if they were financed by any institution, University or company.

Abbreviations

List abbreviations in alphabetical order.

Prot-

ANN	Artificial Neural Network

References

Use APA system. Should not be numbered, nor with bullets, however if necessary numbering will be because reference or mention is made somewhere in the Article.

Use the Roman alphabet, all references you have used should be in Roman alphabet, even if you have cited an article, book in any of the official languages of the United Nations [English, French, German, Chinese, Russian, Portuguese, Italian, Spanish, Arabic], you should write the reference in Roman alphabet and not in any of the official languages.

Citations are classified the following categories:

Antecedents. The citation is due to previously published research and orients the citing document within a particular scholarly area.

Basics. The citation is intended to report data sets, methods, concepts and ideas on which the authors of the citing document base their work.

Supports. The citing article reports similar results. It may also refer to similarities in methodology or, in some cases, to the reproduction of results.

Differences. The citing document reports by means of a citation that it has obtained different results to those obtained in the cited document. This may also refer to differences in methodology or differences in sample sizes that affect the results.

Discussions. The citing article cites another study because it is providing a more detailed discussion of the subject matter.

The URL of the resource is activated in the DOI or in the title of the resource.

Prot-
Mandelbrot, B. B. [2020]. Negative dimensions and Hölders, multifractals and their Hölder spectra, and the role of lateral preasymptotics in science. Journal of Fourier Analysis and Applications Special. 409-432.

Intellectual Property Requirements for editing:

- Authentic Signature in Color of Originality Format Author and Coauthors.
- Authentic Signature in Color of the Acceptance Format of Author and Coauthors.
- Authentic Signature in blue color of the Conflict of Interest Format of Author and Co-authors.

ISSN: 2523-6881
RENIECYT-SECIHTI: 1702902

Reservation to Editorial Policy

Journal Renewable Energy reserves the right to make editorial changes required to adapt the Articles to the Editorial Policy of the Research Journal. Once the Article is accepted in its final version, the Research Journal will send the author the proofs for review. ECORFAN® will only accept the correction of errata and errors or omissions arising from the editing process of the Research Journal, reserving in full the copyrights and content dissemination. No deletions, substitutions or additions that alter the formation of the Article will be accepted.

Code of Ethics - Good Practices and Declaration of Solution to Editorial Conflicts

Declaration of Originality and unpublished character of the Article, of Authors, on the obtaining of data and interpretation of results, Acknowledgments, Conflict of interests, Assignment of rights and Distribution.

The ECORFAN-Mexico, S.C Management claims to Authors of Articles that its content must be original, unpublished and of Scientific, Technological and Innovation content to be submitted for evaluation.

The Authors signing the Article must be the same that have contributed to its conception, realization and development, as well as obtaining the data, interpreting the results, drafting and reviewing it. The Corresponding Author of the proposed Article will request the form that follows.

Article title:

- The sending of an Article to Journal Renewable Energy emanates the commitment of the author not to submit it simultaneously to the consideration of other series publications for it must complement the Format of Originality for its Article, unless it is rejected by the Arbitration Committee, it may be withdrawn.

- None of the data presented in this article has been plagiarized or invented. The original data are clearly distinguished from those already published. And it is known of the test in PLAGSCAN if a level of plagiarism is detected Positive will not proceed to arbitrate.

- References are cited on which the information contained in the Article is based, as well as theories and data from other previously published Articles.

- The authors sign the Format of Authorization for their Article to be disseminated by means that ECORFAN-Mexico, S.C. In its Holding Republic of Peru considers pertinent for disclosure and diffusion of its Article its Rights of Work.

- Consent has been obtained from those who have contributed unpublished data obtained through verbal or written communication, and such communication and Authorship are adequately identified.

- The Author and Co-Authors who sign this work have participated in its planning, design and execution, as well as in the interpretation of the results. They also critically reviewed the paper, approved its final version and agreed with its publication.

- No signature responsible for the work has been omitted and the criteria of Scientific Authorization are satisfied.

- The results of this Article have been interpreted objectively. Any results contrary to the point of view of those who sign are exposed and discussed in the Article.

Copyright and Access

The publication of this Article supposes the transfer of the copyright to ECORFAN-Mexico, SC in its Holding Republic of Peru for its Journal Renewable Energy, which reserves the right to distribute on the Web the published version of the Article and the making available of the Article in This format supposes for its Authors the fulfilment of what is established in the Law of Science and Technology of the United Mexican States, regarding the obligation to allow access to the results of Scientific Research.

Article Title:

Name and Surnames of the Contact Author and the Coauthors	Signature
1.	
2.	
3.	
4.	

Principles of Ethics and Declaration of Solution to Editorial Conflicts

Editor Responsibilities

The Publisher undertakes to guarantee the confidentiality of the evaluation process, it may not disclose to the Arbitrators the identity of the Authors, nor may it reveal the identity of the Arbitrators at any time.

The Editor assumes the responsibility to properly inform the Author of the stage of the editorial process in which the text is sent, as well as the resolutions of Double-Blind Review.

The Editor should evaluate manuscripts and their intellectual content without distinction of race, gender, sexual orientation, religious beliefs, ethnicity, nationality, or the political philosophy of the Authors.

The Editor and his editing team of ECORFAN® Holdings will not disclose any information about Articles submitted to anyone other than the corresponding Author.

The Editor should make fair and impartial decisions and ensure a fair Double-Blind Review.

Responsibilities of the Editorial Board

The description of the peer review processes is made known by the Editorial Board in order that the Authors know what the evaluation criteria are and will always be willing to justify any controversy in the evaluation process. In case of Plagiarism Detection to the Article the Committee notifies the Authors for Violation to the Right of Scientific, Technological and Innovation Authorization.

Responsibilities of the Arbitration Committee

The Arbitrators undertake to notify about any unethical conduct by the Authors and to indicate all the information that may be reason to reject the publication of the Articles. In addition, they must undertake to keep confidential information related to the Articles they evaluate.

Any manuscript received for your arbitration must be treated as confidential, should not be displayed or discussed with other experts, except with the permission of the Editor.

The Arbitrators must be conducted objectively, any personal criticism of the Author is inappropriate.

The Arbitrators must express their points of view with clarity and with valid arguments that contribute to the Scientific, Technological and Innovation of the Author.

The Arbitrators should not evaluate manuscripts in which they have conflicts of interest and have been notified to the Editor before submitting the Article for Double-Blind Review.

Responsibilities of the Authors

Authors must guarantee that their articles are the product of their original work and that the data has been obtained ethically.

Authors must ensure that they have not been previously published or that they are not considered in another serial publication.

Authors must strictly follow the rules for the publication of Defined Articles by the Editorial Board.

The authors have requested that the text in all its forms be an unethical editorial behavior and is unacceptable, consequently, any manuscript that incurs in plagiarism is eliminated and not considered for publication.

Authors should cite publications that have been influential in the nature of the Article submitted to arbitration.

Information services

Indexation - Bases and Repositories

LATINDEX (Scientific Journals of Latin America, Spain and Portugal)
EBSCO (Research Database - EBSCO Industries)
RESEARCH GATE (Germany)
GOOGLE SCHOLAR (Citation indices-Google)
MENDELEY (Bibliographic References Manager)
HISPANA (Information and Bibliographic Orientation-Spain)

Publishing Services

Citation and Index Identification H
Management of Originality Format and Authorization
Testing Article with PLAGSCAN
Article Evaluation
Certificate of Double-Blind Review
Article Edition
Web layout
Indexing and Repository
ArticleTranslation
Article Publication
Certificate of Article
Service Billing

Editorial Policy and Management

1047 La Raza Avenue -Santa Ana, Cusco-Peru. Phones: +52 1 55 6159 2296, +52 1 55 1260 0355, +52 1 55 6034 9181; Email: contact@ecorfan.org www.ecorfan.org

Site Licences

03-2010-032610094200-01-For printed material ,03-2010-031613323600-01-For Electronic material,03-2010-032610105200-01-For Photographic material,03-2010-032610115700-14-For the facts Compilation,04-2010-031613323600-01-For its Web page,19502-For the Iberoamerican and Caribbean Indexation,20-281 HB9-For its indexation in Latin-American in Social Sciences and Humanities,671-For its indexing in Electronic Scientific Journals Spanish and Latin-America,7045008-For its divulgation and edition in the Ministry of Education and Culture-Spain,25409-For its repository in the Biblioteca Universitaria-Madrid,16258-For its indexing in the Dialnet,20589-For its indexing in the edited Journals in the countries of Iberian-America and the Caribbean, 15048-For the international registration of Congress and Colloquiums. financingprograms@ecorfan.org

Management Offices

1047 La Raza Avenue -Santa Ana, Cusco-Peru.

Journal Renewable Energy

2523 6881
ISSN 2523 - 6881